Identification of novel Lis1 protein interaction partners: Investigations towards cellular Lis1 functions

Von der Fakultät für Lebenswissenschaften

der Technischen Universität Carolo-Wilhelmina

zu Braunschweig zur Erlangung des Grades einer

Doktorin der Naturwissenschaften

(Dr. rer. nat.)

genehmigte

D i s s e r t a t i o n

von Bomi Jung

aus Pusan

1. Referent: Professor Dr. Hans-Henning Arnold
2. Referentin: Professorin Dr. Brigitte M. Jockusch
eingereicht am: 20.01.2010
mündliche Prüfung (Disputation) am: 25.02.2010

Druckjahr 2010

Vorveröffentlichungen der Dissertation

Teilergebnisse aus dieser Arbeit wurden mit Genehmigung der Fakultät für Lebenswissenschaften, vertreten durch den Mentor der Arbeit, in folgenden Beiträgen vorab veröffentlicht:

Tagungsbeiträge:

Identification of novel interaction partners with Lis1 protein
B. Jung; A. Holz; H.-H. Arnold
The EMBO Meeting; August 29 – September 1, 2009

When some great sorrow, like a mighty river,
Flows through your life with peace-destroying power
And dearest things are swept from sight forever,
Say to your heart each trying hour:
"This, too, shall pass away."

When fortune smiles, and, full of mirth and pleasure,
The days are flitting by without a care,
Lest you should rest with only earthly treasure,
Let these few words their fullest import bear:
"This, too, shall pass away."

When earnest labor brings you fame and glory,
And all earth's noblest ones upon you smile,
Remember that life's longest, grandest story
Fills but a moment in earth's little while:
"This, too, shall pass away."

By Lanta Wilson Smith

Table of Contents

Summary

Haploinsufficiency of the Lis1 gene in human causes type I lissencephaly owing to a migration defect of cortical neurons during prenatal brain development. Homozygous Lis1 mouse mutants are embryonic lethal, while male mice homozygous for a specific gene trap integration in the Lis1 locus are infertile and display oligozoospermia. These mutations indicate the essential role of Lis1 in different cells, although biochemical mechanisms are not clear.

In a yeast two-hybrid search for Lis1 interaction partners in mouse testis, I isolated three novel potential Lis1-binding proteins, Ranbp9 (Ran binding protein 9), ACT (activator of CREM in testis), and BRAP (BRCA1 associated protein) in addition to the already known binding partner NudeL. GST-pull-down assays, coimmunoprecipitations, and reconstitution of split YFP fluorescence in transfected HeLa cells confirmed these interactions.

Complex formation of Lis1 and Ranbp9 involves the Lis1 WD-40 repeats and the SPRY domain of Ranbp9. ACT binds to Lis1 via the four LIM domains, and BRAP interacts with Lis1 through the coiled-coil domain.

In mouse embryonic fibroblasts (MEFs) with genetically reduced levels of Lis1, Ranbp9 appears reduced at the cell periphery relative to the central, perinuclear region suggesting that Lis1 may play a role in stabilization and/or subcellular localization of Ranbp9. Lis1 forms complexes with ACT in the cytoplasm of spermatogenic cells in testis suggesting that both, Lis1 and ACT may have functions in overlapping processes during late spermatogenesis. BRAP protein also colocalizes with Lis1 in the cytoplasm of HeLa cells where it accumulates close to the nucleus.

Furthermore, Lis1 is a microtubule associated protein that influences microtubule dynamics by affecting microtubule plus-end stability and the frequency of catastrophic breakdown. Analysis of microtubules and plus-end binding proteins in Lis1 deficient-MEF cells revealed reduced levels of acetylated tubulin and increased decoration of microtubule plus-ends by CLIP-115. Moreover, Lis1 affects the velocity of microtubular growth as demonstrated by live cell imaging. These results provide further evidence for an essential role of Lis1 in the regulation of microtubule dynamics.

Zusammenfassung

Die Haploinsuffizienz des *Lis1* führt beim Menschen zu der Lissenzephalie Typ 1, die durch Migrationsdefekte von kortikalen Neuronen während der pränatalen Hirnentwicklung verursacht wird. Mausmutanten mit homozygotem Lis1 sind vorgeburtlich letal, und männliche Mäuse mit einer Genfalle (gene trap) im Lis1 Lokus sind infertil und zeigen eine deutlich verringerte Spermienzahl (Oligozoospermia). Obwohl die biochemischen Mechanismen unbekannt sind, verdeutlichen diese Mutationen die tragende Bedeutung von Lis1 in unterschiedlichen Zellen.

Mit einem Yeast-Two-Hybrid System, bei dem mit Lis1 nach interagierenden Genen des Mäusehodens geforscht wurde, konnten - neben der Detektion des bereits bekannten NudeL - drei neue potentielle Interaktionspartner isoliert werden: Ranbp9 (Ran binding protein 9), ACT (activator of CREM in testis) und BRAP (BRCA1 associated protein). Darüber hinaus wurde die Interaktion mit Lis1 durch die Glutathione S-transferase Methode, Koimmunoprezipitation sowie der Markierung mit fluoreszierendem YFP in transfizierten HeLa-Zellen verifiziert.

Die Komplexbildung zwischen Lis1 und Ranbp9 wird durch WD-40 Domänen in der Lis1-Sequenz sowie durch die SPRY Domäne in Ranbp9 ermöglicht. Die Bindung zwischen ACT und Lis1 wird über vier LIM Domänen und die Interaktion mit BRAP über eine coiled-coil Domäne induziert.

In embryonalen Mäusefibroblasten (MEFs) mit genetisch reduzierter Lis1 Expression erscheint die Lokalisation des Ranbp9 an der Zellperipherie schwächer, im Vergleich zur zentralen perinuklearen Region. Dies deutet auf eine stabilisierende Wirkung hin und/oder eine subzelluläre Lokalisation des Ranbp9 durch Lis1. Mit Act bildet Lis1 Protein-Protein-Komplexe im Zytoplasma von spermatogenen Zellen des Testikels.

Lis1 formt mit ACT Proteinkomplexe im Zytoplasma von ungereiften Spermien (spermatogenic cells) des Hodens. Dies deutet darauf hin, daß Lis1 und BRAP während der späten Spermatogenese an sich überschneidenden Prozessen beteiligt sind. Außerdem befinden sich BRAP und Lis1 kolokalisiert im Zytoplasma von Hela-Zellen, akkumuliert an der Peripherie des Zellkerns.

Zusätzlich interagiert Lis1 mit Mikrotubuli und beeinflußt den Auf- und Abbau der Proteinfilamente durch Einwirkung auf die Stabilität am Plus-Ende und auf die Frequenz des Abbaus am Minusende. In Lis1 defizienten Mäusefibroblasten (MEFs) konnte die Analyse von Mikrotubuli und Mikrotubulus assoziierten Proteinen reduzierte Mengen an acetyliertem Tubulin und eine erhöhte Zahl an Mikrotubulus Plus-Ende assoziierter CLIP-115 aufdecken. Darüber hinaus beeinflußt Lis1 die Geschwindigkeit des filamentösen Wachstums, wie durch "Live Cell Imaging" demonstriert werden konnte. Diese Ergebnisse untermauern zusätzlich die Evidenz, daß Lis1 eine essentielle Funktion bei der Regulation der Mikrotubulidynamik einnimmt.

1. Introduction

Development of the human cerebral cortex is a highly dynamic process which involves migration of neuronal progenitor cells leading to the formation of six distinct cortical layers. Impaired neuronal migration results in cortical layering defects, a smooth brain surface, and abnormal behavior in humans.

Type I (or classical) lissencephaly is a classical example of a severe developmental disorder of the human brain characterized by a smooth surface of the cortex and abnormal neuronal migration during early stages of brain development (Dobyns, 1989; Reiner et al., 1993). Most apparent is the nearly complete absence of gyri, wide ventricles, and heterotopic neuronal cells (Stewart et al., 1975) (Fig. 1). Patients with type I lissencephaly show severe mental retardation, epileptic seizures, and a short lifespan (reviewed in Wynshaw-Boris, 2007).

In humans Lis1 was the first gene shown to be genetically linked to type I lissencephaly suggesting its causal role for the severe brain malformations (Reiner et al., 1993). Haploinsufficiency of Lis1 leads to abnormal cortical layers caused by defects in proliferation and migration of neurons in the developing brain (Reiner et al., 1993; Hattori et al., 1994; Lo Nigro et al. 1997). Homozygous Lis1 mutant mice ($Lis1^{-/-}$) show early embryonic lethality. In contrast, heterozygous mutant mice ($Lis1^{+/KO}$) are viable and resemble the human disease by displaying abnormal organization of layered structures in the central nervous system (CNS) including the cortex, the hippocampus, and the olfactory bulb. All these defects in different brain regions are attributable to neuronal migration defects during early development of the CNS (Hirotsune et al., 1998; Gambello et al., 2003). Additionally, RNA interference studies using Lis1 shRNA indicated that the knockdown of Lis1 leads to complete arrest of cell proliferation, migration, and morphogenesis during neurogenesis (Tsai et al., 2005).

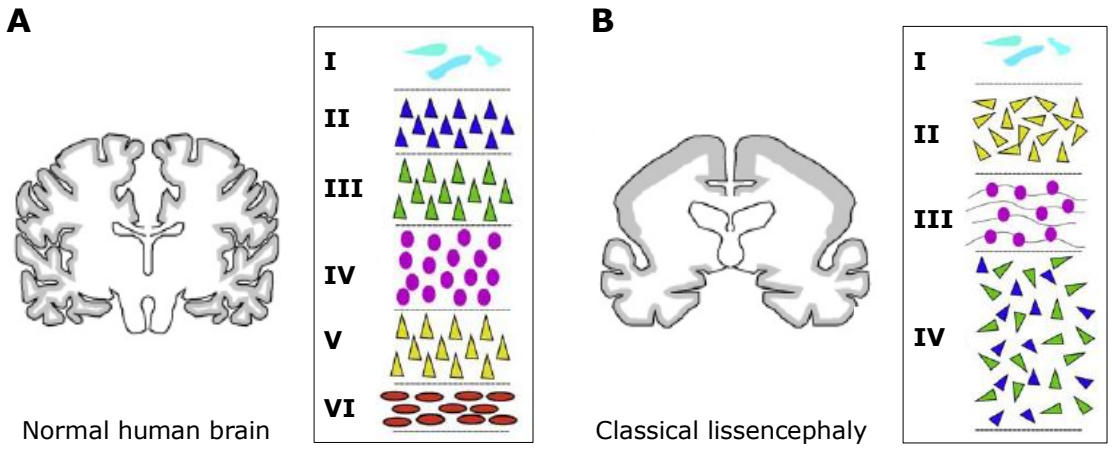

Figure 1. Patients with Lissencephaly have impaired cortical layering.
A. Normal cortical lamination with 6 layers. Layer I: a superficial layer or molecular layer containing mainly extensions of apical dendritic from pyramidal neurons, horizontally-oriented axons, and glial cells. Layer II: consists of pyramidal neurons and satellite neurons. Layer III: contains mainly medium sized pyramidal neurons Layer IV: contains pyramidal neurons and stellate neurons Layer V: consists of the largest pyramidal neurons such as the Betz cells Layer VI: contains large pyramidal neurons and multiform neurons, and spindle shaped pyramidal neurons.
B. Abnormal Cortical layers in type I lissencephaly. Layer I: a superficial layer Layer II: a thin layer dominated by neurons as well as some mislocated cells which are normally located in layers I and II. Neurons are normally located layers IV-VI in normal brain. Layer III: A thin ribbon of white matter Layer IV: a wide layer with heterotopic cells (Stewart et al., 1975) (Adapted and modified from Kerjan and Gleeson, 2007; Guerrini and Parrini, 2009)

The Lis1 gene is evolutionary conserved and homologues can be found in invertebrates like *Drosophila melanogaster* (termed *DLis1*; Liu et al., 2000), *Caenorhabditis elegans* (*lis-1*; Dawe et al., 2001), the fungus *Aspergillus nidulans* (nuclear distribution defective (*Nud*) *F;* Xiang et al., 1995), and in the yeast *Saccharomyces cerevisiae*, where the mammalian Lis1 homologue is termed *Pac1* (perish in the absence of CIN8; Geier et al., 1997).

Lis1 is a microtubule-associated protein (Sapir et al., 1997). Microtubules are dynamic structures of the cytoskeleton with essential functions in cell division, cell migration, and vesicular transport. Microtubules consist of polymerized heterodimers of α- and β-tubulin. Both subunits are highly conserved in all eukaryotes. Interestingly, recent data suggest that perturbation of cortical lamination may also result from mutations in α- or β- tubulin in humans. Since TUBA1 mutant mice also display abnormal laminar architecture of hippocampus and cortex due to impaired neuronal migration (Keays et al., 2007; Jaglin et al., 2009).

Lack of α-tubulin reduces GTP binding and disrupts heterodimer formation of tubulin suggesting that defects of microtubular function are the cause of abnormal neuronal migration (Keays et al., 2007). Mutations in the β-tubulin gene TUBB2B also lead to defects in cortical development resulting in asymmetrical polymicrogyria resembling lissencephaly, including the reduction of gyri and a thick disorganized cortical plate with abnormal lamination (Jaglin et al., 2009). RNAi-based TUBB2B inactivation experiments demonstrated that β-tubulin is essential for neuronal migration (Jaglin et al., 2009). In summary, these data suggest that microtubule-based processes are very important for proper development of the mammalian brain.

Mammalian Lis1 mRNA and protein are ubiquitously expressed in all tissues. However, tissue-specific variations of mRNA splicing and polyadenylation are known in adult brain (5.4kb mRNA), heart (4.4kb mRNA), and testis (2.4kb mRNA) (Peterfy et al., 1998). Especially in testis, an alternatively spliced transcript containing an additional exon 2a was found in the 5'-untranslated region. It is interesting to note, however, that the Lis1 protein encoded by probably all splice isoforms remains unchanged by the alternative splicing events.

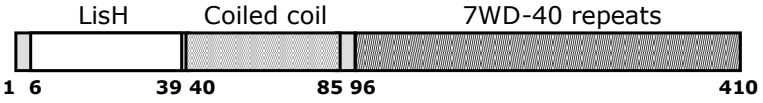

Figure 2. Schematic illustration of the Lis1 protein structure
Full length Lis1 consists of 410 amino acids and contains three main domains. A LisH domain (*aa* 6-39) located at the N-terminus followed by a Coiled coil domain (*aa* 40-85), and, at the C-terminus of Lis1, the 7WD-40 repeat domains (*aa* 96-410) are formed.

The Lis1 gene codes for a cytoplasmic protein of 45kDa consisting of 410 amino acids. The protein contains three known structural motifs. The Lis1-homology (LisH) motif is located at the N-terminus of Lis1 (*aa* 6-39) and has also been found in many other eukaryotic proteins. This region may mediate dimerization and has been implicated in regulating neuronal migration and microtubular dynamics (Emes

and Ponting, 2001). An alpha-helical region (*aa* 40-85) consisting of a coiled-coil domain is located distal to the LisH motif and may mediate important protein-protein interactions (Burkhard et al, 2001; Mason and Arndt, 2004). The N-terminus including the LisH motif together with the coiled-coil domain (*aa* 1-95) is known to be responsible for the homodimerization of Lis1 protein that is an essential subunit in the platelet activating factor-acethylhydrolase (PAF-AH) complex (Cahana et al., 2001; Kim et al., 2004). A heterozygous N-terminal deletion of Lis1 in mouse results in aberrant morphology of cortical neurons and radial glia in the developing cortex owing to retardation of neuronal migration. This emphasizes once again the importance of the N-terminus of the Lis1 protein (Cahana et al., 2001).

The carboxy-terminus of Lis1 is composed of 7 WD-40 repeat motifs (*aa* 96-410). Each of these conserved elements contains around 40 amino acids, often initiated by glycine-histidine (GH), and terminated by tryptophan-aspartic acid residues (WD) (Kim et al., 2004; Li and Roberts, 2001). WD repeat proteins may form a beta-propeller structure which is thought to mediate protein-protein interactions, but may also to be involved in signal transduction, assembly of the cytoskeleton, regulation of vesicular trafficking, cell cycle regulation, and apoptosis (reviewed in Li and Roberts, 2001).

Lis1 functions in two distinct biological pathways. First, Lis1 is part of the Type I platelet activating factor-acethylhydrolase (PAF-AH) complex in which it constitutes the noncatalytic beta subunit (PAF-AH1b) (Reiner et al., 1993; Hattori et al., 1994), besides the two catalytic subunits, α1 and α2 (Arai et al., 2002). All subunits of PAF-AH are highly expressed in the developing brain and testis suggesting a role during neuronal development and spermatogenesis (Koizumi et al., 2003). PAF-AH inactivates platelet activating factor (PAF) by hydrolyzing the acetyl group that is required for the biological function of PAF (Arai et al., 2002). PAF is a potent phospholipid activator present in various organs, particularly in the brain and the reproductive organs. It participates in fundamental physiological processes such as inflammation and vascular permeability (Hattori et al., 1994; Tjoelker et al., 1995; Brkovic and Sirois, 2007). In addition, PAF is essential for sperm motility and acrosomal function, although it seems to be dispensable for sperm development (Roudebush, 2001; Angle et al., 1993). PAF has been implicated also in pathological

processes in the CNS, such as stroke and ischemia (Hattori et al., 1994; Palmer et al., 1997; Umemura et al., 2007). Second, Lis1 participates in the regulation of microtubular dynamics. For this role, Lis1 binds to the plus-ends of microtubules besides interacting with several other proteins, such as cytoplasmic dynein, dynactin, and CLIP-170.

Lis1 directly interacts with the cytoplasmic dynein-dynactin motor complex which requires ATP as the energy source for cargo transport towards the minus-end of microtubules and is essential for various cellular processes including transport of vesicles and organelles, Golgi dynamics, and mitosis (Holzbaur and Vallee, 1994; Hirokawa, 1998; Ahmad et al., 1998). Lis1 has been suggested to be involved in the regulation of the ATPase activity of dynein whereby it may influence motor activity and consequently cargo transport along microtubules (Mesngon et al., 2006). In addition, Lis1 and the cytoplasmic dynein-dynactin complex appears to colocalize at the cell cortex and at mitotic kinetochores indicating that Lis1 may also influence the subcellular localization of cytoplasmic dynein and dynactin as well as mitotic progression and spindle orientation (Siller et al., 2005; Faulkner et al., 2000). Supporting this view, overexpression of Lis1 in cultured cells leads to increased retrograde movement of cytoplasmic dynein and accumulation of microtubules at the cell periphery (Smith et al., 2000). In summary, Lis1 is thought to regulate cytoplasmic dynein-driven retrograde movements along microtubules as well as neuronal migration and axon growth.

NudF, the fungal Lis1 homologue, has been identified as a gene required for dynein-mediated nuclear migration along microtubules indicating that Lis1 plays a role in nucleokinesis in *Aspergillus nidulans* (Xiang et al., 1995). In *Aspergillus*, *NudF* genetically interacts with the microtubule motor machinery including *NudA* and *NudG*, representing the homologues of dynein heavy and light chains, respectively. Other genes such as *NudE* and *NudC* are also required for nuclear migration (Efimov and Morris, 2000). *NudE* was originally identified as a multicopy suppressor of *NudF.* It has two known mammalian homologues, mouse NudE homolog (NudE) and NudE-like (NudeL) which were identified as Lis1 interacting proteins in yeast two-hybrid screens (Feng et al., 2000; Niethammer et al., 2000; Sasaki et al., 2000; Efimov and Morris, 2000). NudE and NudeL are related proteins that both accumulate at the centrosome where they colocalize with Lis1 (Feng et al., 2001; Sasaki et al., 2005). Inhibition of NudE and NudeL leads to metaphase arrest

suggesting that both proteins, together with Lis1, are required for mitotic progression (Stehman et al., 2007). Homozygous NudeL knockout mice show early embryonic lethality, similar to the homozygous Lis1 mutant, whereas viable hypomorphic NudeL mutants exhibit mild defects in neuronal migration. Lis1 and NudeL double mutant mice, heterozygous for each allele, display more severe neuronal migration defects suggesting that both genes interact genetically (Sasaki et al., 2005). Interestingly, Lis1 and NudeL simultaneously interact with cytoplasmic dynein and regulate the distribution of cytoplasmic dynein along microtubules (Sasaki et al., 2000; Stehman et al., 2007).

Lis1 associates with microtubules and it has been implicated in the regulation of microtubule dynamics by preventing microtubule catastrophe events (Sapir et al., 1997). Moreover, different cellular levels of Lis1 affect the distribution of microtubules again suggesting that Lis1 contributes to the regulation of microtubular stability (Smith et al., 2000; Yingling et al., 2008). Lis1 and several proteins specifically bind to the growing plus-ends of microtubules (so called +TIP binding proteins). For instance, the cytoplasmic linker proteins-170 (CLIP-170) was the first identified +TIP binding protein that has been suggested as a regulator of microtubules (Pierre et al., 1992; Binker et al., 2007). CLIP-170 has been shown to associate with $p150^{glued}$, a central component of the dynactin complex as well as Lis1 (Lansbergen et al., 2004). Hence Lis1 might regulate the interactions between the dynein-dynactin complex and CLIP-170 for microtubule dynamics (Coquelle et al., 2002; Tai et al., 2002). Furthermore, $p150^{glued}$ competes with Lis1 for binding to CLIP-170 (Lansbergen et al., 2004). These observations suggest that Lis1 contributes to a complex network of protein-protein interactions required for the regulation of microtubular stability and dynein motor function at the plus-end of microtubules. (Smith et al., 2000; Lansbergen et al., 2004). The precise molecular organization of Lis1 and other +TIP binding proteins is unclear.

Homozygous Lis1 gene trap mutant male mice (Lis1$^{GT/GT}$) with a selective disruption in a testis specific Lis1 transcript show severe defects in spermatogenesis indicating that Lis1 plays an important role during germ cell development (Nayernia et al., 2003).

Spermatogenesis is the developmental process of the generation of male germ cells in the testis. In general, spermatogenesis starts from spermatogonial cells which reside in the basal layer of the germinal epithelium of the testis. Spermatogonia can divide mitotically and by this process maintain the population of spermatogonial cells. However, these cells also produce primary spermatocytes which are able to initiate the first meiotic division and yield secondary spermatocytes. These cells subsequently enter the second meiotic division to produce haploid spermatids. The differentiation of spermatids into mature sperm cells is termed spermiogenesis and corresponds to the final process of spermatogenesis. Not only nuclear condensation and acrosomal formation but also flagellum formation and a significant reduction of cytoplasm all take place during this final stage of spermatogenesis. Although Lis1 is highly expressed in testis, its specific function during spermatogenesis remains unknown.

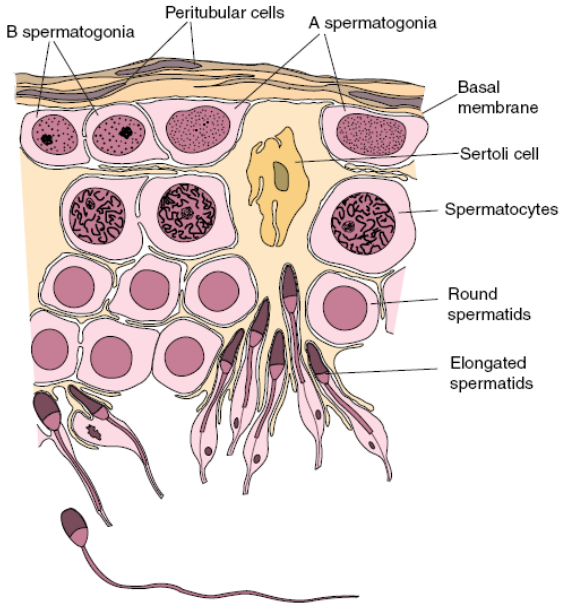

Figure 3. Schematic illustration of cross-section of a mouse seminiferous tubule
The epithelium consists of Sertoli cells and the spermatogenic cells. Spermatogenic cells are in close contact with sertoli cells which support and nourish spermatogenic cells as well as secrete hormones, and phagocytize cell debris. The spermatogonial cells are located in the basal lamina of the seminiferous tubules and spermatogenic cells are migrated toward the lumen. (Adapted from Gilbert et al., 2003)

All subtypes of the Type I platelet-activating factor acethylhydrolase (PAF-AH) are enriched in testes. α2 and Lis1, both are detected in the cytoplasm of all types of spermatogenetic cells enriched in mitotic spermatocytes and elongated spermatids (Koizumi et al., 2003; Nayernia et al., 2003; Yan et al., 2003). In contrast, α1 is restricted to the basal region of seminiferous tubules particularly in the cytoplasm of spermatogonial cells suggesting that this protein might be involved in the proliferation and differentiation of spermatogonia (Koizumi et al., 2003; Yan et al., 2003).

While $\alpha1^{-/-}$ mutant mice are fertile with no apparent phenotype, $\alpha2^{-/-}$mutant males are infertile due to severe defects in spermatogenesis. $\alpha1^{-/-}\alpha2^{-/-}$double-mutants show early defects in spermatogenesis with increased apoptosis in the seminiferous tubule and degeneration at spermatocytes stages suggesting that the catalytic subunits (α1 and α2), particularly α2, are important for male germ cell differentiation (Yan et al., 2003; Koizumi et al., 2003). Up-regulated Lis1 was detected in either $\alpha2^{-/-}$ or $\alpha1^{-/-}\alpha2^{-/-}$ mutant mice. Interestingly, the drastic testis specific phenotypes of $\alpha2^{-/-}$ or $\alpha1^{-/-}\alpha2^{-/-}$ knockout mice can be rescued by reduced Lis1 levels suggesting important doses affect of components of PAFAH1B complex during spermatogenesis (Yan et al., 2003).

Microtubules are dramatically rearranged during spermatogenesis, a process that requires mitotic division of spermatogonia, meiotic division of spermatocytes, manchette formation, and flagella axoneme assembly in spermatids (Koizumi et al., 2003). Lis1 associates with microtubules via microtubule binding proteins, such as dynein (Tai et al., 2002). Lis1 in spermatids indeed colocalizes with α-tubulin and dynein (Nayernia et al., 2003). Lis1 has also been shown to associate with the Golgi complex, the distribution of which is affected by different levels of Lis1 (Nayernia et al., 2003; Smith et al., 2000). This supports the idea that Lis1 may play a role in vesicular transport mediated by dynein motor function during spermiogenesis.

1. 1. Aim of this study

Mutations in the Lis1 gene are known to cause severe developmental defects, such as type I lissencephaly and oligozoospermia (Reiner et al., 1993; Nayernia et al., 2003). However the precise molecular functions of Lis1 for spermatogenesis are not understood.

To get better insights into the role of Lis1 in general and in spermatogenesis in particular, I here present experiments that were designed to identify novel binding partners of Lis1 in testis, confirm their mode of interaction, and examine consequences of Lis1 gene disruption.

I discovered 3 novel Lis1 interaction partners. One of which is testis-specific, the other two are ubiquitously expressed. The formation of complexes between these proteins and Lis1 were confirmed *in vitro* and *in vivo*.

2. Materials and Methods

2. 1. Materials

2. 1. 1. Chemicals, reagents, and solutions

All chemicals and regents were bought from Roth, Merck, Sigma, Promega, Roche, and Fluka. Standard solutions and buffers used in this study were prepared as described in Sambrook et al. (1989).

2. 1. 2. Kits

Kits	Company	Cat#
Qiagen plasmid mini kit	Qiagen	12123
Qiagen plasmid midi kit	Qiagen	12243
Qiagen plasmid maxi kit	Qiagen	12263
MinElute reaction cleanup kit	Qiagen	28204
MinElute gel extraction kit	Qiagen	28604

2. 1. 3. Enzymes

Restriction enzymes and supplied buffers used in this study were purchased from New England Biolabs.

Enzymes		
DNAse	Promega	M-6101
Proteinase K	Roth	7528.2
DNA polymerase I large (Klenow) fragment	Promega	M-2201
Taq DNA polymerase	TaKaRa	R001A
Ex Taq DNA polymerase	TaKaRa	R006A
Pfu DNA polymerase	Promega	M-7741
T4 DNA ligase	Promega	M-1801

2. 1. 4. Oligonucleotides

Oligonucleotides served as primers (1) for RT-PCR to detect the mRNA expression of certain genes, (2) for sequencing to confirm the complete open reading frame, and (3) for genotyping of Lis1 mutant mouse lines and derived murine embryonic fibroblast (MEF) lines, and (4) to amplify DNA fragments for subcloning.

Primers for RT-PCR:

Name	Sequence 5′ to 3′
Lis1-5′	GTGGTCATAGGAGTCCAGTTACTC
Lis1-3′	CCATACGTACCCATTCTCTGTGTC
Ranbp9-5′	CTTCTGGAACTGGACAACCGTATG
Ranbp9-3′	GAACAGTCTGGTCTGTAGATCTGG
ACT-5′	CTTCATCCGCTGCTCTACAA
ACT-3′	CCTGGCATGATGGTTCTCTT
BRAP-5′	CCTGCCAGGAAGAGAAGATAGATG
BRAP-3′	CTGTGTCTCCAGGTAGAACATGAC
GAPDH-5′	ATCCCATCACCATCTTCCAG
GAPDH-3′	CCTGCTTCACCACCTTCTTG

Primers for sequencing:

Name	Sequence 5′ to 3′
GAL4 DBD-5′	GTGCGACATCATCATCGGAAG
GAL4 AD-5′	AAT ACC ACT ACA ATG GAT GAT
GAL4 AD-3′	GTGAACTTGCGGGGTTTTTCA
pGEX-5′	GGGCTGGCAAGCCACGTTTGGTG
pGEX-3′	CCGGGAGCTGCATGTGTCAGAGG
T7	TAATACGACTCACTATAGGG
BGH#1-3′	CAACTAGAAGGCACAGTCGAGGCTG
CRE-3' (160-177)	CCTCATCACTCGTTGCAT
CYFP#1-5′	TCCGCCCTGAGCAAAGAC C
Venus-2-5′	AGTCCGCCCTGAGCAAAGAC
pEGFP-C2-3′	TTTCAGGTTCAGGGGGAGGTG

Name	Sequence 5′ to 3′
pRNA-U6-5′	TACGATACAAGGCTGTTAGAGAG
Cherry#4-5′	GAAGTTGGACATCACCTCCCAC
Cheery#5-5′	ACGGCGAGTTCATCTACAAGGT
Cherry#6-3′	ACCTTGTAGATGAACTCGCCGT

Primers for genotyping:

Name	Sequence 5′ to 3′
Lis1-I3-sense	ATGGTGCATGTGTGAGTATCTGC
Lis1-I7-sense	TGAATGCATCAGAACCATGC
Lis1-I7-antisense	CCTCTACCACTAAAGCTTGTTC

Primers for cloning:

Construct	Name	Sequence 5′ to 3′
pDBD-GAL4-Lis1	Lis1-EcoRI-5′	GAATTCATGGTGCTGTCCCAGAGACAACGAATGAAC
pDBD-GAL4-Lis1	Lis1-SalI-3′	GTCGACTCAATCAACGGCACTCCCACACC
HA-SPRY	Ranbp9-SPRY 5′	GAATTCCTCAACGAGCAGGAGAAGGAG
HA-SPRY	Ranbp9#7 AS-EcoRI+STOP	TGAGGAATTCTCATCCTTCTCGATCCCCGATAGG
HA-LisH+CTLH	HA-Ranbp9-LisH/CTLH-5'-XhoI	CTCGAGATGGACCGCTTTCCTATCGGGGATCGAGAAGGA
HA-LisH+CTLH	HA-Ranbp9-LisH/CTLH-3'-HindIII	AAGCTTCTACAAACACCGCACTTCACTGTCTGTACCATT
HA-ACT-F	ACT-EcoRI-5′	GAATTCATGACAAGTAGTC
HA-ACT-F	ACT-BamHI-3′	GGATCCTTTCTAAGCGTCA
HA-LIM4	HA-ACT-LIM4-5'-EcoRI	GAATTCATGGCTAAAAAGTGTGCAGCCTGCACCAAACCC
HA-LIM4	HA-ACT-LIM4-3'-BamHI	GGATCCTTTCTAAGCGTCAGTGTCTGCCCCGGACGGACA
HA-BRAP-F	BRAP#1-5′	AGATCTCGAGATGGCGTGCAATGGCCGCCAGTT C
HA-BRAP-F	BRAP#2-3′	TAGATAAGCTTGGATGGTCACTTGCCCCTCTTGCTGC
Venus-N-BRAP	BRAP#3-5′-EcoRI	TAGATGAATTCATGGCGTGCAATGGCCGCCA
Venus-C-BRAP & Venus-C-cBRAP	BRAP#5-3′-SalI	TATATGTCGACTCACTTGCCCCTCTTGCTGC
Venus-N-cBRAP	BRAP#4-5′-EcoRI	TAGATGAATTCGCCTTACAGTTAGAGTACTCGTACCTG

Oligo nucleotides serving as DNA linker fragments:

Construct	Name	Sequence 5’ to 3’
pGEX-4T-1-Lis1-C	pGEX-4T-1-Lis1-C	GATCCCCGTCGAC
Venus-N-Ranbp9 & Venus-C-Ranbp9	Venus/ pEGFP-Linker (SalI)-5’	TCGAATGGAGC
Venus-N-Ranbp9 & Venus-C-Ranbp9	Venus/ pEGFP-Linker (SalI)-3’	TCGAGCTCCAT
HA-CRE	CRE-Linker (EcoRI)-5'	GTACGAATTCG
HA-CRE	CRE-Linker (EcoRI)-3'	GTACCGAATTC

2. 1. 5. Antibodies

For Western blot analysis, immunocyto-, or immunohistochemistry several antibodies were used.

2. 1. 5. 1. Primary antibodies

Primary antibodies			Dilution
Mouse monoclonal IgG Anti-Lis1 (N-19)	Santa Cruz	sc-7577	WB 1:2000 IC 1:250
Goat polyclonal IgG Anti-Lis1 (G-3)	Santa Cruz	sc-17817	WB 1:2000 IC 1:250
Goat Anti-ACT (K-18)	Santa Cruz	sc-9368	IC 1:100
Anti-GST	Amersham Biosciences	27-4577-01	WB 1:5000
HA11 Monoclonal Antibody	Covance	MMS-101R	WB 1:2000 IC 1:250
Goat Anti-RanbpM/Ranbp9	ImgeneX	IMX-3686	IC 1:100-250 IH 1:100
Rabbit Anti-Gamma tubulin	Sigma	T5192	WB 1:5000 IC 1:500
Anti-FLAG BioM2	Sigma	F9291	WB 1:2000
Anti-FLAG M2 Monoclonal Antibody	Sigma	F3165	WB 1:2000 IC 1:250
Monoclonal Anti-Lis1 Clone Lis1-338	Sigma	L7391	WB 1:2000
Anti-EB1	BD	610535	WB 1:2000 IC 1:500
Anti-p150glued	BD	610474	WB 1:1000 IC 1:200

WB (Western Blot), IC (Immunocytochemistry)

2. 1. 5. 2. Secondary antibodies

Secondary antibodies			Dilution
Anti-Goat IgG peroxidase conjugate	Sigma	A5420	WB 1:8000
Streptavidin-Peroxidase Streptomyces avidinii	Sigma	S5512	WB 1:2000
Anti-mouse IgG (Cy3)	Sigma	C2181	IC 1:250 IH 1:250
Anti-Rabbit peroxidase conjugate	Amersham Biosciences	NIF 824	WB 1:2000
Anti-mouse IgG+IgM peroxidase conjugate	Jackson ImmunoResearch	115-035-068	WB 1:8000
Anti-mouse IgM (DyLight 549)	Jackson ImmunoResearch	715-505-140	IC 1:250
Anti-mouse IgG (Cy2)	Jackson ImmunoResearch	715-225-150	IC 1:250
Anti-Rat IgG (Cy3)	Jackson ImmunoResearch	712-165-150	IC 1:250
Anti-Rabbit IgG (Cy5)	Jackson ImmunoResearch	711-175-152	IC 1:250
Anti-Goat IgG (Cy3)	Jackson ImmunoResearch	705-165-147	IC 1:250
Anti-mouse IgG+IgM peroxidase conjugate	Jackson ImmunoResearch	115-035-068	WB 1:8000
Anti-mouse igG (H+L) peroxidase conjugate	Dianova	115-035-062	WB 1:8000
Anti-rabbit igG (H+L) peroxidase conjugate	Dianova	111-035-045	WB 1:2000
Anti-rat igG (H+L) peroxidase conjugate	Dianova	112-035-062	WB 1:2000
Anti-mouse IgG (H+L) Alexa Fluor 594	Invitrogen (molecular probes)	A11032	IC 1:200
Anti-Rabbit IgG (H+L) Alexa Fluor 594	Invitrogen (molecular probes)	A11037	IC 1:250
Anti-Rat IgG (H+L) Alexa Fluor 594	Invitrogen (molecular probes)	A11007	IC 1:200

WB (Western Blot), IC (Immunocytochemistry)

2. 1. 6. Yeast strains

The GAL4 based yeast two-hybrid screening as well as corresponding cotransformation assays were performed using the AH109 yeast strain. Alternatively, the L40 yeast strain was used for interaction studies involving the LexA based system.

Yeast strain	Promoter	Reporter genes	Genotype	Reference
AH109	GAL4	ADE2/ HIS3/ LacZ	*MATa trp1 leu2 ura3 his3 Gal4Δ,gal80Δ,LYS:: $GAL1_{UAS}$-$GAL1_{TATA}$-HIS3 $GAL2_{UAS}$-$GAL2_{TATA}$-ADE2 URA3::$MEL1_{UAS}$-$MEL1_{TATA}$-lacZ*	James et al., 1996 A. Holtz, unpublished

Yeast strain	Promoter	Reporter genes	Genotype	Reference
L40	LexA	HIS3/ LacZ	*MATa trp1 his3 leu2 ade2 LYS2::lexAop (4x)-His3 URA::lexAop (8x)-lacZ*	Vojtek, 1993

2. 1. 7. Bacterial strains

For cloning purposes, the E. coli strain XL1-blue was used. The E. coli strain BL21 strain was used for expression of recombinant proteins.

Ecoli strain	Genotype	Purpose	Reference
XL1-blue	recA1, endA1, gyrA96, thi-1, hsdR17, supE44v, rela1,lac$^-$[F',proAB, lacI^{q}ZΔM15,Tn10(Tet^r)]	Cloning	Bullock et al., 1987
BL21	F$^-$ ompT gal dcm lon hsdS$_B$ (r_B^- m_B^-)	Protein expression	Studier et al., 1990

2. 1. 8. Mammalian cell lines

Cells were maintained in Dulbecco's modified Eagle Medium (DMEM, PAA Laboratories) supplemented with 10% fetal calf serum (FCS), 1% penicillin/streptomycin, and 1% L-glutamine at 37℃, 10% CO_2 and 99% humidity incubator.

Mammalian cell lines	Source	Reference
HeLa	Human epithelial carcinoma cell line	Gossen and Bujard, 1992
COS-7	African Green Monkey SV40-transformed kidney fibroblast cell line	Gluzman, Y. 1981
HEK293T	Human embryonic kidney cells transformed with the SV40 Large T antigen	Lebkowski et al., 1985

2. 1. 9. Mouse strains

Mice strain		Reference
Lis1$^{wt/flox}$ and Lis1$^{flox/flox}$ mutants	CRE mediated Lis1 gene excision	Hirotsune et al., 1998

Mouse strain C57BL/6N was used for preparing wild type testis.

2. 2. Methods

2. 2. 1. Molecular biology Methods

2. 2. 1. 1. Plasmid construct

A GAL4-DBD-Lis1 fusion construct was generated to serve as a bait in the yeast two-hybrid screen. A full-length Lis1 cDNA clone (accession number #U95116, a kind gift of Prof. Eichele) was used to synthesize a Lis1 fragment by PCR with primers containing specific restriction sites (Lis1-EcoRI-5' and Lis1-SalI-3') and inserted into the pGEM-Teasy vector. The Lis1 ORF of this plasmid (termed pGEM-Teasy-Lis1) was sequenced completely and no differences to the published Lis1 cDNA were detected. Subsequently, pGEM-Teasy-Lis1 was digested with EcoRI and SalI and the Lis1 fragment was ligated into the EcoRI restriction site of the pBD-GAL4 vector. The resulting pBD-GAL4-Lis1 fusion construct was sequenced at the GSL4-Lis1 junctions to confirm its integrity.

2. 2. 1. 2. Preparation of competent cells

A fresh E. coli colony of the strain XL1-blue was incubated in 2ml of LB-Medium overnight with shaking at 37℃. 450µl of this preculture was used to inoculate 40ml LB-Medium and grown at 37℃ until an OD_{600} value of 0.3 to 0.5. The culture was chilled on ice for 10min and centrifuged at 4000rpm for 10min at 4℃. The bacterial pellet was carefully resuspended in 500µl of ice-cold Solution A. An additional 2.5ml of ice-cold Solution B was added and mixed gently. The competent cells were stored in aliquots at -70℃.

LB-Agar:
10g NaCl
10g Trypton
5g Yeast Extract
20g Agar
Add ddH_2O up to 1000ml
Adjust pH 7.0 with 5M NaOH
Autoclave

LB-Medium:
10g NaCl
10g Trypton
5g Yeast Extract
Add ddH_2O up to 1000ml
Adjust pH 7.0 with 5M NaOH
Autoclave

Solution A:
10mM MgSO4
0.2% Glucose
Add LB-Medium up to 50ml
Filtration
(prepare a fresh Solution A)

Solution B:
36% Glycerin
12% PEG 6000
12mM MgSO4
Add LB-Medium up to 100ml
Filtration
(store at 4℃ for at least several month)

2. 2. 1. 3. Ligation

A standard ligation reaction of linearized vector together with a DNA fragment digested with matching restriction enzymes was carried out as follows:

Ligation	
Vector DNA	30ng
Insert DNA	1:3 molar ratio of vector DNA to insert DNA
10x ligation buffer	1µl
T4 DNA ligase	1µl

Add dH_2O up to 10µl

Ligation was performed overnight at 16℃.

2. 2. 1. 4. Transformation

Competent bacterial cells were thawed on ice and 20-50ng of super-coiled plasmid DNA or ligated DNA was added to 100µl competent cells. This mixture was incubated on ice for 30min and the DNA was introduced into the bacterial cells via heat-shock for 90s at 42℃. 400µl LB medium lacking antibiotics was added to the bacteria and incubated at 37℃ for 30min. 100µl-250µl of the bacterial suspension was plated on LB-Agar plates containing an appropriate antibiotic allowing selection of plasmid containing cells.

2. 2. 1. 5. Purification of plasmid DNA

2. 2. 1. 5. 1. Classical mini preparation

Plasmid DNA was isolated from transformed bacteria by using the mini preparation method.

A single colony was picked and inoculated under selection conditions in 2ml LB medium overnight at 37℃. The culture then was centrifuged and the pellet was resuspended in 100µl GET buffer containing RNase A (100µg/µl). 200µl lysis buffer (0.2M NaOH and 1% SDS) was added and mixed gently by inverting. 150µl high salt buffer was added and mixed gently again. The sample was incubated on ice for 15min and centrifuged at full speed for 10min. The supernatant was transferred to a new tube and centrifuged again at full speed for 10min. The supernatant was transferred to a new tube and 900µl isopropanol was added to precipitate the DNA. The sample was mixed gently, incubated at room temperature for 15min, and then centrifuged at full speed for 10min. The DNA pellet was washed with 70% EtOH, air-dried, and resuspended in 30µl of 1× TE buffer.

GET buffer:
50mM Glucose
10mM EDTA
25mM Tris-HCl (pH 8.0)
Add ddH_2O up to 500ml
Filtration and then storage at 4℃

High-Salt buffer:
3M Potassium acetate
1.6M Formic acid
Add ddH_2O up to 500ml
Filtration and then storage at 4℃

10× TE buffer:
1M Tris (pH 8.0)
0.5M EDTA (pH 8.0)
Add ddH_2O up to 1000ml and then autoclave

2. 2. 1. 5. 2. Classical maxi preparation

To obtain plasmid DNA in large quantities and with high purity, an overnight bacterial culture of 300ml was chilled on ice and centrifuged for 15min at 6000rpm at 4℃. The pellet was washed with 100ml of dH_2O and centrifuged again. The pellet was dissolved in 40ml of cold GET-buffer. 80ml freshly prepared 0.2M NaOH/ 1% SDS was added and incubated for 5min on ice. 50ml High-Salt-buffer was added, mixed gently by inverting, and then incubated again for 15min on ice. The sample was centrifuged for 10min at 10.000rpm at 4℃ and the supernatant was filtrated through a paper filter. To precipitate plasmid DNA, 90ml isopropanol was added, incubated for 15min at room temperature, and centrifuged for 10min at 10.000rpm. The plasmid DNA pellet was air-dried and completely dissolved in 5.5ml 1× TE buffer. Caesium chloride (1.1g/ml) and 80µl ethidiumbromid (10mg/ml) were added and transferred to an ultra centrifugation tube which was filled up with Rebanding mix. Subsequently the sample was centrifuged for 24hrs at 45.000rpm (Beckman L60-ultracentrifuge, rotor 701 Ti) at room temperature. Using appropriate UV illumination, the DNA band was isolated and transferred to a fresh ultra centrifugation tube for a second centrifugation under the same conditions. Isolated plasmid DNA was mixed with an equal amount of isobutanol/ 12% H_2O to extract the ethidiumbromid out of the solution. The solution was subsequently dialyzed against 1× TE buffer for 3hrs at room temperature and then overnight at 4℃. 3M sodium acetate and 2.5 volumes of 96% cold EtOH were added to the solution, which was then incubated for 30min on dry ice allowing the DNA to precipitate. The sample was centrifuged for 30min at 3.600rpm at 4℃. The DNA pellet was washed with 70% cold EtOH, air-dried, and dissolved in 300µl of dH_2O.

Rebanding mix:
333g calcium chloride
350ml 1x TE buffer
11.3ml ethidiumbromid (10mg/ml)
Filtration and then storage at room temperature (dark)

isobutanol/ 12% H_2O:
120ml dH_2O
880ml isobutanol

2. 2. 1. 6. Quantification of DNA and RNA

The concentration of nucleic acids was determined by using an UV spectrophotometer at a wavelength of 260nm. An absorption of 1 at 260nm corresponds to a double stranded DNA concentration of 50µg/ml. The following formula was used to calculate the concentration of double stranded DNA:

$$\frac{\text{OD260 x dilution factor x 50µg/ml}}{\text{1000µg/ml}} = \text{x µg/µl}$$

In addition, the concentration of RNA and single stranded DNA also can be measured at 260nm. However an absorption of 1 at 260nm corresponds to a RNA concentration of 38µg/ml.

2. 2. 1. 7. DNA sequencing

The DNA sequencing procedure was used to confirm the integrity of open reading frames, to check the junctions of fusion protein cDNA constructs, and to identify cDNA clones isolated from the yeast two-hybrid screening. Sequencing reactions were performed by using the Big Dye terminator v1.1 cycle sequencing kit (Applied Biosystems) and a sequence-specific primer.

For 1 reaction	
250-500ng dsDNA	2μl
Premix(BD)	2μl
10pmol primer	1μl
dH_2O	5μl
Total	10μl

Sequencing condition		
Initial denaturing	94℃	2min
Denaturing	94℃	30sec
Annealing^{++}	x℃	15sec
Extension	60℃	4min
Final extension	72℃	10min
Pause	8℃	∞

$^{++}$Annealing temperature is changed depending on a specific primer.
The cycle of denaturing, annealing and extension was repeated 25 times.

Subsequently, 90μl dH_2O, 10μl 3M NaAcO (pH 5.5), and 250μl 100% EtOH were added to the sequencing reaction. The sample was incubated at room temperature for 15min and centrifuged at full speed for 15min. The precipitated DNA pellet was washed with 70% EtOH and dried under vacuum. 12.5μl template suppression reagent (Applied Biosystems) was added. The sequencing reaction was incubated at 90℃ for 2min to denature the labeled single stranded DNA which subsequently was analyzed on an ABI PRISM310 genetic analyzer (Applied Biosystems).

2. 2. 1. 8. Isolation of genomic DNA

Genomic DNA was isolated from mouse tissues using the phenol/chloroform extraction method. Dissected mouse tissues were dissolved in digestion solution at 55℃ overnight. A Phenol:Chloroform mix (1:1) was added, mixed gently by inverting several times, and centrifuged. The aqueous phase containing genomic DNA was carefully transferred to a fresh tube with an equal amount of chloroform, mixed well, and after centrifugation, was transferred into a fresh tube containing isopropanol. Precipitated DNA was collected by centrifugation, washed briefly with 70% ethanol, air-dried, and completely dissolved in 10mM Tris buffer (pH7.5) either at 60℃ for 15min or at 4℃ for overnight. The isolated DNA was used for PCR genotyping.

Digestion solution:
100mM Tris·Cl, pH 8.5
5mM EDTA
200mM NaCl
0.5% Tween 20
0.2mg/ml Proteinase K (diluted 1:500 from a 100mg/ml Proteinase K stock)

2. 2. 1. 9. PCR reaction

A standard PCR was performed as follows:

For 1 reaction	
Template	1µl
10x PCR buffer	2µl
10mM dNTP mix	1.6µl
10µM sense primer	0.5µl
10µM anti-sense primer	0.5µl
Taq polymerase	0.1µl
dH_2O	13.8µl
Total	20µl

PCR condition (for genotyping)		
Initial denaturing	94℃	10min
Denaturing	94℃	30sec
Annealing^{++}	x℃	30sec
Extension	72℃	45sec
Final extension	72℃	10min
Pause	8℃	∞

$^{++}$The annealing temperature was changed depending on the used primers.
The cycle of denaturing, annealing and extension was repeated 35 times.

For cloning purpose, a thermostable DNA polymerase with proof-reading capabilities was used (pfu polymerase, Promega).

2. 2. 1. 10. Isolation of total RNA

Total RNA was isolated from tissues and cells using the peqGold RNAPure reagent (PEQLab, cat# 30-1030). 1ml of peqGold RNAPure reagent was added to 5-10×10^6 cells grown on a 3.5cm petri dish. Cells were lysated and incubated at room temperature for 5min for dissociation of nucleoprotein complexes. 0.2ml of chloroform was added, the mixture was vigorously mixed for 15sec, and incubated on ice for 5min. The tube was centrifuged at 12000×g for 15min at 4℃. Subsequently, the upper aqueous phase was transferred to a new Eppendorf tube and an equal volume of isopropanol was added. The tube was stored at 4℃ for 15min to precipitate the RNA and centrifuged at 12000×g for 15min at 4℃. The RNA pellet was washed with 1ml of 75% ethanol, centrifuged again at 12000×g for 10min at 4℃, air-dried for 5min, and finally resuspended in DEPC-treated H_2O by incubation at 55-60℃ for 10-15min. The RNA concentration was determined using a UV-spectrometer.

2. 2. 1. 11. Reverse transcription-polymerase chain reaction (RT-PCR)

RT-PCR was performed to determine the mRNA expression level of a specific gene. For cDNA synthesis, total RNA (2µg) was isolated from a tissue of interest and used under these conditions:

Reverse Transcription (RT):

For 1 reaction	
Total RNA	2µg
Oligo$(dT)_{15}$ primer	10pmol
DEPC-D.W.	11µl

Incubation at 70℃ for 5min and then cool down on ice for 5min

For 1 reaction	
5x AMV-buffer	5ul
10mM dNTPs	2.5µl
40U RNAsin	1µl
100mM DTT	1µl
15U AMV-RT	0.6µl
DEPC-D.W.	25µl

Incubation at 42℃ for 60min

After reverse transcription, the cDNA template was amplified by PCR using gene specific primers.

2. 2. 1. 12. Annealing of oligonucleotides to complementary sequences

To anneal oligos nucleotides to complementary DNA sequences, an annealing reaction was performed:

Annealing oligos	
10µM Sense primer	10µl
10µM Antisense primer	10µl
10x NEB#3 Buffer	5µl
dH_2O	25µl
Total	50µl

The reaction was heated to 95℃ for 2min and gradually cooled down to 30℃ over a period of 45min-1hr.

2. 2. 2. Biochemistry methods

2. 2. 2. 1. Yeast two-hybrid methods

The yeast two-hybrid system was first described by Fields and song (1989) for the yeast transcription factor GAL4. The system utilizes the fact that in most eukaryotic transcription factors, DNA binding and transcriptional activation domains can be physically separated. Therefore, the GAL4-DNA binding domain can be fused to any protein of which protein interaction shall be tested. This construct is called the bait. The GAL4 activation domain then is fused to a potential interacting candidate to form the so-called prey construct. It also is possible to use an entire cDNA library containing all protein encoding sequences of a particular tissue maybe used as prey (Fields and Song, 1989; Chien et al., 1991). Recapitulation of the functional GAL4 transcription factor depends on interaction of bait and prey proteins. Expression of reporter genes harboring GAL4 upstream activating sequences (UASs) can then be stimulated.

In order to identify novel Lis1 interacting proteins from the mouse testis, the GAL4-DBD-Lis1 plasmid together with a testis cDNA library (BD Biosciences, ML4015AH) was transformed into the AH109 yeast strain using the small scale transformation method. A positive selection screening strategy was used which was based on the Gal4-dependent expression of the HIS3 and ADE2 auxotrophic makers to avoid false-positives (James et al., 1996). When a bait and prey interaction occurs, the HIS3 and ADE2 reporter genes are expressed since they both are brought under the control of a GAL4 responsive element (i.e. GAL1 promoter) in the AH109 yeast strain. Consequently, yeast cells will grow in a selection medium lacking next to histidine also adenine when an adequate protein-protein interaction leads to the activation of the two independent reporter systems.

2. 2. 2. 1. 1. Titering a mouse testis cDNA library

A mouse testis matchmaker cDNA library in E. coli cells (BD Biosciences, ML4015AH) was thawed on ice and mixed by vortexing. 2ml of the cDNA library was diluted in 30ml of LB medium without antibiotics and gently mixed by pipetting. 150µl of the diluted library was plated on LB plates (total around 200 plates) containing an appropriate antibiotic (ampicillin) and incubated overnight (18-20hrs)

at 37℃. The plates were then transferred to a 30℃ incubator and incubated additional 6hrs. 5 ml of LB medium containing ampicillin was added to each plate to collect all E. coli colonies and incubated again at 30℃ for 2hrs with vigorous shaking (200rpm). This culture was stored at 4℃ overnight and plasmid DNA was prepared by maxi preparation as described above (section 2.2.1.5.2.).

2. 2. 2. 1. 2. Yeast small scale transformation (for screening)

To prepare yeast competent cells, several 2-3mm large colonies were inoculated in 1ml of YPDA medium by vortexing to disperse any clumps. The cells then were transferred to a flask containing 50ml of YPDA medium and incubated at 30℃ for 16-18hrs with shaking (250rpm) until they reached the stationary phase (OD600>1.5). The overnight culture was transferred into 300ml of YPDA medium and incubated at 30℃ with shaking (230-270rpm) until an OD_{600} value of 0.5±0.1. The culture was transferred into 50ml tubes and centrifuged at 3600rpm for 5min at room temperature. The cell pellets were resuspended in 50ml of sterile H_2O by vigorous vortexing. Cells were centrifuged again at 3600rpm for 5min at room temperature and the pellet was resuspended in 1.5ml of sterile 1×TE/LiAc. Meanwhile 10ml of PEG/LiAc solution was prepared. 0.1ug of DNA of the binding domain/bait construct, 0.1µg of the activation domain/prey (library or interesting candidate constructs), and 0.1mg of Herring testes carrier DNA were mixed together with 0.1ml of yeast competent cells by vortexing. 0.6ml of sterile PEG/LiAc solution was added, mixed well by vortexing, and incubated at 30℃ for 30min with shaking (200rpm). 70µl of DMSO was added to the mixture by gentle inversion. Heat shock was performed for 15min at 42℃. Cells were chilled on ice and centrifuged for 5sec. The cell pellet was resuspended in 500µl of YPDA medium and plated on SD auxotrophic selection plates lacking the adenine (Ade), histidine (His), tryptophan (Tryp), and leucine (Leu) where adenine and histidine served for the selection of bait/prey interactions. The amino acids tryptophan and leucine were omitted to propagate the BD-bait and the AD-prey plasmids since these plasmids express the selection markers “Trp1” and “Leu2”, respectively. The plates were incubated at 30℃ until colonies appear.

YPDA medium:

YPDA medium is a mixture of peptone, yeast extract, and dextrose for growth of most strains of *Saccharomyces cerevisiae* (Clontech).

20g Difco peptone

10g Yeast extract

20g Agar (for plates only)

2% Glucose

Adjust the volume to 1l with dH_2O / Autoclave

SD medium:

6.7g Yeast nitrogen base without amino acids (Difco #0919-15-3)

20g Agar (for plates only)

2% glucose

100ml 10x Dropout Solution

Adjust the volume to 1l with dH_2O and then autoclave

10x Dropout Solution (-Ade/ -His/ -Tryp/ -Leu) (Media recipes, Clontech):

Nutrient	10× Conc.	Sigma Cat. #
L-Arginine HCl	200mg/L	A-5131
L-Isoleucine	300mg/L	I-7383
L-Lysine HCL	300mg/L	L-1262
L-Methionine	200mg/L	M-9625
L-Phenylalanine	500mg/L	P-5030
L-Threonine	2000mg/L	T-8625
L-Tyrosine	300mg/L	T-3754
L-Uracil	200mg/L	U-0750
L-Valine	1500mg/L	V-0500

To prepare 10x Dropout Solution (-Ade/ -His/ -Tryp/ -Leu), combine the nutrients as indicated above, but not include adenine, histidine, tryptophan, and leucine.

Herring testes carrier DNA (10mg/ml), K1606-A, Clontech

PEG/LiAc solution (polyethylene glycol/lithium acetate):

	Final Conc.	To prepare 10ml of solution
PEG 4000	40%	8ml of 50% PEG
TE buffer	1x	1ml of 10x TE (pH 7.5)
LiAc	1x	1ml of 10x LiAc (pH 7.5)

2. 2. 2. 1. 3. Protein extraction from yeast cultures

To confirm bait protein expression in yeast, the GAL4-DBD-Lis1 plasmid was transformed into the AH109 yeast strain and grown in selection medium (lacking tryptophan). Protein was extracted using the Urea/SDS method as described below. Cells (5ml) were vortexed for 30sec-1min and used to inoculate 50ml YPD medium. The culture was incubated at 30℃ with shaking (250rpm) until the OD_{600} value of 0.4–0.6. The culture was cooled down on ice, placed into a prechilled centrifuge tube, and centrifuged at 1.000×g for 5min at 4℃. The cell pellet was washed with 50ml ice-cold H_2O twice, resuspended in prewarmed cracking buffer, and transferred to a 1.5ml screw-cap centrifuge tube containing 80µl of glass beads per 7.5 OD_{600} units of cells. The sample was incubated at 70℃ for 10min, mixed vigorously by vortexing for 1min, and centrifuged at 14.000rpm for 5min at 4℃. The supernatant was transferred to a new tube and placed on ice. The remaining pellet was treated again by boiling at 100℃ for 5min and mixed vigorously by vortexing for 1min. The sample was centrifuged at 14.000rpm for 5min at 4℃. Both supernatants were combined. The protein concentration was determined by Bradford assay. 10µg from the lysate were loaded on a 10% SDS-PAGE gel, transferred onto a nitrocellulose membrane, and probed with an anti-Lis1 antibody (Sigma).

Protease inhibitor solution:

Name		To prepare 688ul	Type of protease inhibited:
Pepstatin A (Sigma #B4268)	0.1mg/ml	66ul of a 1mg/ml stock solution in DMSO	Carboxyl protease
Leupeptin (Sigma #L2884)	0.03mM	2ul of a 10.5mM stock solution	Some thiol and serine proteases
Benzamidine (Sigma #B6506)	145mM	500ul of a 200mM stock solution	Trypsin, plasmin and thrombin
Aprotinin (Sigma #B6506)	0.37mg/ml	120ul of a 2.1mg/ml stock solution	Some serine proteases
PMSF (Sigma #P7626)			Serine proteases
EDTA			Metalloproteases

PMSF (phenylmethyl-sulfonyl fluoride) 100× stock solution:
0.1742g PMSF
Dissolve in 10ml isopropanol
Warp with foil and store at room temperature

Glass Beads (Sigma #G-8772)

Cracking buffer stock solution:

		To prepare 100ml
Urea	8M	48g
SDS	5% w/v	5g
Tris-HCl (pH6.8)	40mM	4ml of a 1M stock solution
EDTA	0.1mM	20µl of a 0.5M stock solution
Bromophenol blue	0.4mg/ml	40mg
dH_2O		To a final volume of 100ml

Cracking buffer (complete):

	To prepare 1.13ml of Cracking buffer
Cracking buffer stock sol.	1ml
β-mercaptoethanol	10µl
Protease inhibitor sol.	70µl
PMSF	50µl of 100x stock sol.

2. 2. 2. 1. 4. Isolation of plasmid DNA from yeast

Plasmid DNA was isolated from yeast cells by inoculation of a single yeast colony in 5ml prewarmed high stringency selection medium (-Ade/ -His/ -Tryp/ -Leu +2% glucose). The culture was incubated at 30℃ for 16-18hrs with shaking (200rpm) and centrifuged for 1min at 3600rpm at room temperature. The cell pellet was dissolved in 75µl of yeast-suspension buffer and incubated at 37℃ for 30min. Subsequently, 425µl of yeast lysis buffer was added and transferred into an Eppendorf tube containing 400µl of glass beads. 400µl of chloropan was added and mixed for 5min by vortexing. The tube was centrifuged for 10min at 13000rpm. The supernatant containing DNA was transferred to a fresh tube, ammonium-acetate was added (final concentration of 0.4M), and DNA was precipitated with an equal

volume of isopropanol. The tube was centrifuged for 10min at 13000rpm and the DNA pellet was washed with 70% EtOH, air-dried, and dissolved in 20µl of dH_2O. The shuttle vector plasmid DNA was then transformed into competent XL1-Blue bacterial cells and incubated on plates containing ampicillin.

Yeast suspension buffer:

Component	1l
1M tris-HCl (pH 8.0)	10ml
0.5M EDTA	2ml

Adjust the volume to 1l with dH_2O
Sterilize by filtration, store at 4℃ and add Lyticase (4.5units/µl) directly before usage

Yeast lysis buffer:

Component	500ml
Triton X-100	10ml
SDS	5g
NaCl	2.9g
1M Tris-HCl (pH 8.0)	5ml
0.5M EDTA (pH 8.0)	1ml

Adjust the volume to 500ml with dH_2O
Sterilize by filtration

2. 2. 2. 1. 5. Co-transformation assay

Results from the small scale transformation assay were verified by cotransformations into yeast cells. Several controls were included in these assays. Each of the identified Lis1 binding partners linked to the activation domain of GAL4 were cotransformed into yeast strain AH109 together with Lis1 fused to the GAL4 DNA binding domain. Moreover, to assay the specificity of the GAL4-DBD-Lis1 bait construct, a fusion of the SV40 large T-antigen (*aa* 84-708) with the GAL4 activation domain served as control. In addition, a NudeL-GAL4-AD construct served as a positive control for the assay. Additionally, human Lamin C fused to the LexA DNA binding domain was used as a non-specific bait construct in combination with the identified Lis1 binding partners fused to an appropriate activation domain. These constructs were cotransformed into L40 yeast strain containing LexA-responsible auxotrophic markers. All transformed cells were plated on nonselective

and selective plates. Under selection conditions (-Ade/ -His/ -Tryp/ -Leu), cells only can grow when the Ade2 and His3 reporters are activated by protein-protein interactions.

2. 2. 2. 2. GST pull-down methods

For GST pull-down assays, one binding protein physically linked to glutathione-S-transferase (GST fusion protein) is coupled to glutathione sepharose beads which subsequently are incubated with an *in vitro* translated [S^{35}] binding partner protein. After extensive washings, to remove non-specific protein associations, specifically bound protein is separated by SDS-PAGE and detected by autoradiography.

2. 2. 2. 2. 1. Preparation of 50% slurry

Glutathione Sepharose 4B suspension (Amersham) was gently mixed by inversion and transferred to a new container in which it was centrifuged at 500xg for 5min. The supernatant was carefully removed and the pellet was washed three times by adding 10 bed volumes of cold 1× PBS. Finally, an appropriate volume of 1× PBS was added to obtain a 50% slurry.

2. 2. 2. 2. 2. Purification of GST fusion protein

pGEX recombinant plasmids were transformed into the E. coli strain BL21. A single fresh colony was inoculated in 5ml of 2× YTA medium and incubated at 37℃ for 12-15hrs. The culture was diluted 1:100 into prewarmed 2× YTA medium containing 2% glucose and cultivated at 30℃ with shaking (230-270rpm) until the culture reached an OD_{600} of 0.6-0.8. 100mM Isopropyl-β-D-thiogalactopyranosid (IPTG) was added to induce fusion protein production and incubated for an additional 3hrs. The culture was placed on ice for 10min and centrifuged at 8000rpm for 10min at 4℃. The pellet was resuspended in 20ml of an ice-cold 1× PBS. Cells were disrupted by 5 cycles of each consisting of a 30 seconds sonication period (output of 2.0 watts) followed by 1 minute cooling period on ice. To help solubilization of the fusion protein, Triton X-100 was added to the disrupted cells at a final concentration of 1%. The suspension was mixed gently on a rotating wheel for 30min at 4℃. After centrifugation at 10,000rpm for 10min at 4℃, the supernatant was transferred to a fresh container, and incubated with 200µl of a 50% slurry of

Glutathione Sepharose 4B beads on a rotating wheel for 30min at room temperature. After centrifugation at 500xg for 5min, the beads were washed carefully by inverting with 10 bed volumes of 1x PBS and centrifuged again at 500×g for 5min. The washing step was repeated twice more. The purified fusion protein was analyzed on a SDS-PAGE gel. Alternatively 200µl of elution buffer was added to the beads to elute bound protein and incubated using a rotating wheel for 10min at room temperature. After spinning at 500×g for 5min 4℃, eluted protein was transferred to a fresh tube. This elution step was repeated 3 times. Each step of eluted proteins was measured by Bradford assay.

2. 2. 2. 2. 3. *in vitro* translation

In vitro translation was performed following the instruction of the TNT Reticulocyte Lysate System from Promega, a coupled transcription/ translation system requiring SP6, T3 or T7 RNA polymerase promoters to synthesize specific proteins. In vitro translated proteins can be radiolabeled using [^{35}S] methionine and used to analyze protein-protein interactions with GST fusion proteins.

Table TnT Lysate Reactions:

Component	Standard Reaction using [^{35}S]Methionine
TnT Rabbit Reticulocyte Lysate	25µl
TnT Reaction Buffer	2µl
TnT RNA polymerase (T7)	1µl
Amino Acid Mixture, Minus Methionine 1mM	1µl
[^{35}S]Methionine	2µl
RNasin Ribonuclease Inhibitor	1µl
DNA template (0.5µg/ul)	2µl
Nuclease-Free Water to a final volume of	50µl

The reaction was incubated at 30℃ for 90 min. 5µl (10%) of the entire reaction (50µl) was loaded on a SDS-PAGE gel to monitor the translation process. It was mixed with SDS sample buffer and denatured at 95℃ for 5min. Electrophoresis was performed at 100V for 2hrs. The polyacrylamide gel was placed first in destaining solution for 1hr and then in distilled water for an additional 30min. Finally, to enhance the detection sensitivity of radiation signals, the gel was incubated in 1M

sodium salicylate solution for 1hr. The gel was placed on a Whatman filter paper, covered with saran wrap, and dried at 60℃ for 1-2hrs utilizing a vacuum gel dryer. The dried gel then was exposed on an X-ray film at room temperature.

2. 2. 2. 2. 4. GST pull- down assay

20μg of purified beads to which GST-Lis1 fusion protein had been bound were incubated with a sample of 45μl of [^{35}S] radiolabeled in vitro translated proteins on a rotating wheel over night at 4℃. To avoid unspecific binding, the beads were 3 times washed by carefully inverting with 10 bed volumes of 1× PBS and subsequent centrifugation at 500×g for 5min. Bound proteins were denatured with SDS-sample buffer and heating at 95℃ for 5min and separated on a SDS-PAGE. Dried gels were exposed on X-ray films.

Reagents for purification of pGEX recombinants:

Product	Catalog #	Company
Glutathione Sepharose 4B	17-0756-01	Amersham
TnT Coupled Reticulocyte Lysate system	L4610	Promega
Rnasin Ribonuclease inhibitor	N2111	Promega
Redivue L-[^{35}S] Methionine	AG1094	Amersham
isopropyl-β-D-thiogalactoside (IPTG)	27-3054-03	Amersham
Anti-GST antibody	27-4577-01	Amersham

2× YTA medium:
2× YT + 100μg/ml ampicillin
16g tryptone
10g yeast extract
5g NaCl in 900ml of distilled H_2O.
Adjust the pH to 7.0 with NaOH.
Adjust the volume to 1l with dH_2O
Autoclave
Add ampicillin stock solution to a final concentration of 100μg/ml

100mM IPTG:
Dissolve 500mg of isopropyl-β-D-thiogalactoside (IPTG) in 20ml of distilled H_2O
Filter-sterilize and store at -20℃

Elution buffer:
50mM Tris-HCl
10mM reduced glutathione
pH 8.0
store at -20℃
Avoid more than five freeze/thaw cycles

Destaining solution:
450ml Methanol
100ml acetic acid
450ml dH_2O

Sodium Salicylate:
32g sodium salicylate
Add 200ml dH_2O

TBST:
20mM Tris-HCl (pH 8.8)
140mM NaCl
0.1% Tween 20

2. 2. 2. 3. Coimmunoprecipitation assay

Coimmunoprecipitation allows the detection of protein-protein interactions in a tissue or a cell line and utilizes an antibody specifically binding to one of the interaction partners. Protein-G sepharose functions to "precipitate" this immune complex including proteins associated with the antibody bound antigen. Interaction partners can then be visualized by Western blot using appropriate antibodies. For this assay, Lis1 and candidate interacting proteins were subcloned into a mammalian expression vector pcDNA3.1 containing Flag or HA epitope tags.

4×10^5 of COS-7, HeLa or HEK293T cells were seeded in 6 well dishes and on the following day, cells were transiently transfected with expression plasmid of Flag tagged Lis1 and HA tagged candidate interacting proteins using Lipofectamine 2000. HA antibody coupled beads were prepared by washing of Protein G-sepharose

beads (Ezview red protein G affinity gel, Sigma) with lysis buffer and incubation with HA antibody for 2hrs at 4℃. These antibody coupled beads were washed 3times with lysis buffer. Cells were lysed by adding 100μl of lysis buffers (RIPA or 1% Triton X-100 lysis buffer containing a protease inhibitor cocktail (Roche) including 1mM EDTA. Extracts were centrifuged at 13,000rpm for 15min 4℃ for two times to remove cellular debris and incubated with 20μl of HA antibody coupled protein G-Sepharose beads using rotary agitation overnight at 4℃. Immunoprecipitates were washed with lysis buffer. Proteins were separated on a SDS-PAGE gel. Flag-tagged binding partners could be detected by an anti-Flag antibody.

Reagents for coimmunoprecipitation:

Product	Catalog #	Company
EZview Red Protein G Affinity Gel	E3403	Sigma
HA11	MMS-101R	Covance
Anti-Flag BioM2	F9291	Sigma
Streptavidin-Peroxidase	S5512	Sigma
Lipofectamine 2000	11668-019	Invitrogen
protease inhibitor cocktail tablets, EDTA-free	04 693 159 001	Roche

RIPA buffer (for NudeL, ACT and BRAP):
10% NaDoC (Deoxycholic acid Sodium salt monohydrate)
100mM Tris-HCl (pH 7.5)
20% SDS
5M NaCl
1% NP-40

1% Triton X-100 lysis buffer (for Ranbp9):
1% Triton X-100
20mM Tris-HCl (pH 7.5)
50mM NaCl
50mM NaF
15mM $Na_4P_2O_7 \cdot 10H_2O$
2mM Na_3VO_4

The protease inhibitor cocktail, EDTA free (Roche) is able to inhibit efficiently serine and cysteine proteases. Metalloproteases were blocked by the addition of EDTA (1mM).

2. 2. 2. 4. Determination of protein concentration using Bradford assay

The protein concentration was determined by Bradford assay (Bradford reagent #5000205, Biorad). A standard curve was always prepared using BSA (Bovine Serum Albumin standard set #5000207, Biorad) at different concentrations (ranging from 0.125 to 2.0mg/ml). 10ul samples were incubated with 990µl of Bradford reagent for 10min. OD values were measured using a spectrophotometer at 595nm.

2. 2. 2. 5. SDS-PAGE gel electrophoresis

SDS-PAGE gels were used to separate proteins according to their molecular weight (Laemmli, 1970). For this purpose, protein extracts were incubated in SDS-sample buffer (1.75mM Tris-HCl pH 6.8, 10.28% SDS, 36% glycerol, 0.012% bromphenol blue, 5% 2β-mercaptoethanol) at 95℃ for 5min, then cooled on ice, and centrifuged at 4℃ for 5min at full speed. Samples were loaded on the SDS-PAGE gel always together with a standard molecular weight maker. Different concentrations of acrylamide gels were used depending on the molecular weight of the proteins to be separated.

Compositions of separating SDS-PAGE gels:

Component	8%	10%	12%	15%
H_2O	2.7ml	2.45ml	2.2ml	1.825ml
4x separating buffer	1.25ml	1.25ml	1.25ml	1.25ml
40% acrylamide	1ml	1.25ml	1.5ml	1.875ml
10% APS	50µl	50µl	50µl	50µl
TEMED	2µl	2µl	2µl	2µl

Compositions of stacking SDS-PAGE gels:

Component	15%
H_2O	1.22ml
4x stacking buffer	500µl
40% acrylamide	250µl
10% APS	20µl
TEMED	2µl

Gels were run at a constant voltage of 100V. Proteins were subsequently visualized by staining with Coomassie brilliant blue solution (0.025% Coomassie brilliant blue R250, 40% methanol, 7% acetic acid in 2 liters).

2. 2. 2. 6. Western blotting

Proteins were transferred to nitrocellulose membranes using a semidry blotting apparatus (Biometra) for 2hrs at constant current of 57mA. After blotting, membranes were usually stained with Ponceau S solution (Sigma #7170) to confirm transfer efficiency. The membrane was then blocked with 5% skimmed milk powder in TBST at room temperature for 1hr and subsequently incubated with a primary antibody at 4℃ overnight (16-18hrs). The membrane was washed 3times for 10min with TBST before an appropriate the secondary antibody conjugated to horseradish peroxidase was added for 1h at room temperature. The membrane was rinsed 3 times for 10min in TBST. Enhanced Chemiluminescence (ECL)(Amersham and Thermo) following the manufacture instructions was performed and exposed to an X-ray film (Fuji). The antibody dilutions are given in section 2.1.6.

4× Separating buffer:

Component	100ml
2M tris-HCl (pH 8.8)	75ml
10% SDS	4ml
H_2O	21ml

4× Stacking buffer:

Component	100ml
1M tris-HCl (pH 6.8)	50ml
10% SDS	4ml
H_2O	46ml

10× Running buffer (pH 8.3):

Component	1l
Tris-base	30.3g
Glycine	144g
SDS	10g

Adjust the volume to 1l with dH_2O

10× Blotting buffer (pH 8.3):

Component	1l
Tris-base	30.3g
Glycine	144g

Adjust the volume to 1l with dH_2O

1× Blotting buffer (pH 8.3):

Component	1l
Methanol	200ml
10x blotting buffer	100ml
H_2O	700ml

6× SDS-sample buffer:

Component	10ml
1.75M tris-HCl (pH 6.8)	2ml
SDS	1.028g
100% glycerol	3.6ml
2β–mercaptoethanol	500µl
Bromophenol blue	0.0012g

Adjust the volume to 10ml with dH_2O

2. 2. 2. 7. Bimolecular fluorescence complementation assay

To examine the protein-protein interactions in living mammalian cells, bimolecular fluorescence complementation (BiFC) assays were performed. In principle, this technique is based on a fluorescent reporter protein which is divided into two fragments, an amino- and a carboxy-terminal part. Each fragmented reporter protein is linked to candidate binding protein partners, so that reconstitution of the fluorescent reporter protein depends on the interaction between the fusion proteins. The reconstituted fluorophore is able to emit defined fluorescent signals which can be detected by confocal microscopy or quantified by FACS (fluorescence activated cell sorting).

2. 2. 2. 7. 1. Procedure to detect the Venus fluorophore signals using a confocal laser-scanning microscopy

1×10^5 HeLa cells were seeded on 24 well plates containing sterile cover slides. After 24hrs, appropriate Venus fusion constructs of Lis1 and interaction partners were cotransfected into HeLa cells using the Lipofectamine 2000 transfection reagent (Invitrogen). 24hrs after transfection cells were washed one time with 1× PBS and fixed then by 95% ethanol in the dark for 10min at room temperature. Cells were washed with 1× PBS and subsequently nuclei were stained by 4'-6-Diamidino-2-phenylindole (DAPI) (1µg/ml) for 10min at room temperature. The cells were washed with 1x PBS and mounted using aqueous mounting medium to prevent fading of the fluorescence. The Venus fluorophore signals were analyzed using a Carl Zeiss LSM510 confocal microscopy and with 488nm laser light for excitation.

2. 2. 2. 7. 2. Procedure to quantify the Venus fluorophore signals using a FACS

1×10^5 HeLa cells were transfected as described above. 24hrs later, cells were washed with 1× PBS and detached from the wells by trypsin-EDTA in the dark. DMEM growth medium (10% FCS, 1% penicillin/streptomycin, and 1% L-glutamine) was added and cells were centrifuged at 1000rpm for 5min. The cell pellet was resuspended in FACS buffer (2% FCS in 1× PBS containing 0.5mM EDTA pH. 8.0). 10,000 cells were analyzed in the FL1 channel of a FACS machine (Becaman) able to excite and detect Venus fluorophore signal at 530nm (+/-10nm).

2. 2. 2. Cell biology methods

2. 2. 2. 1. Mammalian cell cultivation

Cells were maintained in Dulbecco's modified Eagle Medium (DMEM, PAA Laboratories) supplemented with 10% fetal calf serum (FCS), 1% penicillin/streptomycin, and 1% L-glutamine in an incubator at 37℃, 10% CO_2, and 99% humidity.

2. 2. 2. 2. Generation of immortalized mouse embryonic fibroblast cells

Primary mouse fibroblast cells (MEFs) were prepared using wild type as well as $Lis1^{wt/flox}$ and $Lis1^{flox/flox}$ embryos at embryonic day E13.5. The embryo head were collected for genotyping. After removal of the internal organs from the embryo, body tissues were used to generate immortalized mouse embryonic fibroblast cells. The tissues were mechanically dissociated by pipetting and subsequently dissociated using trypsin/EDTA. 2ml DMEM growth medium supplemented with 10% FCS, 2% chicken extract, 1% penicillin/streptomycin, and 1% L-glutamine were added to the suspension and mechanically dissociated again using a Pasteur pipette. Single cell suspensions were maintained in DMEM growth medium. To establish a stable cell line, cells were transferred every 2-3 days to a new culture dish until cells stopped dividing and underwent crisis. After then, cells were able to grow again and maintained in DMEM medium supplemented with 10% FCS, 1% penicillin/streptomycin, and 1% L-glutamine.

2. 2. 2. 3. Transfection

1×10^5 cells were seeded in 24 wells in DMEM medium supplemented with 10% FCS and 1% L-glutamine without antibiotics one day before transfection. At the following day, each of 0.8µg plasmid DNA and 2µl Lipofectamine 2000 (Invitrogen, cat# 11668-019) was diluted in 50µl of DMEM medium without FCS and antibiotics. Subsequently, both solutions were gently combined and incubated for 20min at room temperature. This mixture was directly added to the culture plate and gently mixed again. Cells were maintained at 37℃ and 10% CO_2 incubator for various time points.

2. 2. 2. 4. Adenovirus-CRE recombinase infection

0.2-0.5×10^5 cells were seeded in 24 well plates with DMEM growth medium supplemented with 10% FCS, 1% penicillin/streptomycin, and 1% L-glutamine. 24hrs later, 1.5×10^7 PFU of recombinant adenovirus able to express CRE recombinase tagged with the GFP fluorophor (AD-CRE, Vector Biolabs, cat# 1700) was diluted in DMEM growth medium. Cells were incubated with the virus diluted growth medium in a 37℃, 5% CO_2 incubator for various time points.

2. 2. 2. 5. Amplification of adenovirus

The used recombinant adenovirus (Vector Biolabs) can replicate in the HEK293T cells supplying the missing viral genes such as E1 and E3 (Graham et al., 1977). 2-3×10^5 HEK293T cells were seeded in 6 well plates with DMEM growth medium supplemented with 10% FCS, 1% penicillin/streptomycin, and 1% L-glutamine. 24hrs later, cells were incubated with 1.5×10^7 PFU virus in growth medium. The virally infected cells were harvested after 40-48hrs and centrifuged at 4000 rpm for 15min at 4℃. The supernatant was carefully removed and the cell pellet was resuspended in 2× viral storage buffer. The cells were immediately frozen on dry ice and stored at -80℃. Cells were thawed rapidly and frozen using dry ice. This step was repeated 3 times and then the tubes were centrifuged at 3200rpm for 10min at 4℃. The supernatant containing recombinant adenovirus was removed and transferred to a fresh tube. A small aliquot used to determine the viral titer.

2× viral storage buffer:
10mM Tris (pH8.0)
100mM NaCl
0.1% BSA
50% glycerol
After filtration, storage at 4℃

2. 2. 2. 6. Titration of recombinant adenovirus

Titration of recombinant adenovirus was monitored by GFP expression (He et al., 1998). 0.8×10^5 MEF cells were seeded on 24 wells with 13 mm round coverslips. At the following day, cells were infected with serially diluted samples of the virus

containing cell lysate (1, 2, 5, 7, and 10μl) (prepared as described in 2.2.2.6.) for 72hrs. After then, cells were fixed using 4% PFA for 10min at room temperature, and counterstained with DAPI (1μg/ml). The coverslips were mounted using an aqueous non-fading mounting medium to preserve the GFP fluorescence. The GFP positive cells infected by recombinant adenovirus were counted using the fluorescence microscope (Zeiss).

2. 2. 2. 7. Immunocytochemistry

1×10^5 cells were plated on 24 wells with 13mm round coverslips. Cells were washed with PBS and fixed with an appropriate fixation solution at room temperature for various time points. Cells were washed three times with PBS to remove remaining fixation solution. To reduce nonspecific antibody binding, cells were first blocked in blocking buffer (2-3% FCS in PBS) for 1hr at room temperature and then subsequently incubated with the diluted primary antibody for 2hrs at room temperature or overnight at 4℃. Cells were washed with blocking buffer and the diluted secondary antibody was added for 1hr at room temperature. Cells again were washed three times with blocking buffer. 4', 6-Diamidino-2-phenylindole, dihydrochloride (DAPI) at 1μg/ml was added for 10min to visualize nuclei. Cells were washed two times with PBS. Coverslips were mounted using an aqueous mounting medium able to prevent fading of the fluorescence.

Fixation solutions and blocking buffers in different antibodies staining on cells:

Staining	Fixation solution	Blocking buffer	1° AB	2° AB
Tagged in Hela cells (HA, Flag and eGFP)	95% Ethanol for 10min	2% FCS in PBS	1:250	1:250
Anti-goat Ranbp9 in Hela cells	4% PFA for 10min	2% FCS in PBS	1:250	1:250
Anti-mouse Lis1 in Hela cells	95% Ethanol for 10min or 4% PFA for 10min	2% FCS in PBS	1:250	1:250
Anti-mouse Lis1 in MEF cells	Methanol for 5min at -20℃ 4% PFA for 10min	0.2% Triton X-100 3% FCS in PBS	1:250	1:200
Anti-goat Ranbp9 in MEF cells	Methanol for 5min at -20℃ 4% PFA for 10min	0.2% Triton X-100 3% FCS in PBS	1:100	1:200
Anti-mouse α-tubulin in MEF cells	95% Ethanol for 10min	0.2% Triton X-100 3% FCS in PBS	1:500	1:500

Staining	Fixation solution	Blocking buffer	1° AB	2° AB
Tagged in MEF cells (HA and eGFP)	4% PFA for 10min	0.2% Triton X-100 3% FCS in PBS	1:250	1:200

Fixation solutions and blocking buffers for microtubule (MT) and MT-TIP binding proteins:

Staining	Fixation solution	Blocking buffer	1° AB	2° AB
Anti-mouse-α-tubulin	Methanol containing 1mM EGTA for 10-15min at -20℃ 4% PFA for 15-20min at RT Permeablization for 10min in 0.15% Triton X-100 in PBS	0.05% Tween 20 1% BSA in PBS	1:50,000	1:200
Anti-mouse-Glu-tubulin			1μg/μl	1:200
Anti-rat-Tyrosinated-tubulin			1μg/μl	1:200
Anti-mouse-Acetylated-tubulin			1:200	1:200
Anti-rabbit-CLIP115			1:250	1:500
Anti-rabbit-CLIP170			1:250	1:500
Anti-mouse-EB1			1:500	1:200
Anti-mouse-p150glued			1:200	1:200

2. 2. 2. 8. Staining the Golgi complex in living cells

1×10^5 cells were plated on 24 wells with sterile round cover slides. Cells were rinsed with Hanks' buffered salt solution containing 10mM HEPES (pH 7.4) (HBSS/HEPES) and incubated with 5μM BODIPY TR C_5 ceramide-BSA (Molecular Probes, B-34400) in HBSS/HEPES for 30min at 4℃. To remove remaining ceramide-BSA complexes, cells were washed three times with ice-cold growth medium and then incubated in fresh growth medium at 37℃ for an additional 30min. Cells were washed once more and fixed with 4% PFA at room temperature for 10min. After washing the cells with 1× PBS, nuclei were counterstained by DAPI (1μg/ml) for 10min at room temperature. The cells were washed with 1x PBS once more and then mounted using aqueous mounting medium containing an anti-fading agent. The signals were analyzed using a confocal microscopy and a laser at 589nm excitation.

2. 2. 3. Histology methods

2. 2. 3. 1. Paraffin section of tissues

Mouse testes were collected in 1× PBS and fixed in a solution of 4% formaldehyde in PBS at 4℃ overnight with gently shaking or rotating. Subsequently, the samples were washed with 1× PBS at 4℃ for 30min and then washed again twice with 1× TBS at 4℃ for 30min. The tissue was permeablized with 0.3% Triton X-100 in 1× TBS containing 5% BSA for 2hrs at 4℃ and washed with 1× TBS containing 1% BSA at 4℃ for 1hr. The testes were dehydrated through a EtOH series (25%-100% EtOH) and cleared in Xylenes. Subsequently, paraffin infiltration was performed with Xylene: Paraffin (1:1 dilution) at 60℃ for 1hr and then the testes were incubated in melted paraffin at 60℃ overnight. At the following day, the testes were embedded in paraffin and stored at room temperature.

Paraffin embedded sections were cut at 10μm and collected on poly-D-lysine coated slides which were dried at 40℃ for 30min and then stored at room temperature for further analysis.

2. 2. 3. 2. Immunohistochemistry

Paraffin sections were deparaffinized through Xylene and EtOH series steps. After deparaffinization, the slides were washed with PBS. Most antigens are not recognized by specific antibodies due to the fixation and the paraffin embedding procedure. For this reason, an antigen-retrieval procedure was performed. 2.4ml antigen unmasking solution (Vector Lab. Inc. #H-3300) was dissolved in 250ml H_2O and boiled in a microwave oven. When antigen unmasking solution had cooled down to 55℃, the slides were added to this solution and boiled for 3-4min in a microwave oven. Subsequently the slides were cooled down to 55℃ at room temperature and then shortly boiled again in a microwave oven. The slides were allowed to cool and then washed in PBS. To prevent non-specific antibody binding, the sections were blocked with 2% FCS in PBS containing 0.1% Tween 20 for 2hrs at room temperature and then incubated with the primary antibody (antibody dilutions are given in section 2.1.6 Antibodies) overnight at 4℃. The slides were rinsed in PBS and subsequently incubated with an appropriate secondary antibody for 2hrs at room temperature. The slides were washed in PBS and nuclei were

stained with DAPI (1μg/ml). The slides were mounted using aqueous non-fading mounting medium (Gel/Mount, cat# 17985-10). The protein expression was examined using a fluorescence microscope (Zeiss).

2. 2. 4. Image acquisition and analysis

Most of images were taken using either a fluorescence microscope (40× oil-immersion objective, Zeiss) controlled by the Metamorph software or a Carl Zeiss LSM510 confocal microscopy.

2. 2. 4. 1. Analysis of +TIP comets of CLIP-170 and CLIP-115

The fluorescence images of +TIP comets of CLIP-170 and CLIP-115 at growing microtubule plus ends was acquired using a 63× oil-immersion objective of microscope (Zeiss) controlled by the Metamorph software. The comet tail lengths of the end-decorating CLIP-170 and CLIP-115 were measured by using the NIH ImageJ program. More than 1000 comets from over 10 independent cells were examined for statistical analysis. The comet tail length of CLIP-170 and CLIP-115 is expressed by the mean ± standard deviation.

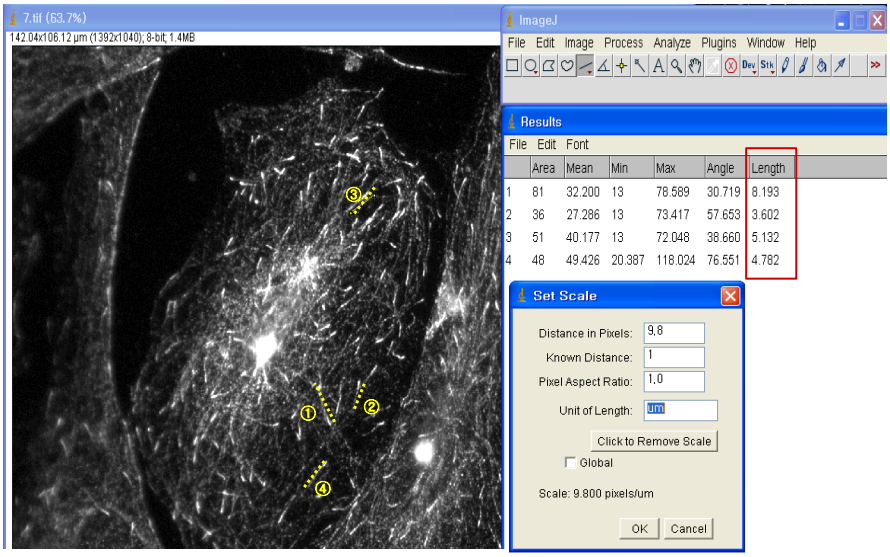

Figure 4. Analysis of comet tail lengths of the CLIP-170 and CLIP-115 in mouse embryonic fibroblast cells
To analyze 63x images of comet tail lengths of CLIP-170 and CLIP-115, the NIH ImageJ program was used in this study. For measurement of distance in pixels, the scale set up of 1μm corresponds to 9.8 pixels as descried in the reference to ImageJ.

2. 2. 4. 2. Imaging of GFP-EB1 labeled the plus-end of growing microtubules and analysis

GFP-EB1 (a kind gift of Prof. Wehland) and mCherry-CRE recombinase were transiently cotransfected into wild type and $Lis1^{flox/flox}$ MEFs using Lipofectamine 2000. 24hrs later, single cells coexpressing GFP-EB1 and mCherry-CRE were imaged every 4s for 5min using a 100× oil-immersion objective (Zeiss) controlled by the Metamorph software. Growth velocity of microtubules was determined by Metamorph software using the point segment tool. For quantitative analysis, wild type (105 MT ends in 8 cells) and $Lis1^{flox/flox}$ MEFs (75 MT ends in 5 cells) were examined. Each displayed value represents the mean value ± standard deviation. Statistical significance was evaluated by *t*-test.

3. Results

3. 1. The identification of novel interaction partners of Lis1 protein

3. 1. 1. Yeast two-hybrid screening of mouse testis

In order to investigate the cellular functions of Lis1 during spermatogenesis, I identified novel interaction partners of Lis1 using the yeast two-hybrid method. The screen was performed with a mouse testis cDNA library.

In this study, the bait vector was constructed by inserting the entire open reading frame of murine Lis1 cDNA (U95116) downstream of the GAL4 DNA binding domain (DBD) as described in detail under Material and Methods (Fig. 5A). DNA sequencing of the GAL4-DBD-Lis1 junction confirmed the continuous open reading frame (ORF). The recombinant GAL4-DBD-Lis1 fusion protein has a calculated molecular weight of 62kDa. Expression of the Lis1 fusion protein in yeast was confirmed on a Western blot (Fig. 5B).

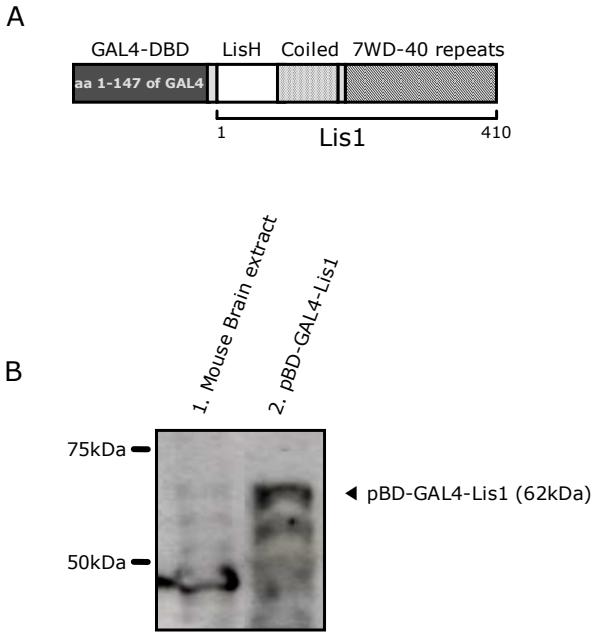

Figure 5. The Lis1 fusion protein as bait for yeast two-hybrid analysis
A. Schematic representation of the GAL4-DNA binding domain (DBD)-Lis1 fusion protein. Individual structural domains are indicated.
B. Expression of a Lis1 fusion protein in the yeast strain AH109. Proteins were identified on Western blot with α Lis1 mono clonal antibody. Lane 1: endogenous Lis1 protein (45kDa) in a mouse brain extract. Lane 2: GAL4-DBD-Lis1 fusion protein (62kDa) in yeast. Lower bands indicate some degradation.

The high stringency yeast two-hybrid screen yielded 26 positive clones (Table 1). To further characterize these clones by sequence analysis, E. coli was transformed with plasmid DNA from individual yeast clones at low DNA concentration. For each yeast clone, two individual E. coli colonies were picked, amplified, and isolated plasmid DNA was sequenced. All DNA sequences were annotated by alignments in the GenBank database (NCBI). The sequencing results confirmed that all obtained clones were in frame with the GAL4 activation domain.

Among the 26 yeast clones, 6 coded for NudeL, a protein already known to interact with Lis1. This repetitive isolation of NudeL provided good evidence that in principle the bait construct was functional in the yeast two hybrid screening. Another 6 yeast clones coded for the Ran binding protein 9 (Ranbp9). Four individual clones were isolated coding for the LIM-only protein ACT, while 3 additional clones contained sequences of BRCA1-associated protein (BRAP). Further single clones were found for tubulin alpha 3B, protamine 1, non-metastatic cells 5, ring finger protein 138, and histone H3B. Three clones could not be identified due to failing transformation or sequencing.

Since Ranbp9, ACT, and BRAP clones were independently isolated several times in the screen, their association with Lis1 protein was considered significant. Therefore, these clones were subjected to further analysis.

Table 1. List of potential Lis1 interacting proteins identified in yeast two-hybrid clones

Yeast colonies	E·coli clones	Accession	Description
A1	A1-2	NM_023668	Mus musculus nuclear distribution gene E-like homolog 1 NudeL protein
A2	A2-1 A2-2		
7	7-1		
11	11-1		
14	14-1 14-2		
18	18		
A4	A4-1 A4-2	NM_028227	Mus musculus BRCA1 associated protein (BRAP)
17	17		
22	22-1 22-2		
3	3-1	NM_019930	Mus musculus RAN binding protein 9 (Ranbp9)
6	6-1 6-2		
9	9-1 9-2		
16	16-1 16-2		
19	19-2		
20	20-1 20-2		
5	5-1 5-2	NM_021318	Mus musculus four and a half LIM domains 5 (Fhl5) LIM-only protein ACT
8	8-1 8-2		
10	10-1		
12	12-1 12-2		
A1	A1-1	NM_013637	Mus musculus protamine 1 (Prm1)
A3	A3-1	NP_542368	Mus musculus non-metastatic cells 5 (Nme5)
2	2-1	NM_009449	Mus musculus tubulin, alpha 3B (Tuba3b)
4	4-1	NM_019706	Mus musculus ring finger protein 138 (Rnf138)
13	13-2	NM_008211	Mus musculus H3 histone, family 3B (H3f3b)
1			Transformation failure
15			Sequencing analysis of failure
21			Sequencing analysis of failure

A total of 26 yeast colonies were isolated from a mouse adult testis cDNA library. Note that the number A1 yeast positive colony contained two different AD plasmids which coded NudeL and protamine whereas all other yeast colonies contained only one clone. 6 clones coded for NudeL, which is already known to interact with Lis1. 7 clones coded for Ranbp9, 4 clones coded the LIM-only protein ACT, and 3 clones coded the BRCA1-associated protein BRAP. Further single clones represented tubulin alpha 3B, protamine 1, non-metastatic cells 5, ring finger protein 138, and histone H3B cDNA. Three clones were not able to be transformed into E·coli or did not produce any readable sequence for technical reasons.

First, the size of the DNA inserts in Ranbp9, ACT, BRAP and NudeL clones was determined by digestion with restriction enzymes followed by separation on agarose gels. The pACT-AD plasmid was found at the expected size of around 8.1kb and inserts were detected ranging in size between 3530bp and 564bp (Fig. 6a). Each individual clone started at different nucleotide positions compared to the reference sequence indicating that each identified cDNA clone represented a unique protein-Lis1 interaction event (Fig. 6b).

NudeL protein consists of 345 amino acids and the N-terminus of the protein (aa 27-191) forms a typical coiled-coil structure that interacts with Lis1 protein (Toyo-oka et al., 2003). Sequencing of the identified NudeL cDNA showed that most isolated clones contained the entire coding sequence and all included the coiled-coil region in agreement with previous data on Lis1 binding (Toyo-oka et al., 2003).

Mouse Ranbp9 protein consists of 710 amino acids and contains four known structural domains referred to as SPRY (dual-specificity kinase splA and in ryanodine receptor), LisH (lissencephaly-1 like homology), CTLH (C-terminal to LisH), and CRA (or CT11-RanBPM) domains. All these motifs have been associated with protein-protein interactions (Murrin and Talbot, 2007). All but one of the isolated Ranbp9 cDNA clones included all of these domains. The single incomplete clone lacked the C-terminal CRA domain suggesting that this region is not essential for Lis1 binding.

ACT protein consists of 285 amino acids and contains 4 and a half LIM domains. LIM domains are composed of double zinc-fingers that mediate protein-protein interactions (Dawid et al., 1998; reviewed in Curtiss and Heilig, 1998). All isolated ACT cDNA clones encoded the complete 4 LIM domains but one lacked the half LIM domain located at the N-terminus suggesting that this region of the protein was not important for binding to Lis1.

Full length BRAP consists of 374 amino acids with three known domains referred to as Ring Finger, Znf-UBP, and Coiled-coil domain (Li et al., 1998). Interestingly, all identified BRAP cDNA clones only contained sequences encoding the coiled-coil domain. This coiled-coil domain shows no primary sequence homology to that of NudeL or Lis1.

A. NudeL

(a)

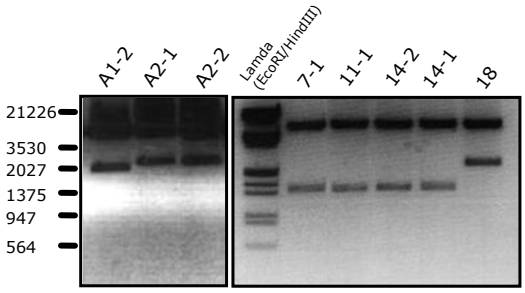

(b)

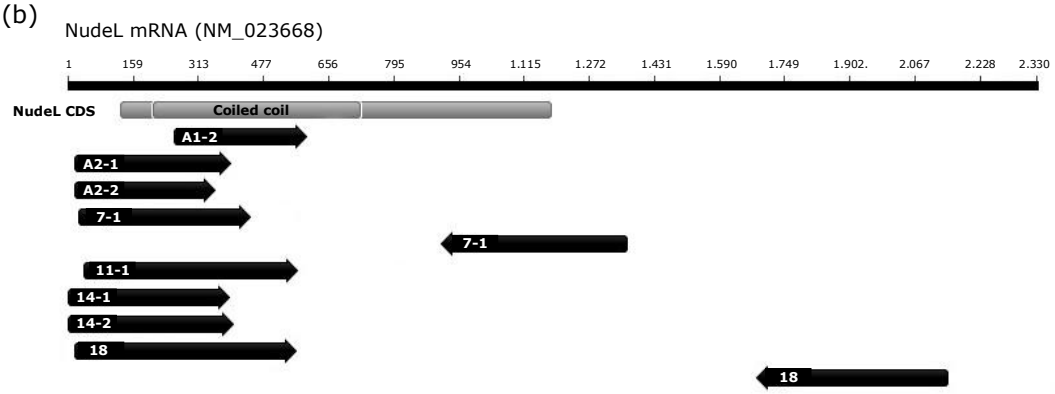

B. Ranbp9

(a)

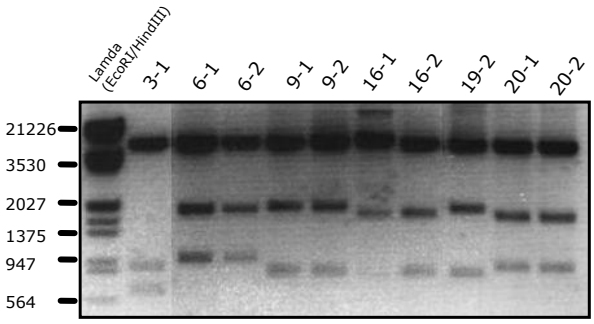

(b)

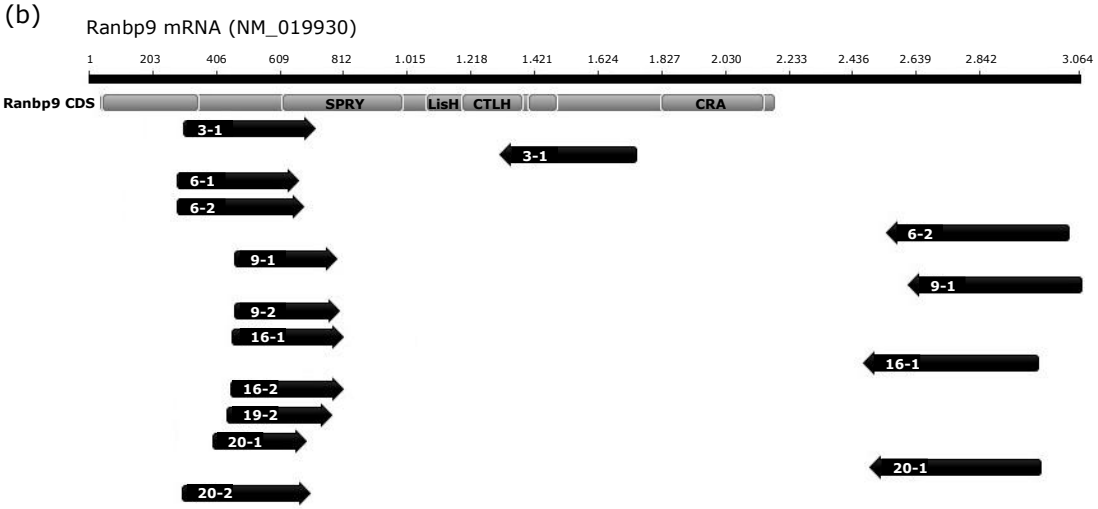

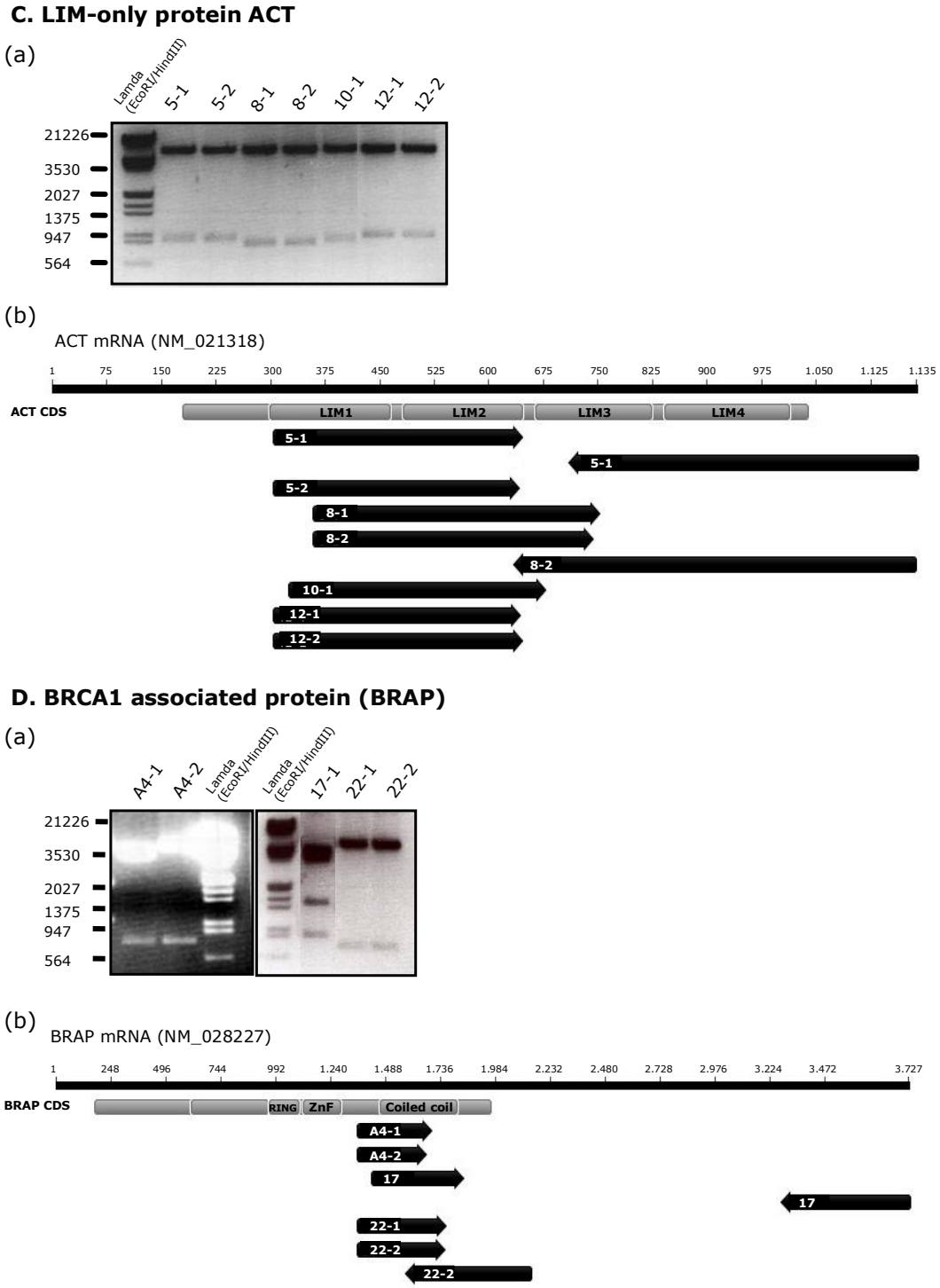

Figure 6. Analysis of the clones obtained from yeast 2 hybrid screen using restriction digestions and multiple sequence alignments

(a) The size of each individual insert of the Ranbp9, ACT, BRAP and NudeL clones was determined by digestion with EcoRI and XhoI restriction enzymes. The pACT2 plasmid has a size of 8.1Kb and the inserts ranged from 564bp to 3530bp according to the cDNA size of each clone.

(b) To confirm the exact insert size of the plasmid DNA, clones were sequenced from 5' and 3' end sides. The Blast (bl2seq) program was used for the sequence alignments of the identified clones with an according reference sequences. Each individual clone initiated at different nucleotide position of the reference sequence shown by DNA sequence analysis.

To investigate whether Lis1 indeed interacted with Ranbp9, ACT, and BRAP, the clones containing the longest cDNA inserts (#18 for NudeL, *aa* 1-345; #6-2 for Ranbp9, *aa* 40-710; #5-1 for ACT, *aa* 41-285; and #17 for BRAP, *aa* 401-592) were selected and further analyzed.

3. 1. 2. The verification of the protein-protein interaction in yeast

To verify binding of Ranbp9, ACT, and BRAP proteins to Lis1, the candidate clones and several control plasmids were cotransformed into a yeast strain with auxotrophies for several amino acids (outlined in Fig. 7). As shown in the left panel of the figure, all used bait constructs grow in the control medium lacking tryptophan. The amino acid tryptophan was omitted from the medium to propagate the bait constructs as these constructs express the selection marker, Trp1. In contrast, under selection conditions (lacking adenine, histidine, tryptophan and leucine) cells could only grow when bait and prey protein interaction occurred to overcome the requirements for adenine and histidine, due to Ade2 and His3 makers (Fig. 7, right panel).

Independent cotransformations of Lis1 and candidate clones demonstrated that Lis1 indeed interacts with Ranbp9, ACT, and BRAP (Fig. 7, right panel #3). Lis1 also bound efficiently to NudeL as has been shown previously (Toyo-oka et al., 2003 and Fig. 7, right panel #2). The specificity of the interaction was confirmed by unrelated bait proteins, such as Lamin C and SV40 large T-antigen which failed to show any interactions (Fig. 7, right panels #5 and #6).

In conclusion, the various cotransformation assays in yeast demonstrated that the proteins isolated from the yeast two-hybrid screen specifically associated with Lis1 protein but not with other unrelated baits.

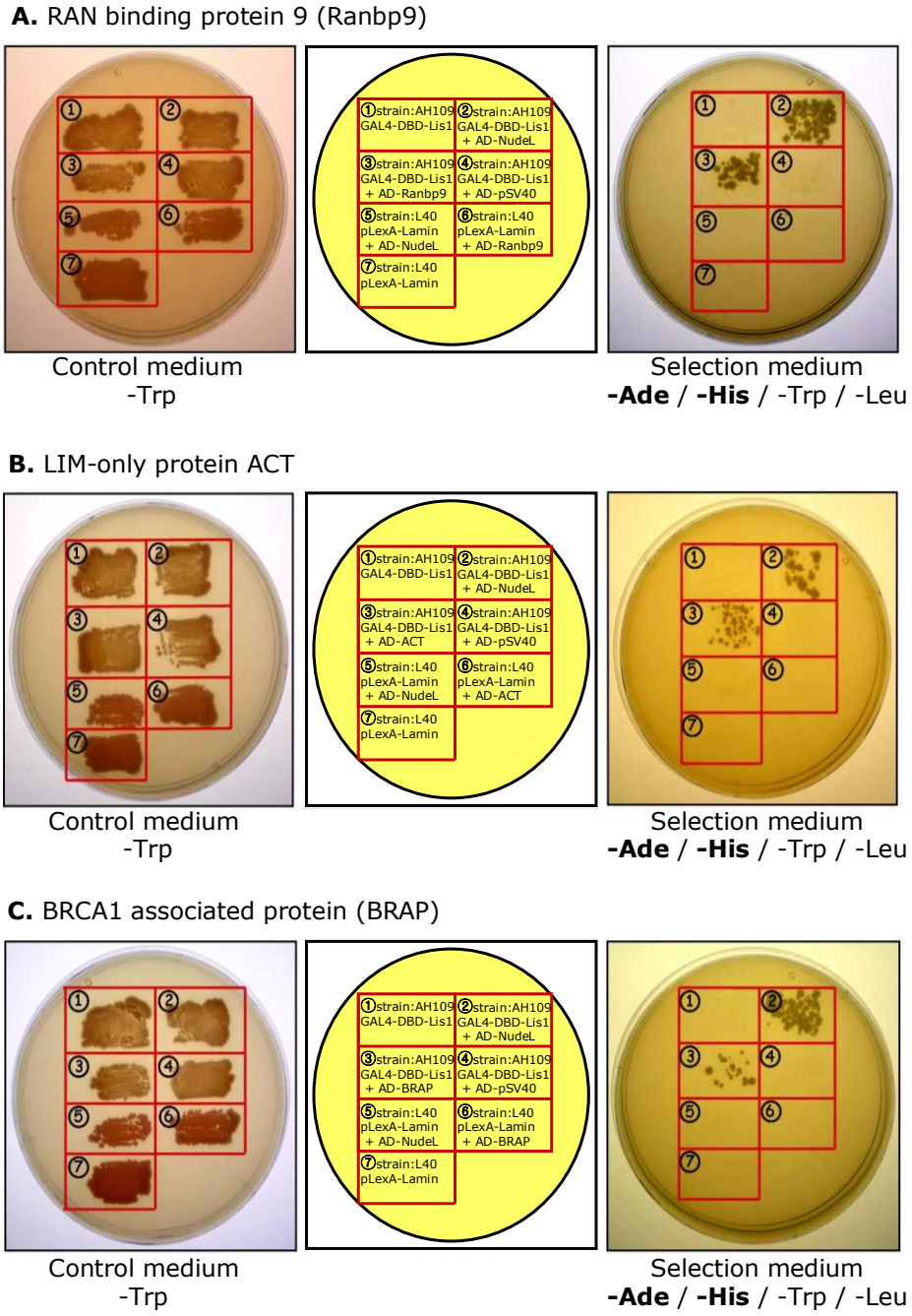

Figure 7. Verification of the Lis1-interacting clones on selection plates
The interaction of Lis1 with Ranbp9, ACT, and BRAP was investigated using selection plates lacking adenine, histidine, tryptophan and leucine. The GAL4-DBD-Lis1 and the GAL4-AD fusion of novel Lis1 candidate interaction partners were cotransformed into the yeast strain AH109 (#3). In a set of controls, the AD-psV40 served as an unrelated control GAL4 AD vector (#4) whereas NudeL used as a positive control (#2). To further investigate the specificity of interaction, the pLexA-Lamin was used as a non specific bait (#5-6). GAL4-AD fusion of novel Lis1 candidate interaction partners were cotransformed into the yeast strain L40 with pLexA-lamin (#6). Individual transformants and cotransformants respectively were plated on control medium lacking tryptophan and the selection medium lacking adenine, histidine, tryptophan and leucine. The cotransformants of Lis1 with NudeL as well as Ranbp9, ACT and BRAP (right panel, #2 and #3) grew on high stringency selection plates whereas the negative controls (right panel, #4, #5, and #6) were not able to grow under these conditions.

3. 2. Assessment of protein interactions between Lis1 and Ranbp9, ACT, or BRAP proteins in vitro

Ranbp9, ACT, and BRAP were isolated from a mouse adult testis library as putative Lis1 interacting proteins. So far, these three proteins had not been identified as interaction partners of Lis1.

Here, I present various experimental approaches to confirm the protein-protein interactions between Ranbp9, ACT, and BRAP with Lis1 as suspected from the yeast two-hybrid data described before.

3. 2. 1. GST pull-down assays

GST pull-down assays were performed using different length Lis1-glutathione-S-transferase fusion proteins to probe for protein-protein interactions. Full length Lis1 (*aa* 1-410) protein, the N-terminus of Lis1 (*aa* 1-95) containing the LisH and coiled-coil domain, and the C-terminus of Lis1 (*aa* 96-410) containing the 7 WD-40 repeat domains were separately fused to GST. In this way, the protein binding region of Lis1 that is required for the association with other proteins could be determined. All hybrid proteins and native GST protein used as control were expressed in E. coli and purified on glutathione sepharose beads. The highly enriched recombinant proteins were checked on SDS-PAGE (Fig. 8B).

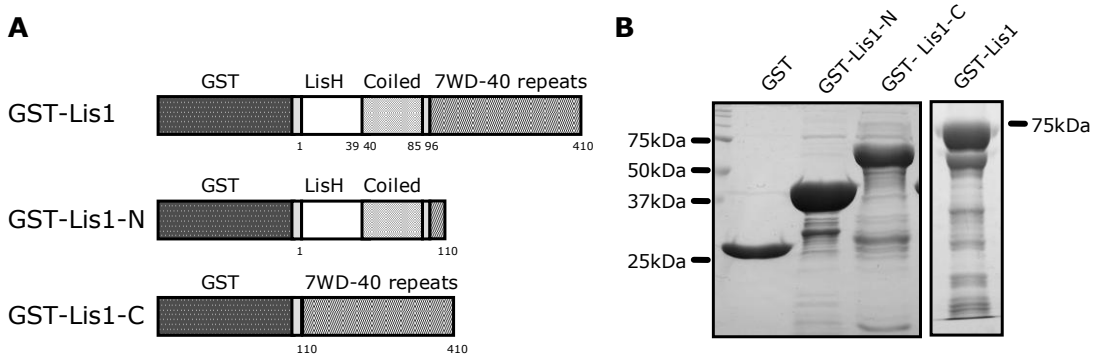

Figure 8. Expression and affinity purification of Lis1-GST fusion proteins
A. Schematic illustration of full length Lis1 GST fusion protein and two truncated forms, one containing the N-terminal LisH and the coiled-coil domains (*aa* 1-110) and the other containing the C-terminus including the 7WD-40 repeats (*aa* 110-410).
B. Purified fusion proteins (20ug) were separated on a 12% SDS-PAGE and stained with Coomassie brilliant blue. Lane1: GST (26kDa) Lane 2: GST-Lis1-N (38kDa) Lane 3: GST-Lis1-C (59kDa) Lane 4: GST-Lis1 (71kDa). Smaller bands may be due to protein degradation.

In a first experiment, full length Lis1 GST fusion protein was tested for its association with *in vitro* translated, radioactively labeled Ranbp9 (*aa* 40-710), ACT (*aa* 1-285), and BRAP (*aa* 1-374) proteins. As shown in Fig. 9, full length Lis1 binds efficiently to all three candidates. Control experiments with purified GST protein alone showed no binding confirming the specificity of these interactions. NudeL protein (*aa* 1-345) is known to interact with Lis1 and served as a positive control. These results lent further support to the idea that Lis1 interacts with the identified proteins also in the GST pull-down assay *in vitro*.

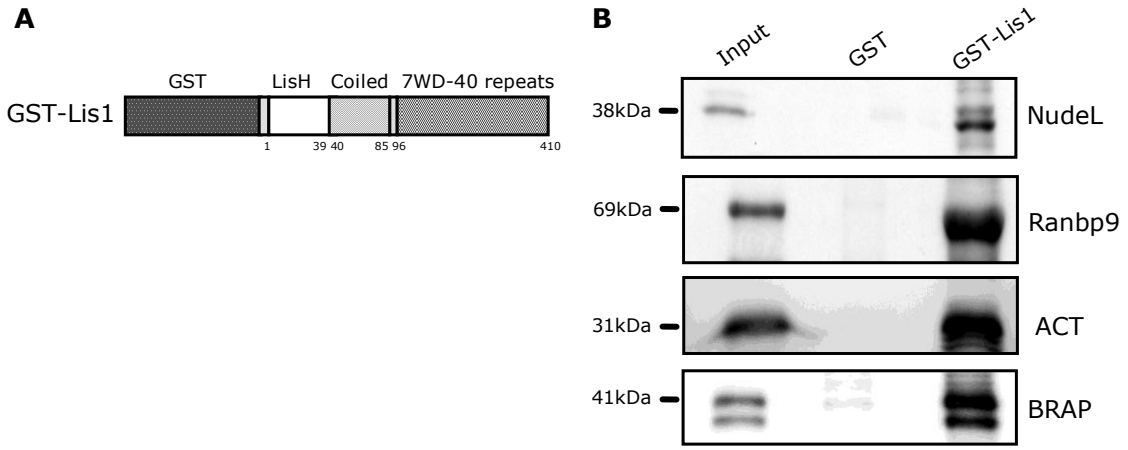

Figure 9. Lis1 binds to Ranbp9, ACT, and BRAP
A. Schematic representation of the GST-Lis1 fusion protein.
B. GST-Lis1 protein or GST protein were coupled to Glutathione-sepharose and used to pull-down *in vitro* translated [S^{35}]-labeled NudeL, Ranbp9, ACT, and BRAP proteins. Bound proteins were separated by SDS-PAGE and visualized by autoradiography. Input shows 10% of the *in vitro* translated protein used in the binding experiment. The lower band of BRAP corresponds to a second translation product using a different start codon.

3. 2. 1. 1. The seven WD-40 repeats of Lis1 is necessary for the interaction with all candidate proteins

To dissect the region of Lis1 that is responsible for the association with the binding partners, two truncated forms of Lis1 protein (GST-Lis1-N and GST-Lis1-C) were generated and used in pull-down assays. As shown in Figure 10, the C-terminus of Lis1 strongly interacted with Ranbp9, ACT, and BRAP proteins, whereas the N-terminus of Lis1 (*aa* 1-110) failed to bind Ranbp9 and ACT proteins (Fig. 10B). In contrast, BRAP protein showed some binding to the Lis1 N-terminus which was, however, much weaker than the one observed with the Lis1 C-terminus. GST protein alone was unable to pull down any of the tested proteins, as observed previously.

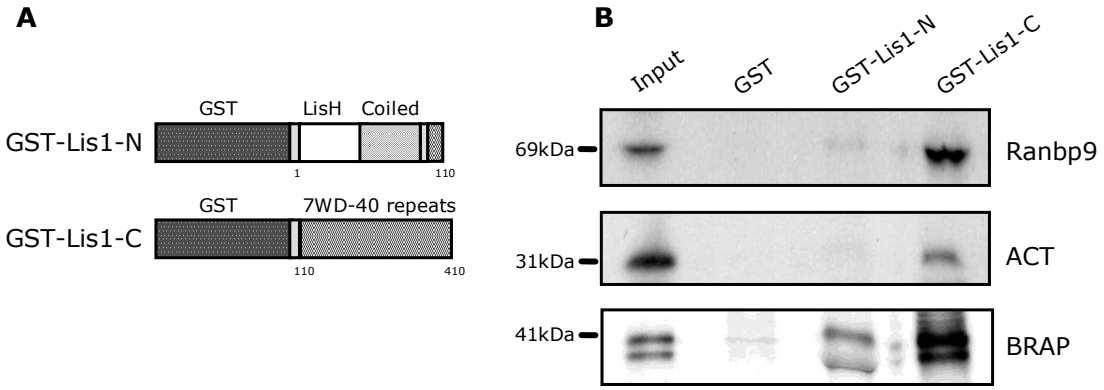

Figure 10. The C-terminus of Lis1, 7WD-40 repeats binds Ranbp9, ACT, and BRAP proteins
A. Schematic illustration of two truncated forms of Lis1 GST fusion proteins.
B. Bound proteins were separated on SDS-PAGE followed by autoradiography. Note that all proteins are pulled-down efficiently by GST-Lis1-C. The protein can be recovered with GST protein alone and GST-Lis1-N although BRAP showed a weak binding to the GST-Lis1-N. 10% of the vitro translated protein served as reference for input.

Taken together the pull-down experiments with GST fusion proteins suggested that primarily the C-terminal 7 WD-40 repeat domains mediate interactions of Lis1 with Ranbp9, ACT, and BRAP. For BRAP binding, there appears to be an additional contribution of the Lis1 N-terminus.

3. 2. 2. Bimolecular Fluorescence Complementation (BiFC) assays confirm interaction of Lis1 with Ranbp9, ACT, and BRAP in tissue culture cells

The bimolecular fluorescence complementation (BiFC) assay was performed to analyze the Lis1 protein interactions with Ranbp9, ACT, and BRAP in living cells. The principle of the method is based on a fluorescent reporter protein which has been split into two parts, the N-terminal and C-terminal fragments. Each of these separated protein fragments is unable to emit fluorescent light. However, when both fragments reassociate via fused protein domains (Fig. 11A), fluorescence can be reconstituted (Fig. 11B-C) (Morell et al., 2008). Intracellular signals can be detected by confocal microscopy which under certain circumstances allows to identify the cellular localization of the interacting proteins with high resolution. Moreover, fluorescence activated cell sorting (FACS) can be used to quantify protein interactions in a cell population. In this study, the YFP derivative Venus fluorophore (a kind gift of Dr. S. Illenberger) was utilized for the BiFC assay.

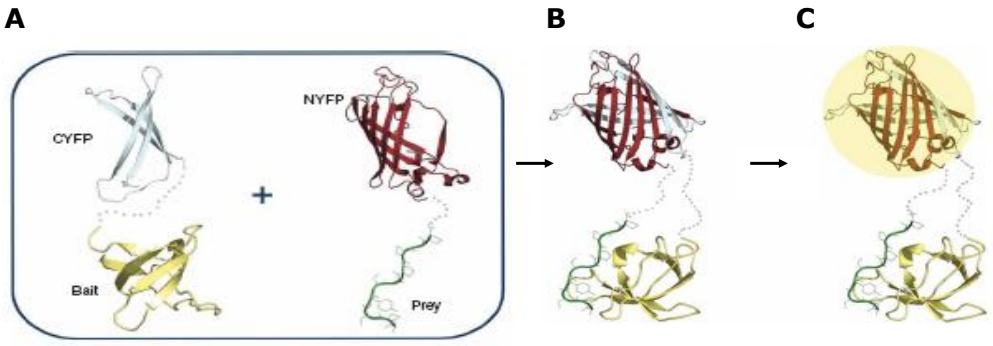

Figure 11. Principle of the bimolecular fluorescence complementation assay
A. A bait protein is fused to the C-terminus of YFP fluorescence reporter protein (CYFP) and a prey protein is linked to the N-terminus of YFP (NYFP).
B-C. When bait and prey interact, the YFP fluorescence reporter protein is reconstituted and is able to emit fluorescence upon activation with laser light of λ=488nm. (adapted in Morell et al., 2008)

In a first step, full length Lis1 (*aa* 1-410) and the identified Ranbp9 (*aa* 40-710), ACT (*aa* 1-285), and BRAP (*aa* 1-374) proteins were linked to the amino- and the carboxyl-terminal fragments of the Venus fluorophore, respectively, by molecular cloning (Fig. 12). Expression of these hybrid proteins in HeLa cells was confirmed on a Western blot using antibodies against Flag and HA protein tags that were part of the various constructs (data not shown).

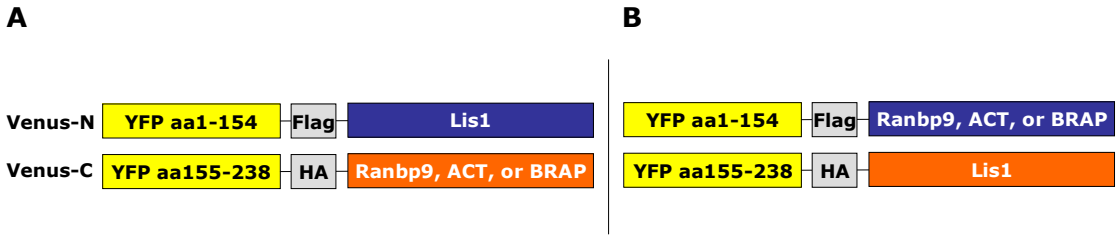

Figure 12. Schematic representation of Venus fusion proteins
cDNAs for Lis1 and all identified proteins were cloned into the multiple cloning sites of Venus-N and Venus-C vectors. Venus-N vector contains the N-terminus of Venus (*aa* 1-154) and can also be recognized by its Flag-tag. Venus-C consists *aa* 155-238 of the Venus fluorophore followed by an HA epitope tag.

3. 2. 2. 1. The detection of protein-protein interactions using confocal microscopy

Combinations of the amino- and carboxyl-terminal portions of the Venus fusion proteins were transiently expressed in HeLa cells (Fig. 13). When only the amino and carboxyl parts of Venus fluorophore were expressed, no fluorescent cells could be detected (Fig. 13A). Clearly, the sole overexpression of both fluorophore fragments was not sufficient to reconstitute a stable and active structure of the Venus fluorophore. Likewise, combining Venus-N or Venus-C fragments alone with any of the Venus fusion proteins also did not generate fluorescent cells (Fig. 13 I and J). However, overexpression of the Venus-N-Lis1 with Venus-C-Lis1 enabling Lis1 homodimerization (Cahana et al., 2001) allowed the detection of strongly fluorescent HeLa cells (Fig. 13 B). Fig. 13 shows that the Lis1-dimers are exclusively present in the cytoplasm and spare the nucleus as described before (Cahana et al., 2001). These results provide good evidence for Lis1 interaction in HeLa cells detected by the bimolecular complementation assay of the Venus fluorophore. Moreover, using the lambda scanning ability of a Zeiss LSM confocal microscope, the maximum emission wavelength of the observed fluorescent signal was determined to be at λ=520-530, consistent with the reconstituted Venus signal (emission maximum at 528nm) (data not shown). Most interestingly, the coexpression of Venus-N-Lis1 and Venus-C-Ranbp9, Venus-C-ACT, and Venus-C-BRAP in HeLa cells also generated fluorescent cells with similar absorption spectra (Fig. 13 C, E, and G). Comparable results were obtained when Venus-N-Ranbp9, Venus-N-ACT, and Venus-N-BRAP and Venus-C-Lis1 were coexpressed (Fig. 13 D, F, and H). The Lis1-Ranbp9 interaction signal was always detected in the cytoplasm suggesting the cytoplasmic localization of this protein-protein complex. The Lis1-ACT protein interaction also seemed to occur predominantly in the cytoplasm of HeLa cells, although ACT alone is frequently found in the nucleus of spermatids (Fimia et al., 1999). Lis1-BRAP protein interaction was also mainly seen in the cytoplasm including some punctate signals in the perinuclear region.

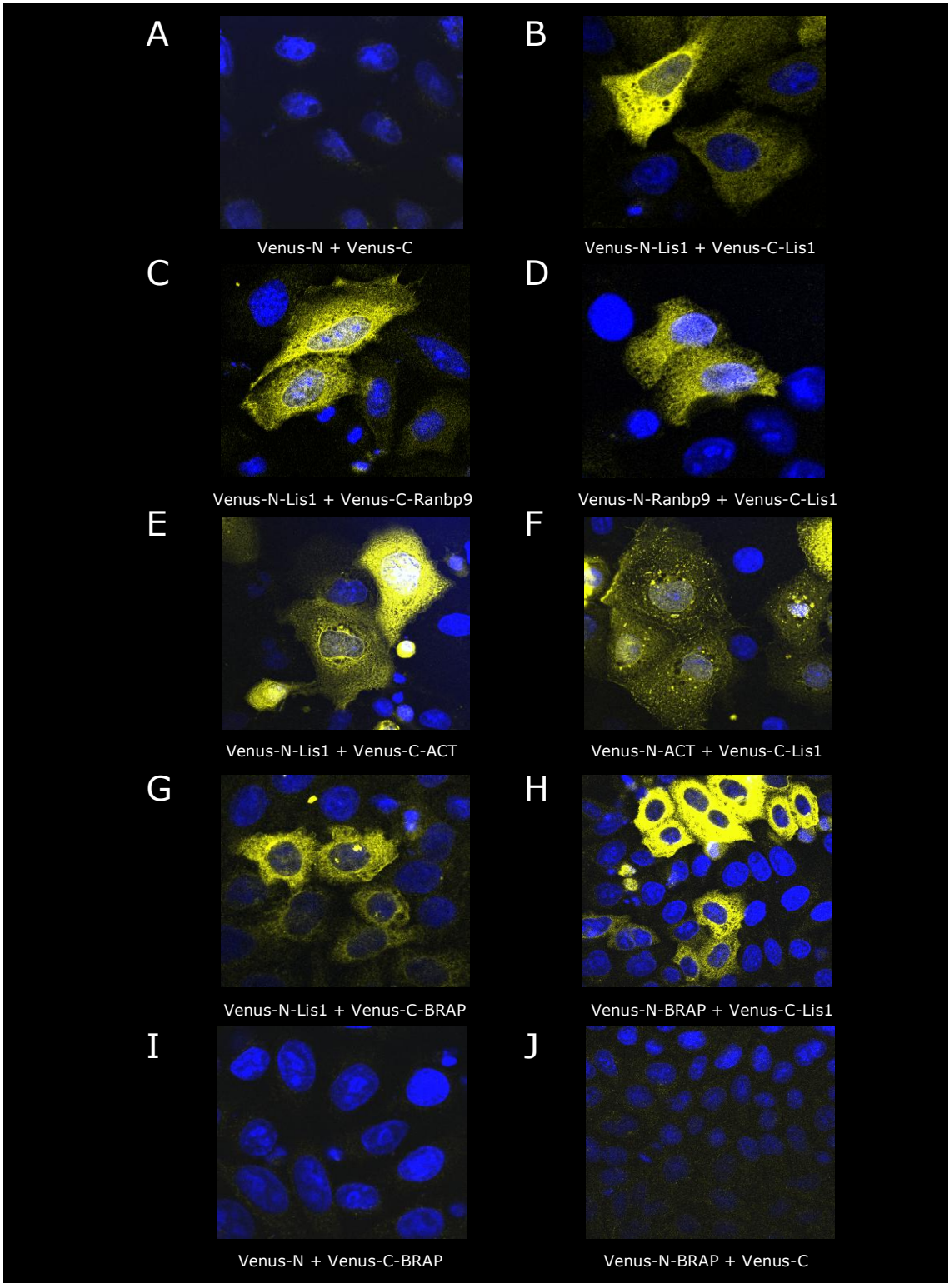

Figure 13. Lis1 interaction with Ranbp9, ACT, and BRAP proteins in HeLa cells demonstrated by BiFC assay HeLa cells were transiently cotransfected with expression plasmids for Venus-N and Venus-C (A), and the indicated combination of Venus-N and Venus-C fusion proteins with Lis1 (B), Ranbp9 (C, D), ACT (E, F), and BRAP (G, H). Note the yellow YFP signals that the Venus fluorophore has been reconstituted by protein-protein interactions. Cells were analyzed by confocal microscopy. Blue nuclei were stained with DAPI. Background was determined in cells transfected with Venus-N-BRAP protein and Venus-C terminus or vice versa (I, J).

3. 2. 1. 2. Protein-protein interactions in cells were quantified by FACS analysis

For better quantitative analysis, Venus fluorophore activation was measured by FACS analysis (Fig. 14). Fluorescence intensity and the cell size were determined and dots in the G1 quadrant indicated cells with protein-protein interactions. As expected, coexpression of amino- and carboxyl- termini of Venus showed essentially no protein interaction with background signals in about 0.6% of cells. In agreement with the results of the confocal microscopy, transient overexpression of Venus-N-Lis1 and Venus-C-Lis1 caused a significant number of cells (18.3%) to emit fluorescence. Coexpression of Venus-N-Ranbp9, Venus-N-ACT, and Venus-N-BRAP together with Venus-C-Lis1 caused Venus fluorescence in 9.4% to 16.5 % of cells. In contrast, only few fluorescent cells were detected when the Venus-N-Ranbp9, ACT, or BRAP fusion proteins were coexpressed with Venus-C alone used as negative control.

In summary, these results provide first evidence that Lis1 is able to associate with Ranbp9, ACT and BRAP in living mammalian cells. The site of the formation of these stable complexes seemed to be predominantly in the cytoplasm.

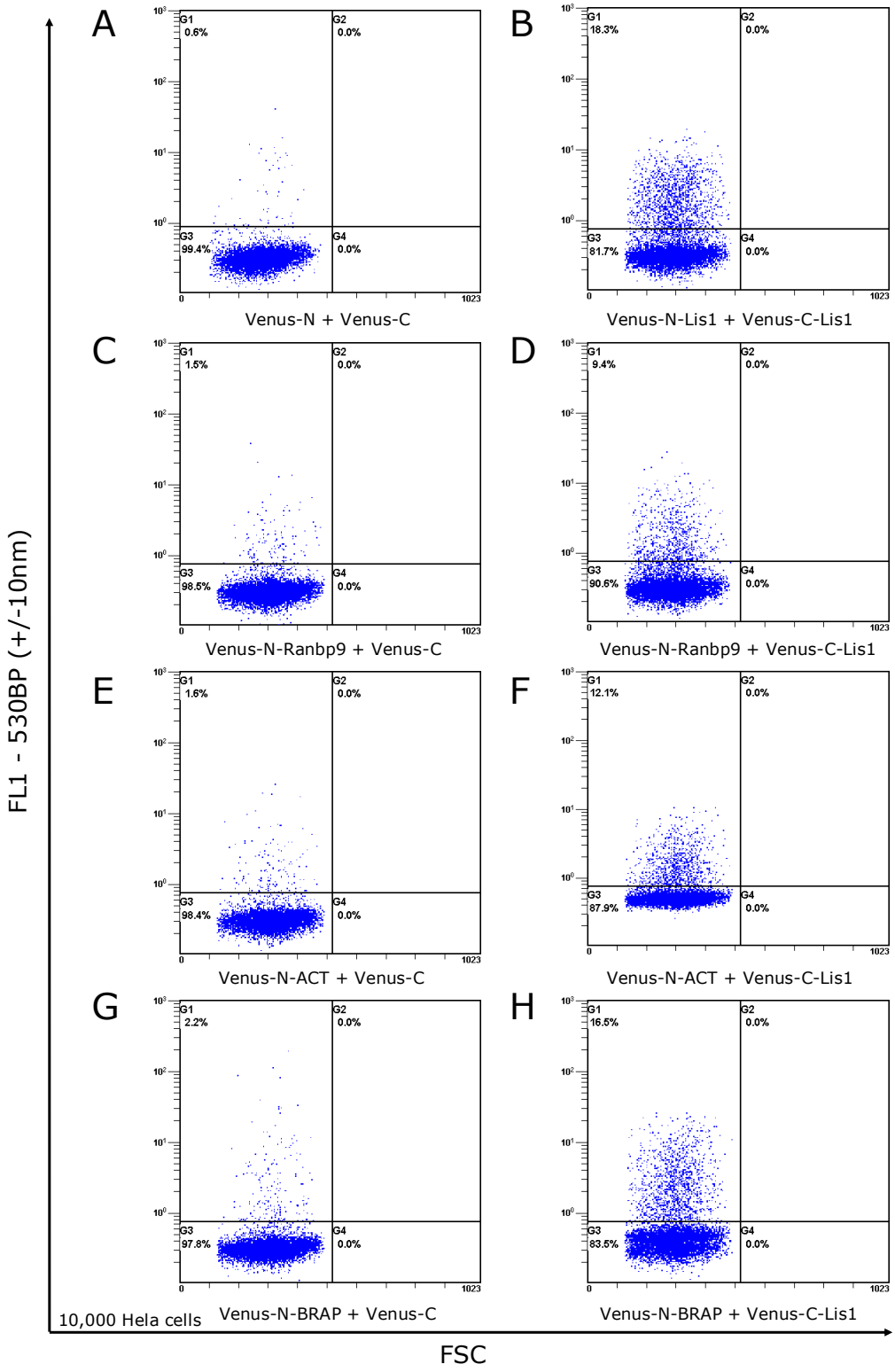

Figure 14. Lis1-Ranbp9, ACT, or BRAP protein interaction demonstrated in HeLa cells by BiFC assay

FSC (Forward scatter) is used to identify the cell size while the emitted Venus fluorescent signal was detected at 530nm (+/-10nm) using the FL1 (Fluorescent green light) channel. The G1 quadrant shows the percentage of the cells emitting YFP signals as a result of protein-protein interactions. 10,000 viable HeLa cells were analyzed by FACS.

3. 2. 3. Mutational analysis of individual binding domains in Lis1 interacting proteins

The previous experiments showed that the 7 WD-40 repeat domains of Lis1 were required for the association with Ranbp9, ACT, and BRAP. To identify the regions of Ranbp9, ACT, and BRAP that are essential for the interactions with Lis1, truncated versions of each of these proteins were used in various binding assays.

3. 2. 3. 1. Ranbp9 binds to Lis1 via the SPRY domain

First, the BiFC assay was performed with two truncated forms of Ranbp9, containing either *aa* 40-393 covering most of the amino terminus of Ranbp9 with the SPRY and LisH domains or *aa* 394-710 containing the CTLH and CRA domains. Either of these coding regions were fused to the carboxy-terminus of the Venus fluorophore. Expression levels of the fusion proteins in HeLa cells were determined on Western blots (Fig. 15A).

The BiFC experiments showed that the N-terminal *aa* 40-393 of Ranbp9 protein are sufficient to mediate the interaction with Lis1, while the C-terminus failed to form complexes (Fig. 15). This suggests that the SPRY and/or the Lis1H domains are the key for the association with Lis1 protein. Apparently, the CTLH and the carboxyl-terminal CRA domains of Ranbp9 are not required for the interaction. Interestingly, the isolated amino terminal part of Ranbp9 interacted significantly more efficient with Lis1 than the full length Ranbp9, based on the observed mean fluorescence intensity and the frequency of fluorescent cells (Fig. 15).

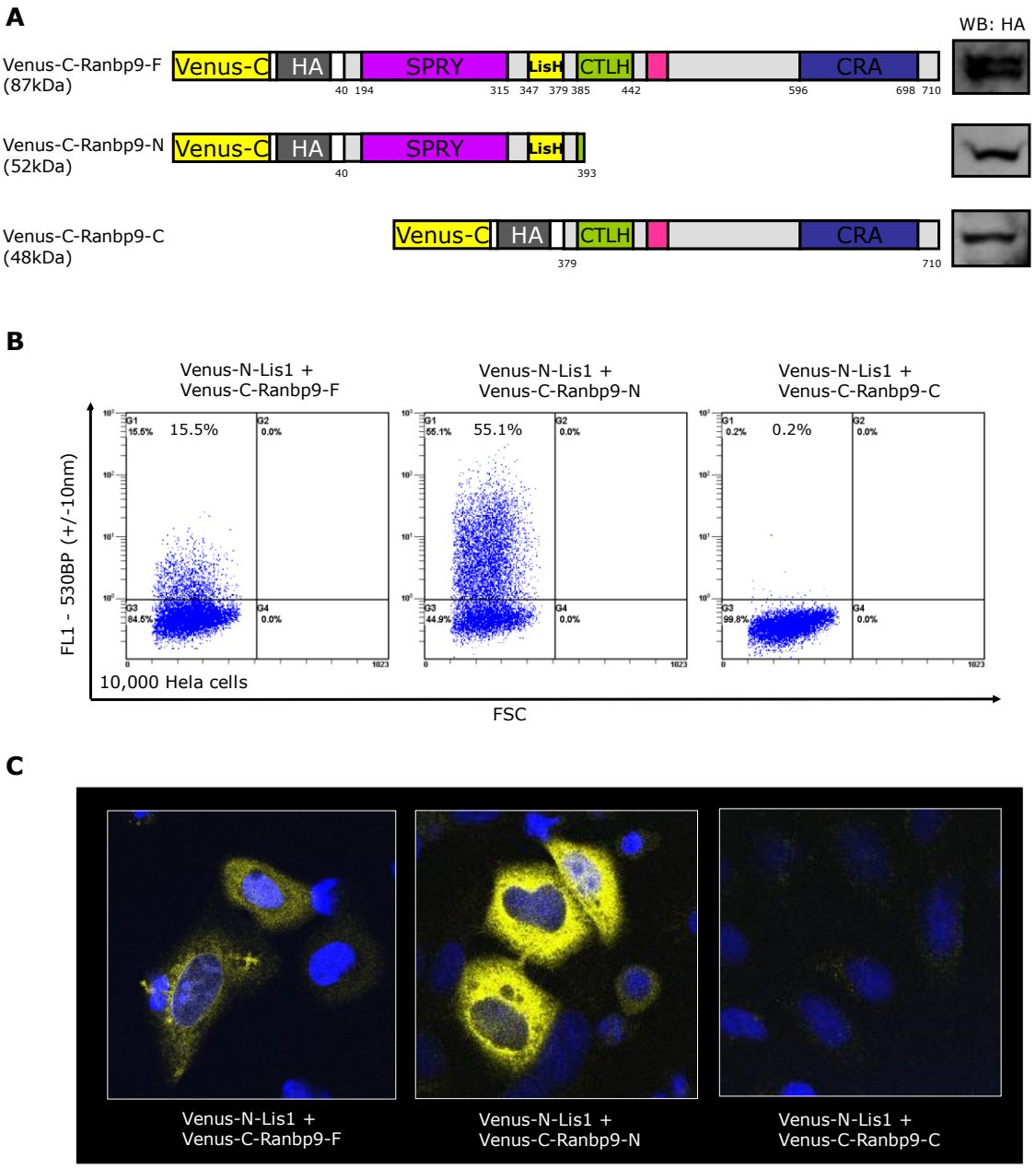

Figure 15. Lis1 binds to N-terminus of Ranbp9 protein
A. Schematic illustration of the used Ranbp9 expression constructs all of which were fused to the carboxy terminal fragment of the Venus fluorophore. All constructs were expressed in HeLa cells and proteins expression was detected by Western blotting using HA antibody (right side).
B-C. Interaction between Lis1 and Ranbp9 truncations were demonstrated by BiFC assay. HeLa cells were transiently cotransfected with indicated combination of Venus-N-Lis1 and Venus-C fusion proteins with Ranbp9, Ranbp9-N or Ranbp9-C. The cells emitting YFP signals as a result of protein-protein interactions were analyzed by FACS using the FL1 channel (B) and confocal microscopy (C).

To obtain confirmation and to extend the finding that the N-terminus of Ranbp9 was required and sufficient to mediate the association with Lis1, co-immunoprecipitation (Co-IP) assays were performed. A set of Ranbp9 truncations was prepared by molecular cloning, all of which were fused to the HA epitope (Fig. 16). Similarly, Lis1 was tagged with Flag epitope. Overexpression of these constructs in HEK293T cells allowed to perform Co-IPs in which full length Lis1 protein was tested for the association with various fragments of Ranbp9 protein (Fig. 16A). The Co-IP experiments confirmed the previous results that Ranbp9-N terminus (*aa* 40-710) binds to Lis1 protein (Fig. 16B lane2). Moreover Lis1 coimmunoprecipitated with the SPRY+LisH containing fragment (*aa* 40-393) from transfected HEK293T cells, but not with the CTLH+CRA domains (*aa* 379-710) (Fig. 16B lane 3 and 4). These observations argue that only the amino terminal region of Ranbp9 is required for binding of Lis1.

To elucidate which of the two potential binding domains, LisH or SPRY of Ranbp9 mediates the interaction with Lis1, Co-IP assays were performed with appropriate expression constructs. As shown in Fig. 16C, the Co-IP experiments confirmed that the N-terminus of Ranbp9 associates with Lis1 protein. Interestingly, Lis1 coimmunoprecipitated with the single SPRY domain but not with the LisH+CTLH suggesting that the SPRY domain of Ranbp9 alone is sufficient for binding. Moreover, this data indicates that both proteins do not interact via their LisH motifs.

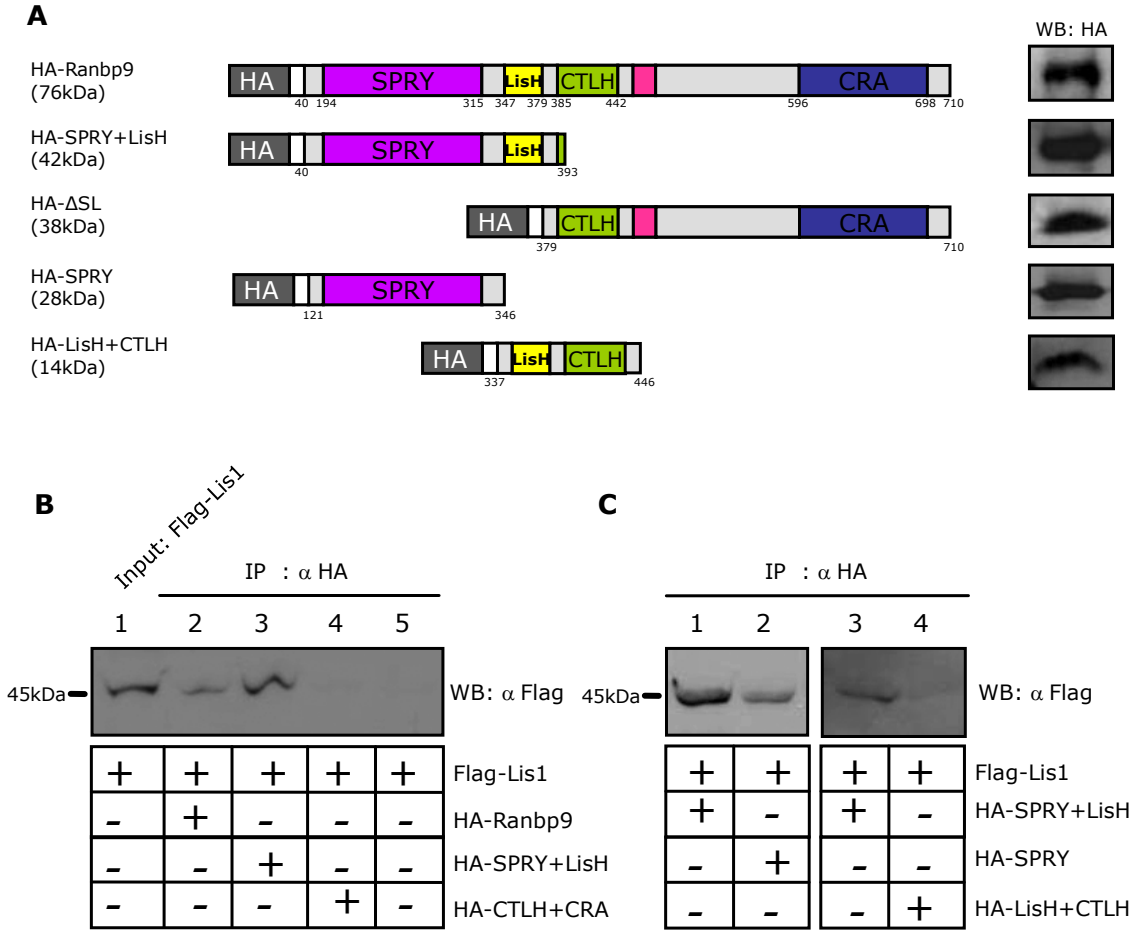

Figure 16. Ranbp9 binds to Lis1 via the SPRY domain
A. Schematic representation of Ranbp9 expression constructs which all were in frame with an amino-terminal HA epitope. The expression of these Ranbp9 deletions in HEK293T cells was detected on Western blots using an HA antibody specific for the HA epitope.
B-C. HEK293T cells were cotransfected with expression plasmids for Flag-Lis1 and HA-Ranbp9 truncations. 24hrs after transfection, the cell lysates were subjected to immunoprecipitation with HA antibody. Protein interactions were analyzed by Western blots with Flag antibody. Input shows 10% sample of Flag-Lis1 protein used in the binding assay (B. Lane1). Lis1 was able to interact with Ranbp9 and the N-terminal region (SPRY+LisH) (B. Lane 2 and 3; C. Lane 1 and 3) but not with the C-terminal region (CTLH+CRA) (B. Lane 4). Moreover, Lis1 bound to the SPRY domain (C. Lane 2), but not to the LisH+CTLH domains (C. Lane 4). A control experiment with Flag-Lis1 alone showed no signal demonstrating the specificity of this assay (B. Lane 5).

3. 2. 3. 2. The 4 complete LIM domains of ACT are required for interaction with Lis1

ACT contains four and a half LIM domains. The third LIM domain has been suggested to be important for interaction with CREM (Fimia et al., 1999), while all LIM domains are necessary for interaction with KIF17b (Kotaja et al., 2005). Interestingly, all ACT clones isolated in the yeast two-hybrid assay contained four intact LIM domains (*aa* 41-285), but lacked the half LIM domain. To further define the domains necessary for Lis1 binding, various mutant forms of ACT protein were tested in coimmunoprecipitation (Co-IP) assays with Lis1 protein.

Truncated forms of ACT were fused to the HA epitope and transiently expressed in COS-7 or HEK 293T cells together with Lis1 tagged with the Flag epitope. The expression of all proteins was monitored by Western blotting (Fig. 17A).

The Co-IP experiments verified the protein interaction of the four complete LIM domains of ACT excluding the half LIM domain (*aa* 41-285) with Lis1 protein (Fig. 17B). Also, full length ACT (*aa* 1-285) coimmunoprecipitated with Lis1 from transfected HEK293T cell extracts. In contrast, none of the truncated LIM domain constructs was able to associate with Lis1 (Fig. 17C). This data suggests that all complete LIM domains of ACT are required for the interaction with Lis1, probably via the 7 WD-40 repeats.

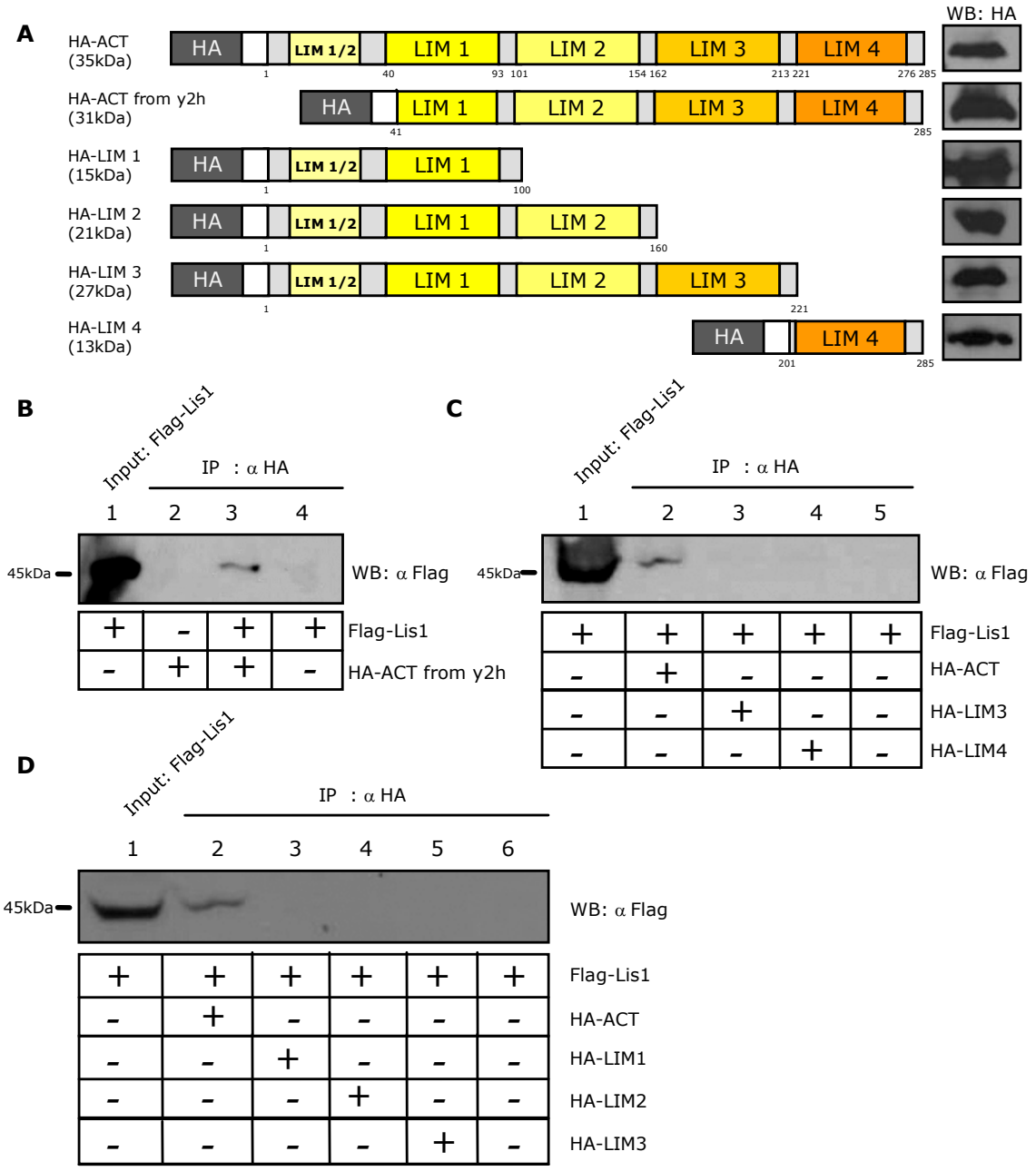

Figure 17. The intact 1-4 Lim domains of ACT are required for interaction with Lis1
A. Schematic illustration of ACT truncations. All ACT constructs were tagged with the HA epitope and expressed in COS-7 or HEK293T cells and the protein expression were detected on Western blots using HA specific antibody.
B-D. COS-7 or HEK293T were cotransfected with different combination of Flag tagged Lis1 and HA tagged ACT truncations as indicated. 24hrs after transfection, the cell lysates were immunoprecipitated with HA antibody and immunoprecipitates were separated on SDS-PAGE and analyzed by immunoblotting with Flag antibody. 10% sample of Flag-Lis1 protein used in the binding assay was served as input (B-D. Lane1). Lis1 was sufficient to interact with the intact 4 LIM domains (B. Lane 3) and full length ACT protein (C-D. Lane 2). However a series of truncated forms of the LIM domains did not show any binding to Lis1 protein (C. Lane 3 and 4; D Lane 3, 4, and 5). A control experiment with either Flag-Lis1 or HA-ACT (derived from the yeast two-hybrid screen) alone did not illustrate any signals demonstrating the specificity of this assay (B. Lane 2 and 4; C. Lane 5; D. Lane 6).

3. 2. 3. 3. Complex formation of Lis1 and BRAP involves the coiled-coil domain of BRAP

The full length BRAP (BRAP) protein contains 374 amino acids and three known distinct domains (Fig. 18A). Interestingly all BRAP clones isolated in the yeast two-hybrid screen encoded only the carboxy-terminus of BRAP with the coiled-coil domain (Section in 3.1.1. Fig. 6D). Only one study so far described the C-terminal region of BRAP to be involved in the association with a binding partner (Asada et al., 2004). Since the interaction of Lis1 with the coiled-coil domain of BRAP was already seen in yeast, it seemed very likely that only this BRAP domain was involved in Lis1 binding. Similar to experiments described above for Ranbp9 and ACT, I investigated the Lis1 and BRAP association in COS-7 cells by Co-IP assays. First, the coiled-coil domain of BRAP (cBRAP) was fused to the HA epitope and its expression was confirmed on a Western blot (Fig. 18A). Co-expression of HA-cBRAP together with Flag-Lis1 revealed that the coiled-coil domain of BRAP alone was sufficient for interaction with Lis1 protein (Fig. 18C).

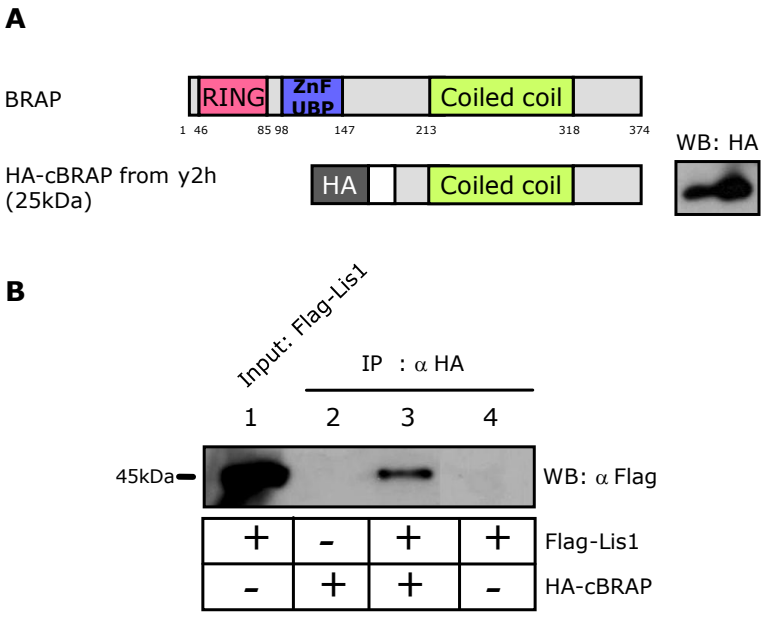

Figure 18. The C-terminal, Coiled coil domain, associates with Lis1
A. Schematic illustration of the BRAP construct. Overexpressed HA tagged coiled-coil domain of BRAP was analyzed from COS-7 cell lysate by Western blot with a HA specific antibody.
B. The expression plasmids for Flag-Lis1 and HA-cBRAP were coexpressed in COS-7 cells and 24hrs after transfection, the cell lysates were immunoprecipitated with HA antibody. Protein interactions were verified by Western blots with a Flag specific antibody. 10% input illustrates the sample of Flag-Lis1 protein used in the binding assay (B. Lane1). The specificity of this assay was demonstrated by control experiment with either HA-cBRAP or Flag-Lis1 alone showing no signals (B. Lane 2 and 4).

Also a BiFC assay confirmed this result (Fig. 19). Lis1 and cBRAP proteins fused to Venus-N and Venus-C fragments, respectively, were transiently coexpressed in HeLa cells and produced fluorescent cells with an emission wavelength of λ=520-530nm. Protein interaction was detected in the cytoplasm. Interestingly, punctate signals were also observed in the perinuclear region similar to the results obtained with the full length BRAP protein.

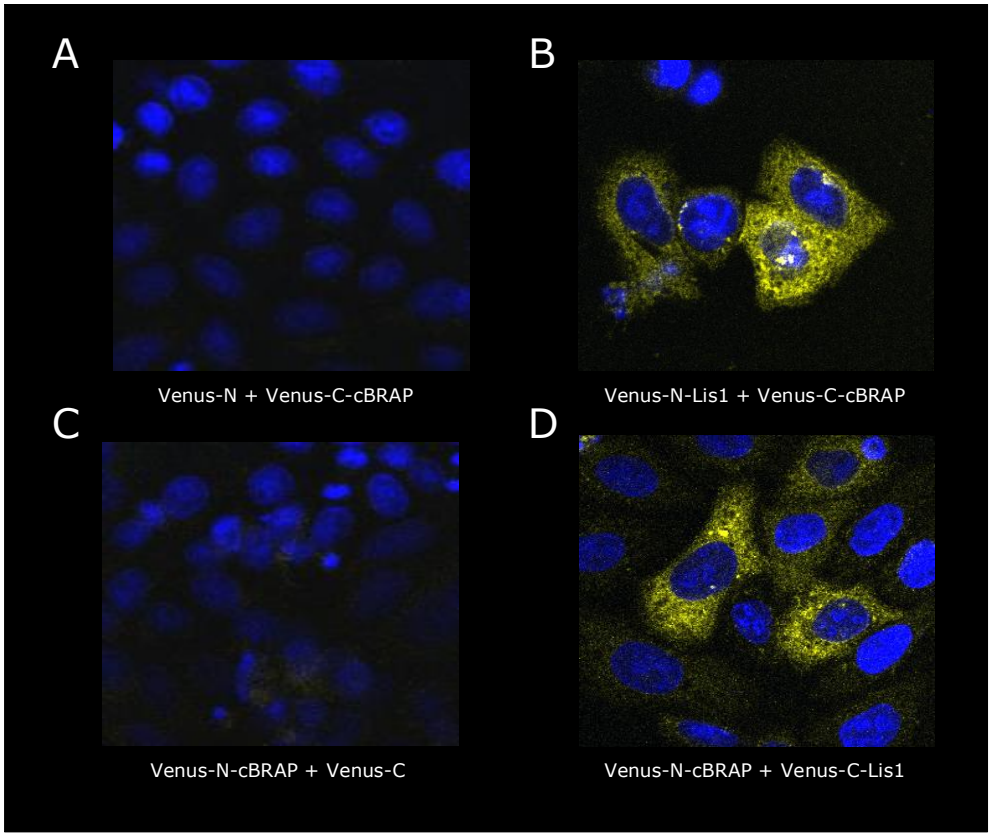

Figure 19. The interaction between Lis1 and Coiled-coil domain of BRAP was demonstrated by bimolecular fluorescence complementation assay.
The indicated combination of Venus-N and Venus-C fusion proteins with Lis1 and cBRAP (B and D) were transiently coexpressed in HeLa cells and the reconstitution of Venus Fluorophore due to protein-protein interactions were analyzed by confocal microscopy. The specificity of interaction was verified in cells transfected with Venus-N terminus and Venus-C-cBRAP protein or vice versa (A and C). Nuclei were counterstained with DAPI (blue).

Taken together, these observations provide conclusive evidence that the coiled-coil domain of BRAP is sufficient for complex formation with Lis1. However, additional parts of BRAP are also able to bind to Lis1. The N-terminal region of BRAP possesses a conserved C_2H_2–type zinc finger motif that has been shown to be involved in binding to the nuclear localization signal (NLS) of BRCA1 (Li et al., 1998). To explore the potential of the N-terminus of BRAP to also associate with Lis1, GST pull-down assays were performed. Fig. 20A shows that full length Lis1 interacts with the N-terminus of BRAP including the zinc finer domains. This data suggests that BRAP binding to Lis1 involves at least two regions, the C-terminus and the N-terminus, which both can mediate the interaction independently.

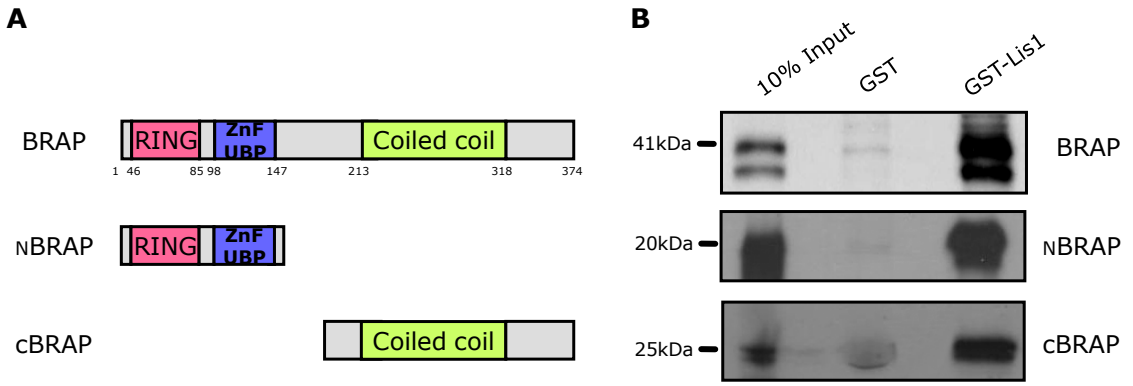

Figure 20. The determination of BRAP domains for interaction with Lis1
A. Schematic illustration of full length BRAP and two truncated forms.
B. The interaction between Lis1 and BRAP truncations was analyzed by GST pull-down assay. Bound proteins and 10% input of *in vitro* translated protein were resolved on SDS-PAGE and followed by autoradiography. GST-Lis1 interacts with full length BRAP as well as the N- and the C-terminus of BRAP while GST protein alone did not show any interactions with BRAP.

3. 2. 4. Colocalization in mammalian cells

3. 2. 4. 1. Cellular localization of Lis1 and Ranbp9 protein in HeLa cells

The cellular localization of recombinant as well as endogenous Lis1 and Ranbp9, proteins were investigated by immunocytochemistry in HeLa cells (Fig. 21). Endogenous Lis1 was found throughout the cytoplasm with high concentration around the nucleus. This observation is in good agreement with previous studies of the cellular distribution of Lis1 protein (Assadi et al., 2003; Smith et al., 2000). Previous reports showed that endogenous Ranbp9 is mainly in the cytoplasm, although in cells of the immune system Ranbp9 also seems to localize to the plasma membrane (Denti et al., 2004). In addition, a truncated form of Ranbp9 (called RanbpM) has been observed at the centrosome (Nakamura et al., 1998). HA tagged or endogenous Ranbp9 in HeLa cells were found by immunofluorescence exclusively in the cytoplasm and not in the nucleus or at the cell membrane of HeLa cells. Superimposition of stainings for Lis1 and Ranbp9 revealed that both proteins partially overlapped within the cytoplasm.

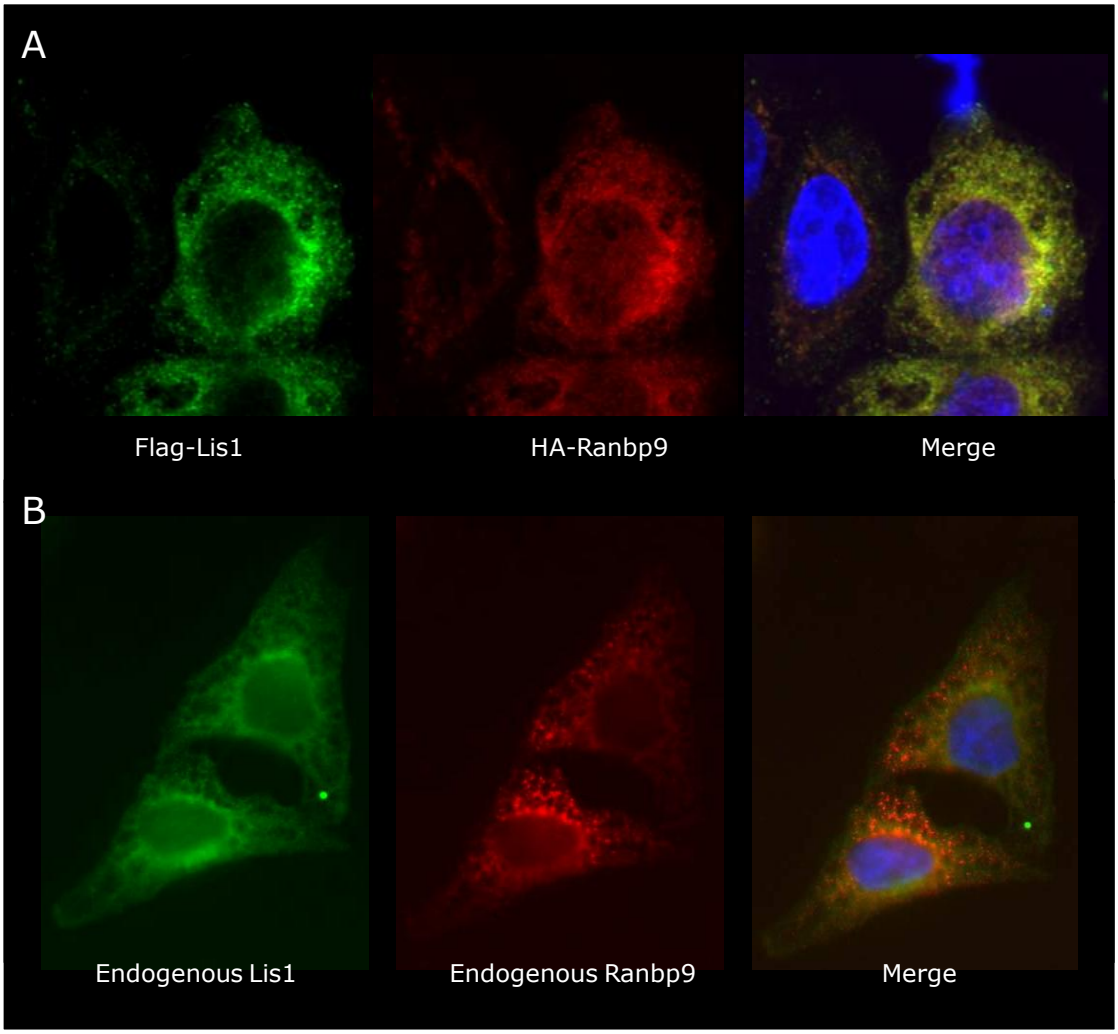

Figure 21. Cellular localization of recombinantly expressed and endogenous Lis1 and Ranbp9
Overexpressed as well as endogenous Lis1 was found to partially associate with Ranbp9.
A. To examine the distribution of overexpressed Lis1 and Ranbp9 proteins, HeLa cells cotransfected with Flag tagged Lis1 (green) and HA tagged Ranbp9 (red) were detected by Flag and HA specific-antibodies.
B. Endogenous Lis1 (green) and Ranbp9 (red) proteins were detected by specific antibodies.
In all figures, the nucleus was counter-stained with DAPI (blue).

3. 2. 4. 2. The subcellular localization of Lis1 and ACT protein in HeLa cells

The subcellular distribution of Lis1 and ACT proteins was also studied in mammalian cells. Endogenous ACT protein is only expressed in testis during primary spermatogenesis. Therefore, overexpression studies with tagged forms of ACT were performed. HeLa cells were transiently transfected with eGFP tagged Lis1 (*aa* 1-410) and HA tagged ACT (*aa* 1-285) and subsequently stained with HA-specific antibody. As expected, overexpression of Lis1 protein resulted in intense signals within the cytoplasm (Smith et al., 2000) (Fig. 22A) and overexpressed ACT protein was observed both, in the nucleus and the cytoplasm (Kotaja et al., 2005) (Fig. 22B). This result demonstrates that both proteins when coexpressed in the same cell accumulate and partially colocalize in the cytoplasm, while ACT alone is also found in the nucleus (Fig. 22C).

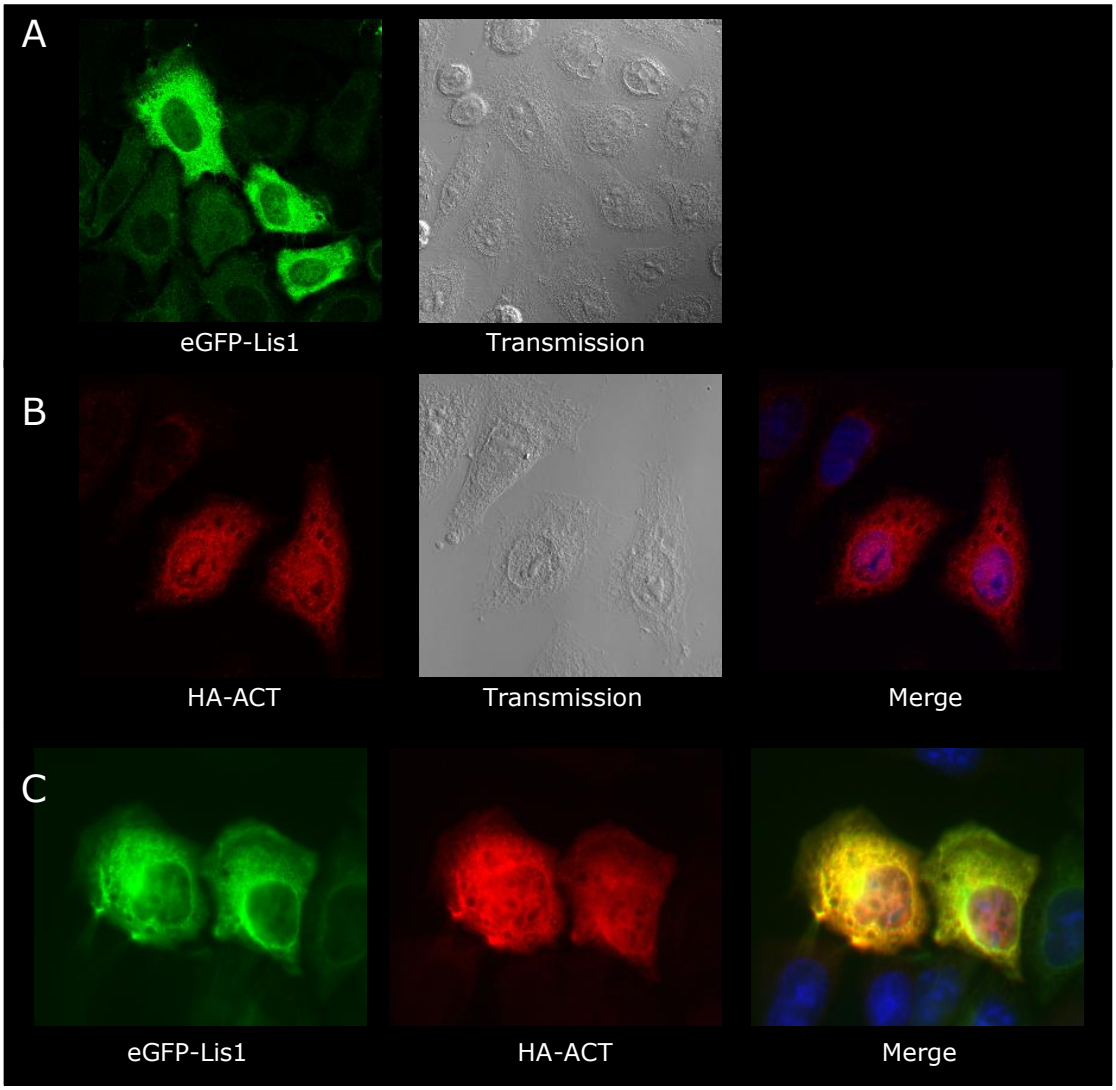

Figure 22. Subcellular localization of Lis1 and ACT
A. eGFP-Lis1 (green) was transfected into HeLa cells and over expressed protein was observed through the cytoplasm of HeLa cells.
B. Overexpressed HA-ACT was detected in cytoplasm and nucleus. Localization of ACT protein was determined by HA antibody after HA-ACT transient transfection into HeLa cells. ACT (red) was detected in the cytoplasm and nucleus.
C. Colocalization of Lis1 and ACT was predominately detected at the cell cortex.
The nucleus was stained with DAPI (Blue).

3. 2. 4. 3. Lis1 protein colocalizes with BRAP in HeLa cells.

The subcellular localization of BRAP protein in mammalian cells was also determined by immunocytochemistry. There is no available antibody for BRAP, therefore overexpression studies were performed with a tagged BRAP. HA tagged full length BRAP was expressed in HeLa cells and found in the cytoplasm in agreement with previous studies (Li et al., 1998) (Fig. 23A). When Lis1 and BRAP proteins were coexpressed in HeLa cells, both proteins displayed tightly overlapping expression domains (Fig. 23A). Occasionally, in about 5-10% of cells overexpressing BRAP, the protein was clustered close to the nucleus (Fig. 23B).

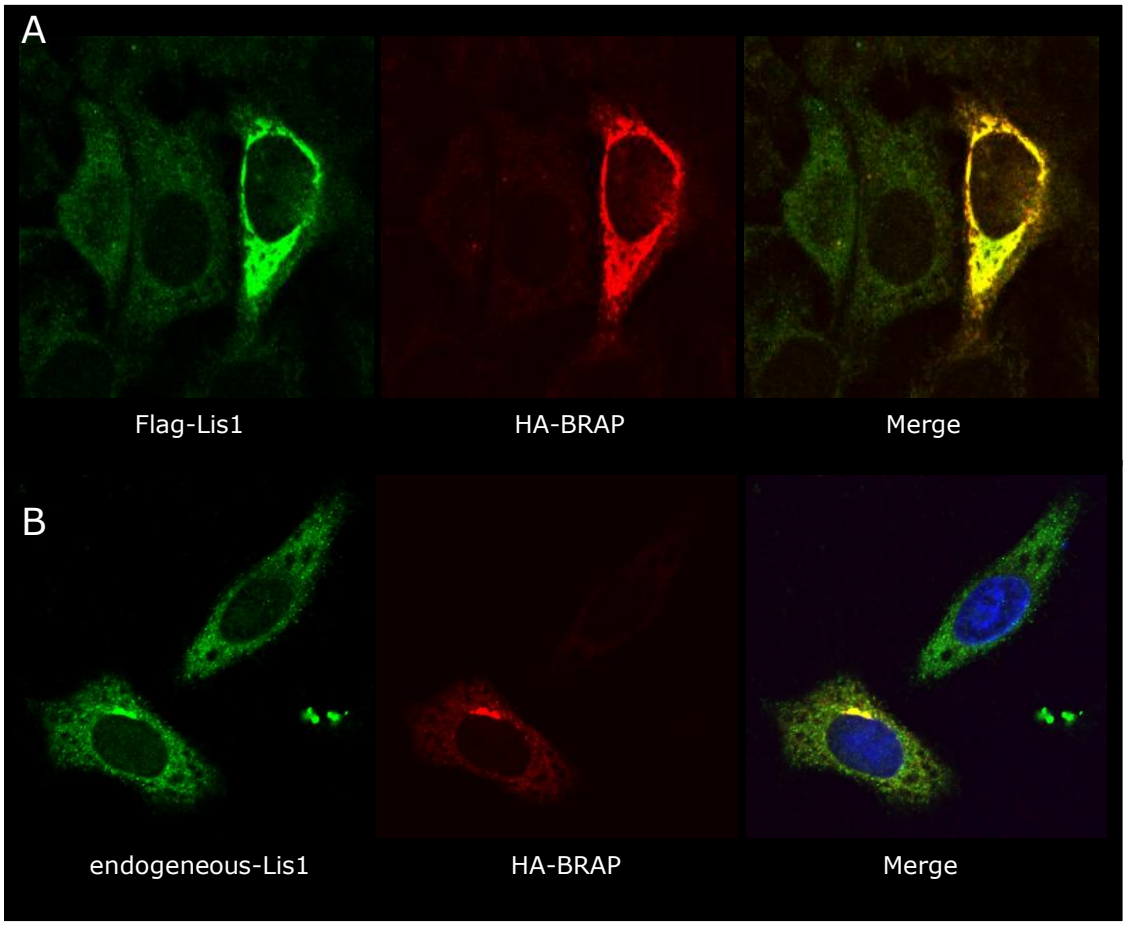

Figure 23. Lis1 protein colocalize with full length of BRAP in the cytoplasm of HeLa cells
A. Overexpressed Lis1 (green) and BRAP (red) were detected in the cytoplasm and seem to colocalize (yellow). Flag tagged Lis1 together with HA tagged BRAP were transiently transfected into HeLa cells. 24hrs after transfection, cells were fixed and stained with HA and Flag specific antibodies.
B. Endogenous Lis1 protein (green) was observed with overexpressed BRAP (red). Both proteins were localized predominantly in cytoplasm and more concentration of BRAP expression was sometimes detected at a point next to the nucleus. HA tagged BRAP were transiently transfected into HeLa cells. 24hrs after transfection, the cells were fixed and stained with Lis1 and HA specific antibodies.

Since in previous experiments the coiled-coil domain of BRAP (cBRAP) showed interaction with Lis1, I investigated also its potential to colocalize with Lis1 in HeLa cells. HA-tagged cBRAP and Flag-tagged Lis1 were subjected to immunocytochemistry which revealed cBRAP protein expression in a punctate staining next to the nucleus overlapping with Lis1 protein (Fig. 24).

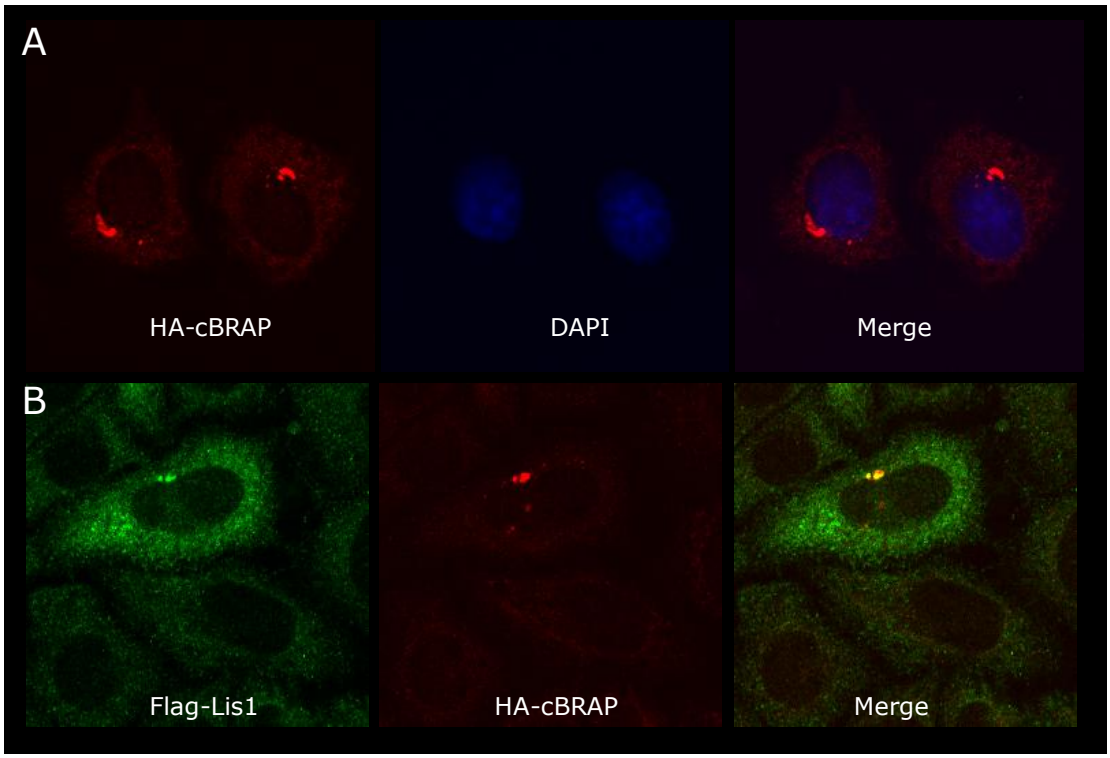

Figure 24. Lis1 protein colocalizes with cBRAP in HeLa cells
To determine the localization of cBRAP and to exam the colocalization of Lis1-cBRAP, Flag-Lis1 and HA-cBRAP were transiently transfected into HeLa cells. 24hrs after transfection, the cells were fixed and stained with antibodies.
A. When cBRAP was overexpressed in cells, the protein expression was detected at a certain point next to the nucleus.
B. Overexpressed Lis1 (green) and cBRAP (red) were detected mainly at a point near the nucleus where they seem to colocalize (yellow).

This result suggests that the cluster-like accumulation of BRAP in the perinuclear region maybe mediated by the C-terminal coiled-coil domain, possibly in association with Lis1. To examine the BRAP staining next to the nucleus, an antibody to gamma-tubulin that specifically recognizes the centrosome was applied.

Lis1 is known to interact with the centrosome and may play an important role for positioning of the centrosome (Smith et al., 2000). BRCA-1, one of the BRAP interacting proteins, was also discussed for the activity of microtubule nucleation in the centrosome (Sankaran et al., 2005). Immunostaining revealed that neither full length BRAP (Fig. 25A) nor the coiled-coil domain of BRAP (Fig. 25B) costained with gamma-tubulin, indicating that BRAP is not part of the centrosome but may rather be associated with the Golgi complex.

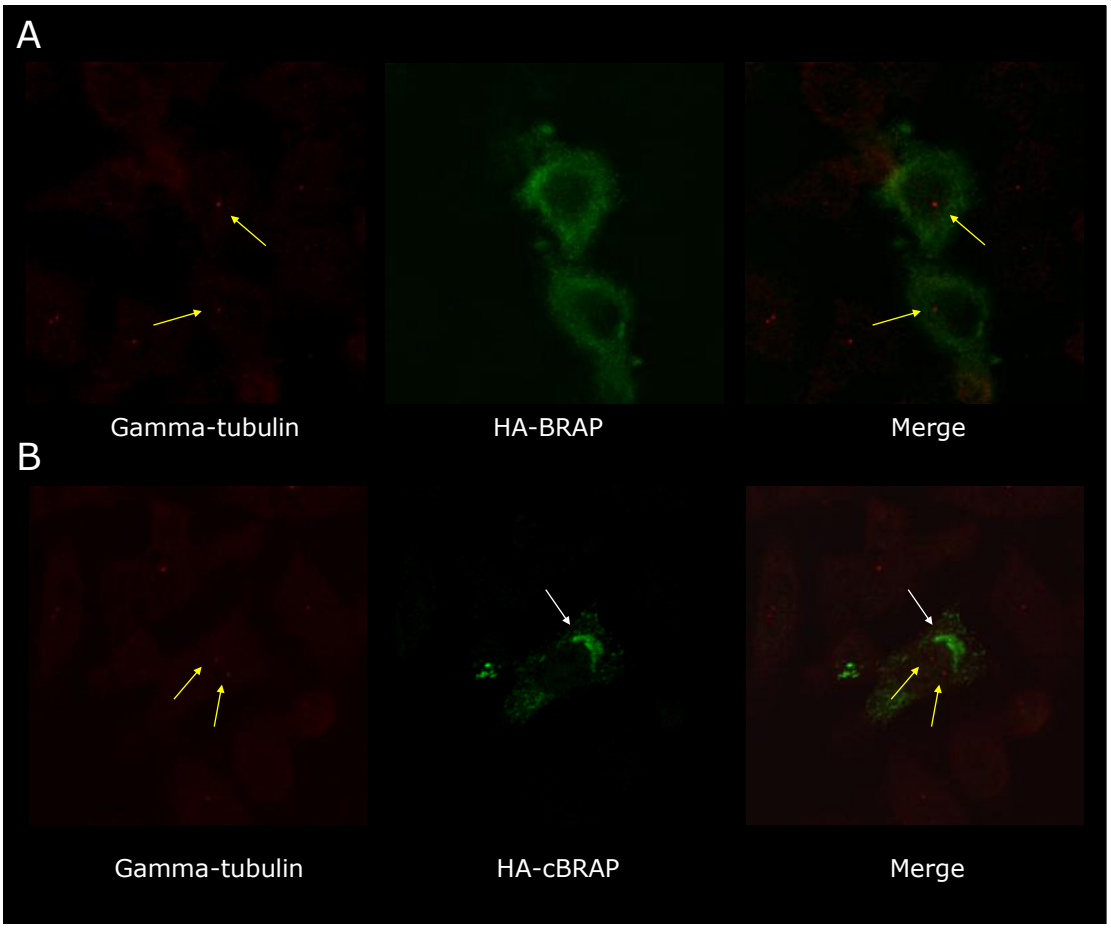

Figure 25. Full length BRAP as well as coiled-coil domain of BRAP does not seem to colocalize with gamma tubulin in HeLa cells
To exam the colocalization of full length BRAP or cBRAP and centrosome, HA-BRAP or HA-cBRAP was transiently transfected into HeLa cells. 24hrs after transfection, the cells were fixed and stained with specific antibodies for gamma tubulin and HA epitope.
A. Full length BRAP (green) was localized in throughout the cytoplasm and not associated with gamma-tubulin (yellow arrow indicates).
B. When cBRAP was overexpressed in cells (white arrows indicate), protein expression was detected at certain points next to the nucleus but cBRAP did not colocalize with gamma-tubulin (indicated by the yellow arrow).

The Golgi complex is usually located close to the nucleus to perform vesicular transport mediated by dynein motor function along microtubules (Harada et al., 1998; Presley et al., 1997). Lis1 protein has been shown to localize to the Golgi complex and different levels of Lis1 affect the cytoplasmic distribution of the Golgi complex (Nayernia et al., 2003; Smith et al., 2000). As illustrated in Fig. 26, the Golgi complex, visualized by a specific marker and eGFP-BRAP partially overlapped allowing the interpretation that BRAP protein may at least in some instances associates with Golgi structures.

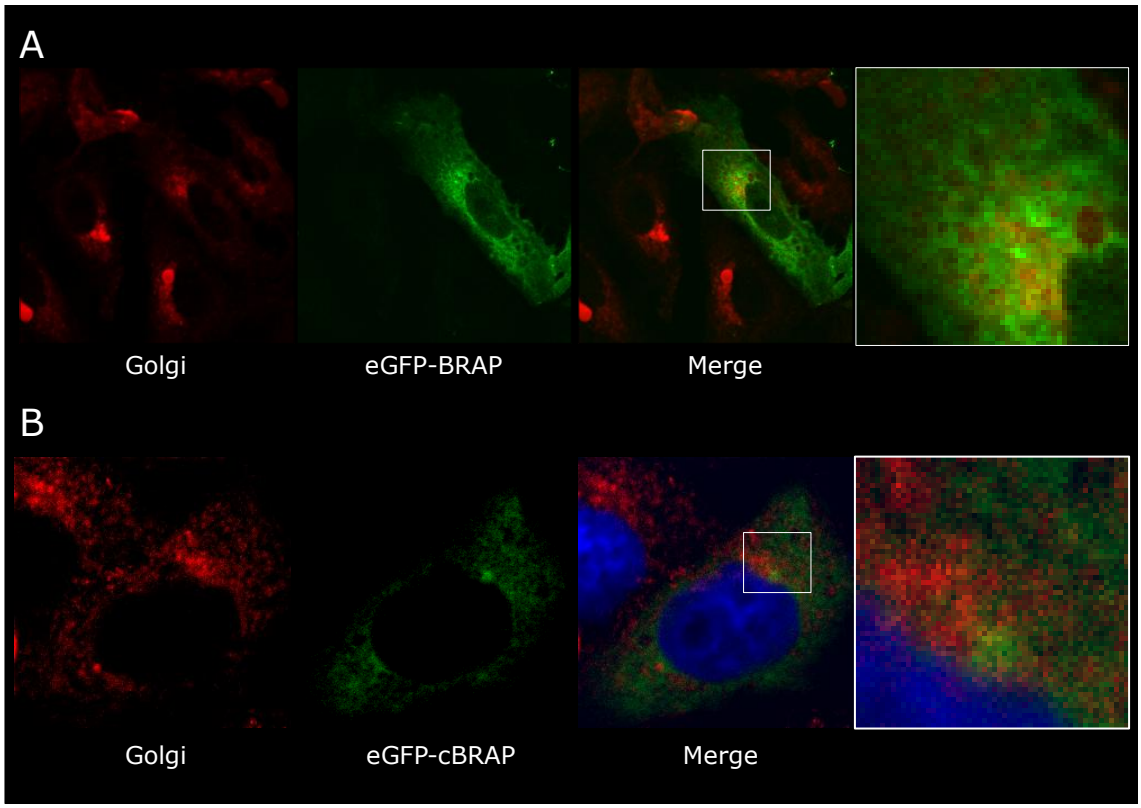

Figure 26. BRAP associates with Golgi complex in the cytoplasm of HeLa cells
To investigate the subcellular colocalization of full length BRAP (A) or coiled-coil domain of BRAP (B) and Golgi, HeLa cells were transiently transfected with either eGFP-BRAP or eGFP-cBRAP. Colocalization of eGFP-BRAP or eGFP-cBRAP (green) with a Golgi marker, BODIPY TR-ceramide (red), in living HeLa cells reveals that BRAP is partially overlapped with Golgi complex.

3. 2. 5. Analysis of Lis1, Ranbp9, ACT, and BRAP in testis

To characterize mRNA expression of the Lis1 gene and its identified interacting partners in various mouse tissues including the testis, RT-PCR was performed. In agreement with previous studies, it was found that Lis1, Ranbp9, and BRAP are expressed in most of the mouse tissues but ACT is specifically confined to testis (Fig. 27) (Nishitani et al., 2001; Li et al., 1999; Fimia et al., 1999).

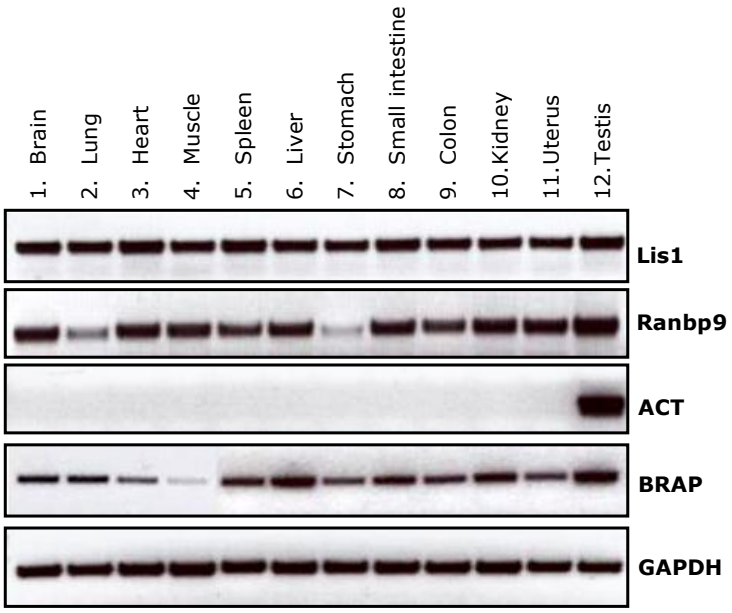

Figure 27. RT-PCR analysis in adult mouse tissues
mRNA expression of Lis1, Ranbp9, and BRAP were detected in all mouse tissues whereas mRNA expression of ACT was observed only in testis. GAPDH transcripts served for as a control for the use of equal amounts of template. Total RNA from 12 different organs of adult mouse tissues was analyzed by RT-PCR.

I also analyzed testis RNA from different mouse mutants (a kind gift of Prof. W. Engel) that specifically arrest spermatogenesis at different stages (Fig. 28). Lis1, Ranbp9, and BRAP were expressed in testis of wild type and all mutant animals, except the one of the W/W^{v} mouse which lacks all spermatogenic cells (Rooij and Boer, 2003). This indicates that Lis1, Ranbp9, and BRAP transcripts are expressed throughout spermatogenesis. In contrast, ACT transcripts were only detected in mutants with defects in late spermatogenesis, such as the olt/olt and qk/qk strains but not in mutants that block early spermatogenesis (Fig. 28) (Bennett et al., 1971; Moutier, 1976). This result validates previous studies that ACT is specifically expressed during late stages of spermatogenesis (Fimia et al., 1999). It also shows that the Lis1 gene is active throughout spermatogenesis. Lis1 binding partners Ranbp9, ACT, and BRAP are expressed during over-lapping periods of spermatogenesis.

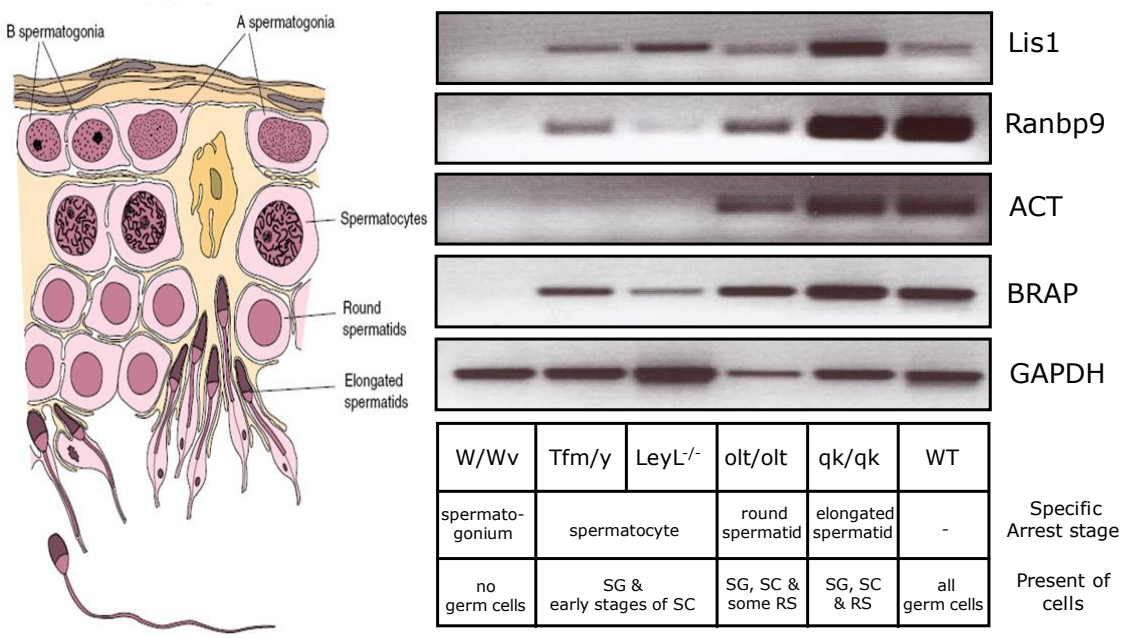

Figure 28. mRNA expression from testes in various mutants with defects of spermatogenesis
Total RNA from mice testes of different mutants with defects in spermatogenesis was analyzed by RT-PCR using specific primers for Lis1, Ranbp9, ACT, and BRAP. GAPDH gene expression served as a control. W/W^{v} mice are characterized by lack of any germ cell (Rooij and Boer,2003). Tfm/y and $Leyl^{-/-}$ mutants are arrested at the spermatocytes stage (Lyon and Hawkes, 1970; Zimmermann et al., 1999), while in olt/olt spermatogenesis stops at the round spermatids stage and in qk/qk at the elongated spermatids stage (Bennett et al., 1971; Moutier, 1976). Spermatogonium: SG; Spermatocytes: SC; Round spermatids: RS Left panel illustrate cross-section of a mouse seminiferous tubules (Adapted from Gilbert et al., 2003)

Next I determined the presence of the corresponding proteins in the adult wild type testis by immunohistochemistry. As illustrated in Fig. 29, Lis1 and Ranbp9 proteins were expressed in the cytoplasm of all types of spermatogenetic cells, but ACT was restricted to the late stages of spermatogenesis. Lis1 appeared to be enriched in spermatocytes and in elongated spermatids. Significant expression of Ranbp9 was observed in the cytoplasm of spermatocytes while expression levels of Ranbp9 in spermatogonia and spermatids were considerably lower. The double immunofluorescence reveals that Lis1 and Ranbp9 proteins are prominently coexpressed in the cytoplasm of spermatocytes and that Lis1 only colocalizes with ACT in late spermatogenetic cells.

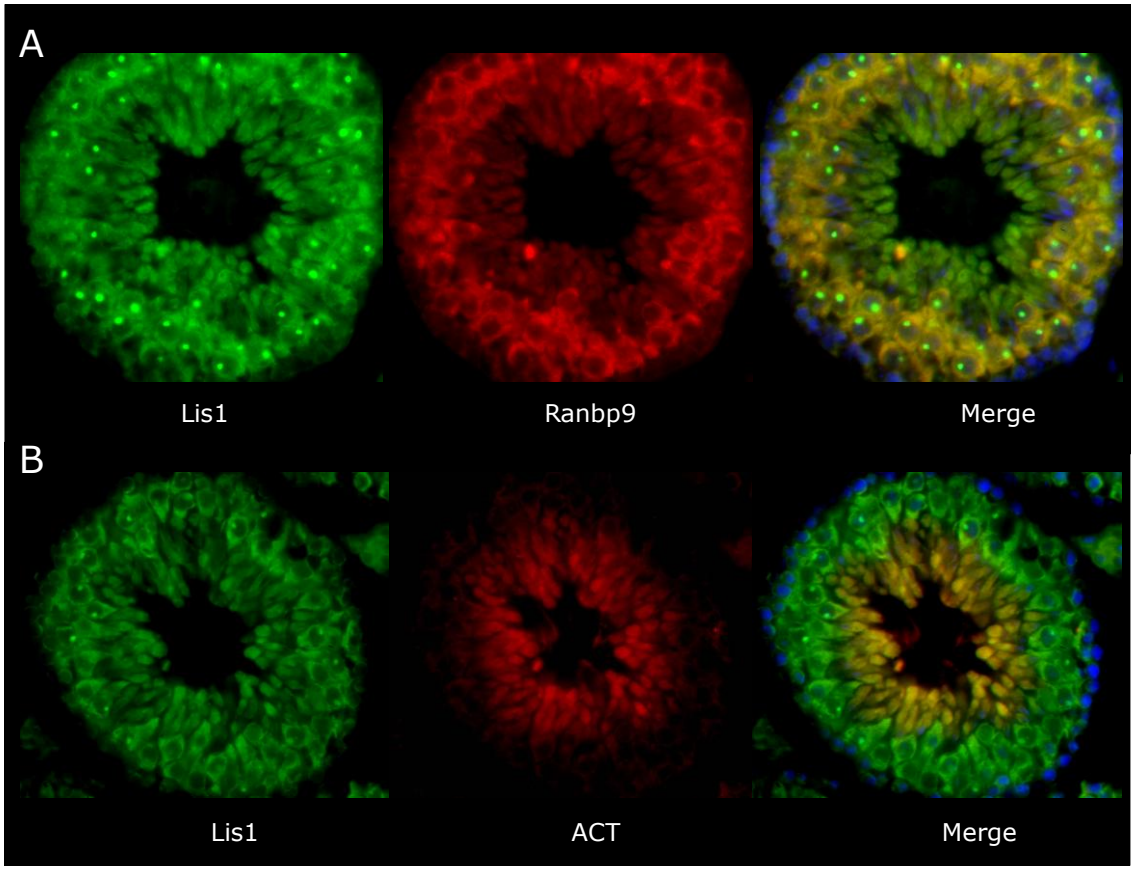

Figure 29. Colocalization of Lis1 and Ranbp9 or ACT in mouse testis
Double immunofluorescence staining was performed on mouse testis sections using specific antibodies for Lis1, Ranbp9, and ACT. Lis1 and Ranbp9 proteins are present in all spermatogenetic cells and a significant expression of both proteins is detected in the cytoplasm of spermatocytes (A). ACT protein is only found in the late stages of spermatogenic cells where ACT overlaps with Lis1 (B). Nuclei were counterstained with DAPI (Blue).

3. 3. Functional analysis of Lis1 in genetically manipulated cells

3. 3. 1. Generation of immortalized mouse embryonic fibroblast (MEF) cells from mice carrying a floxed Lis1 allele

To investigate the cellular function of Lis1 in more detail, immortalized mouse embryo fibroblasts (MEFs) were generated from E13.5 wild type, $Lis1^{wt/flox}$, and $Lis1^{flox/flox}$ mouse embryos. The mouse mutant was generously provided by Dr. Wynshaw-Boris A (University of California, USA). The murine Lis1 gene contains 11 exons. $Lis1^{flox/flox}$ MEFs have two loxP sites inserted in Lis1 introns 3 and 7 to allow CRE mediated excision of exons 4 and 7 (Fig. 30A) (Hirotsune et al., 1998). CRE mediated deletion of both loxP alleles *in vivo* results in early embryonic lethality soon after implantation during embryogenesis (Hirotsune et al., 1998). Heterozygous Lis1 mutant mice are viable but display morphological abnormalities in the brain including the cortex, hippocampus, and olfactory bulb (Hirotsune et al., 1998). Allele-specific PCR confirmed the genotypes of the established MEF lines (Fig. 30B). All established MEF cells were polyclonal and showed similar growth behavior in culture.

For CRE recombinase mediated site-specific recombination, wild type, $Lis1^{wt/flox}$, and $Lis1^{flox/flox}$ MEFs were either transiently transfected with an expression plasmid encoding CRE recombinase tagged with fluorescent eGFP (hereafter eGFP-CRE) or infected with recombinant adenovirus expressing CRE recombinase and GFP to visualize CRE expressing cells (hereafter termed AD-CRE). Gene recombination was observed in $Lis1^{wt/\Delta Lis1}$ and $Lis1^{\Delta Lis1/\Delta Lis1}$ MEFs at various time points following CRE expression but not in Lis1 wild type MEFs, as determined by PCR analysis (Fig. 30C).

While the expression of CRE recombinase in wild type MEFs had no effect on growth behavior (data not shown), heterozygous and homozygous Lis1-deficient cells grew fairly normal for 48 to 72 hours after transfection or infection but after that time period showed severe morphological changes, such as blebbing, rounding up, and eventually cell death. These observations indicate that Lis1 is essential for long term survival of cells, although the used experimental system allowed to study short term effects of Lis1 deficiency for approximately 3 days in culture.

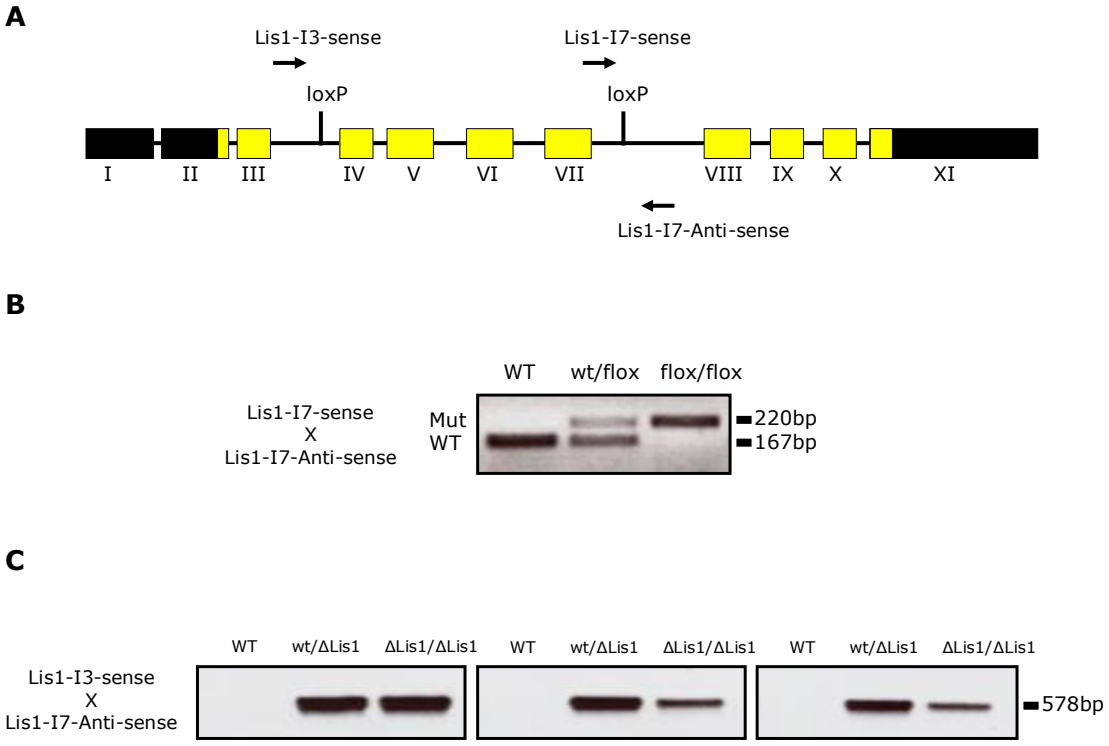

Figure 30. Analysis of Lis1 mutant mouse embryo fibroblasts (MEFs)
A. Schematic representation of the Lis1 allele present in the mouse mutant used to isolate MEFs. Note the two loxP sites located in introns 3 and 7. Primers for PCR genotyping are indicated.
B. Representative results of PCR genotyping from genomic DNA of wild type, $Lis1^{wt/flox}$, and $Lis1^{flox/flox}$ MEFs. Diagnostic fragments for Wild type (167bp) and mutant (220bp) alleles are indicated.
C. PCR analysis of recombined floxed Lis1 alleles (578bp) 24, 48, and 72hrs after infection of MEFs with CRE recombinase.

3. 3. 2. CRE recombinase decreases Lis1 protein levels in MEFs

To ensure that Lis1 protein levels in MEFs are reduced after deletion of the Lis1 gene, Western blot analysis and immunofluorescence staining of cultured cells was performed. Protein extracts from wild type, Lis1$^{wt/\Delta Lis1}$ and Lis1$^{\Delta Lis1/\Delta Lis1}$ MEFs on Western blot showed substantial reduction of Lis1 protein, while actin levels used as control remained unchanged (Fig. 31A and C). Reduction of Lis1 protein in heterozygous and homozygous Lis1-deficient MEFs compared to wild type cells was confirmed by immunofluorescence analysis. While Lis1 protein in wild type cells appeared throughout the cytoplasm, only residual Lis1 protein was found in heterozygous and homozygous mutant MEFs around the nucleus but not in peripheral regions of the cytoplasm (Fig. 31B and D). Similar results were obtained in MEFS transfected with CRE-recombinase expressing plasmid and with adenoviral mediated expression of CRE recombinase.

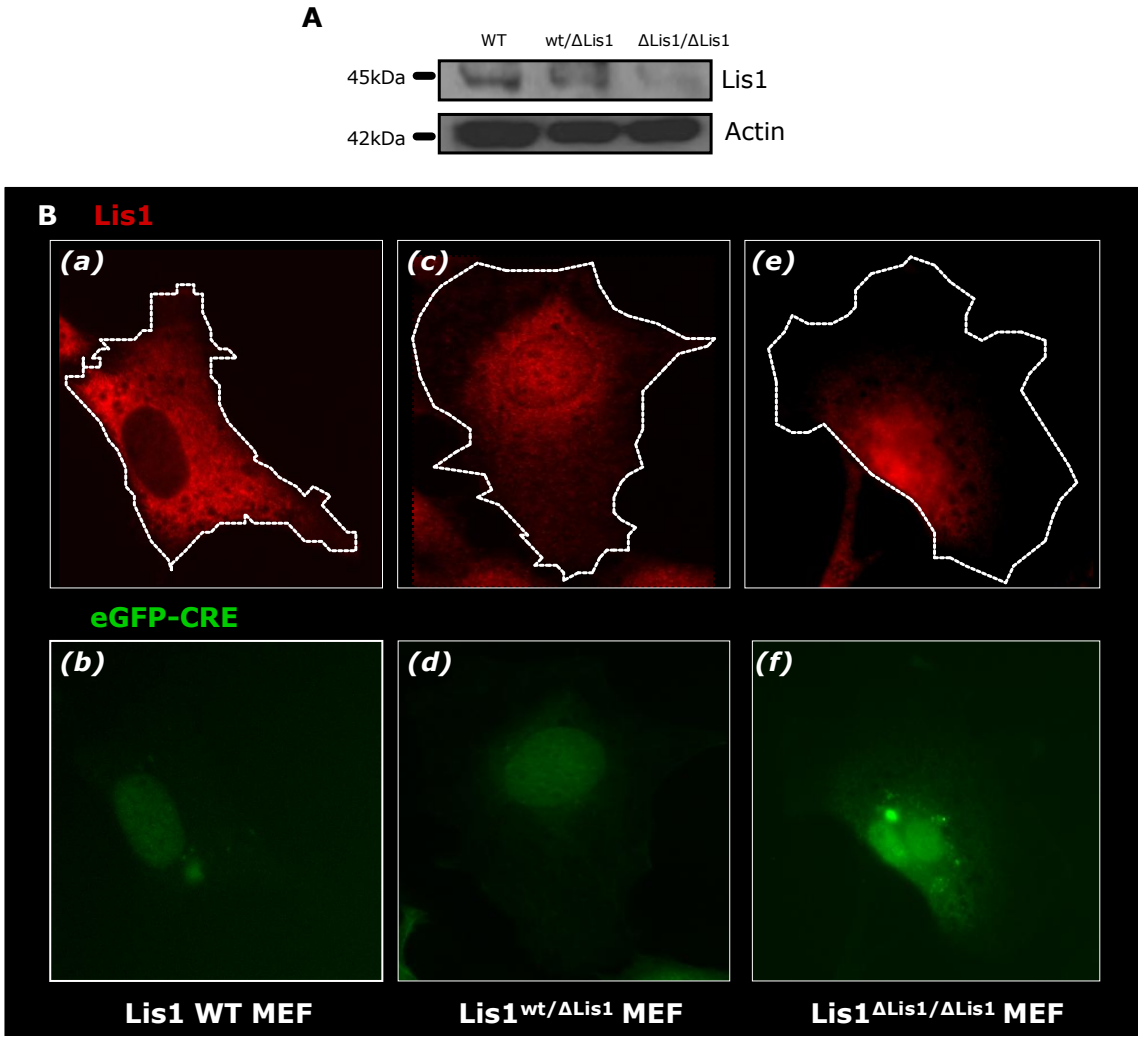

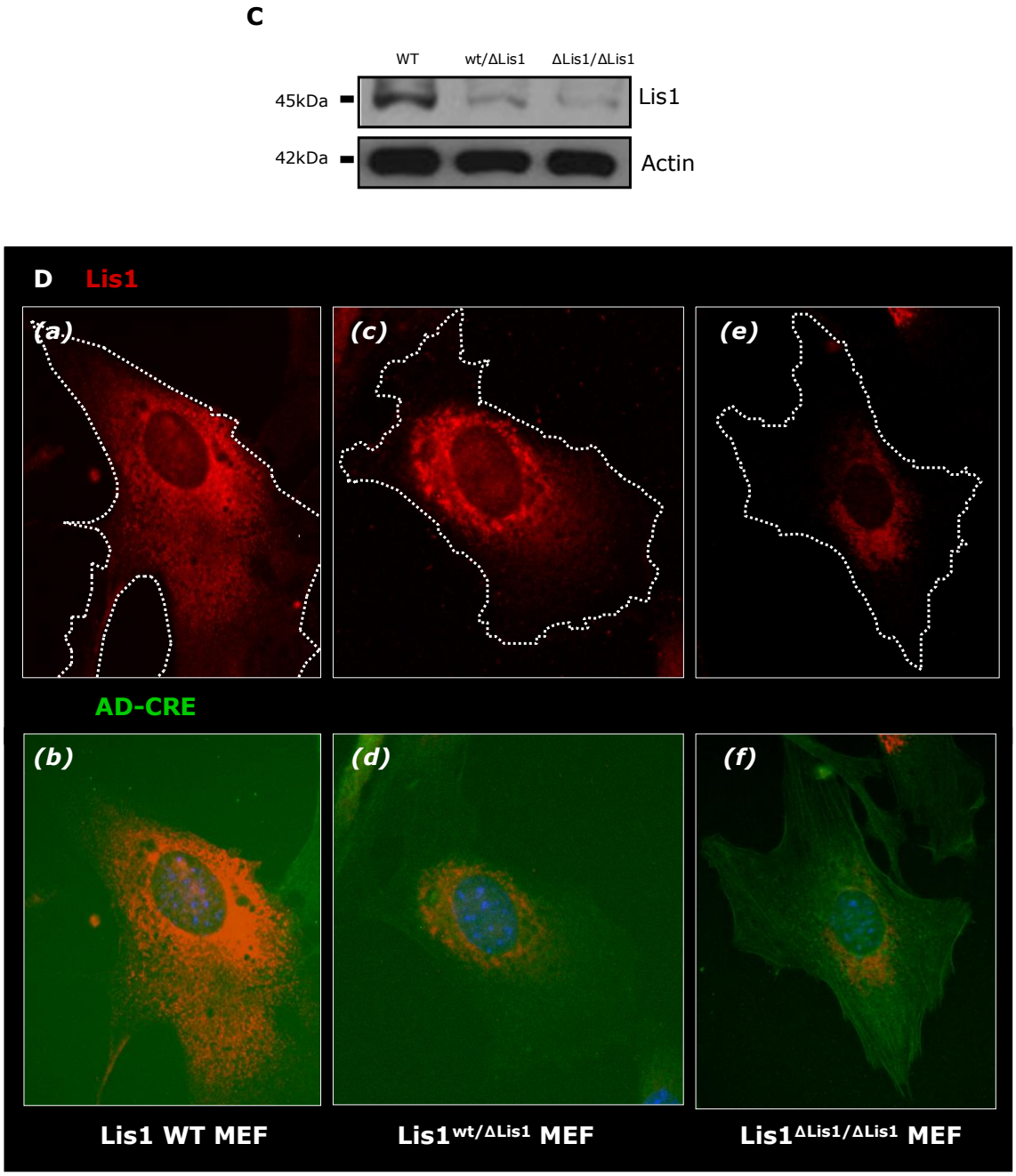

Figure 31. Accumulation of Lis1 protein in mutant MEFs after CRE recombinase mediated Lis1 gene deletion

MEFs were either transiently transfected with eGFP-CRE (A, B) or infected with AD-CRE (C, D). Cells were analyzed 48 and 72hrs after transfection and infection, respectively.

A, C. Western blot of protein extract (10µg total protein) from wild type, Lis1$^{wt/flox}$ and Lis1$^{flox/flox}$ MEFs probed with an α-Lis1 specific monoclonal antibody. Gel loading was controlled with an α–actin specific antibody.

B, D. Immunofluorescence analysis of MEFs illustrates reduction of Lis1 protein and distribution of residual Lis1 in the perinuclear region. Lis1 protein is shown in red (a, c, e) and GFP is indicated in green (b, d, f). Dotted lines were drawn to illustrate the outer margin of cells. The nucleus was stained with DAPI (blue)

3. 3. 3. Reduced levels of Lis1 may affect the steady state levels of Ranbp9 protein

Ranbp9 may play a role as a scaffolding protein during various cellular processes (reviewed in Murrin and Talbot, 2007). A recent study demonstrated that Ranbp9 controls cell morphology and may be involved in the exchange process between the cytoplasm and the nucleus (Valiyaveettil et al., 2008).

Based on the previously demonstrated interaction of Ranbp9 with Lis1, I here wanted to investigate whether Lis1 affects the accumulation and distribution of Ranbp9 protein. To this end, immunofluorescence staining of cultured cells was performed. In heterozygous and homozygous Lis1-deficient MEFs, differentially distributed Ranbp9 protein compared to wild type cells was observed by immunofluorescence analysis. Ranbp9 protein was located throughout the cytoplasm in wild type cells, whereas in heterozygous and homozygous mutant MEFs reduced levels of Ranbp9 were found mainly in the perinuclear region and possibly also in the nucleus (Fig. 32A and C). Similar results were obtained for overexpressed HA-tagged Ranbp9 and the endogenous Ranbp9 protein.

To control that the reduction of Ranbp9 protein was actually depended on the loss of Lis1 due to CRE recombinase, $Lis1^{wt/flox}$, and $Lis1^{flox/flox}$ MEFs were tested. These cells exhibited no apparent difference in Ranbp9 protein without CRE-recombinase indicating that the amount of Ranbp9 is only reduced in cells with low levels of Lis1.

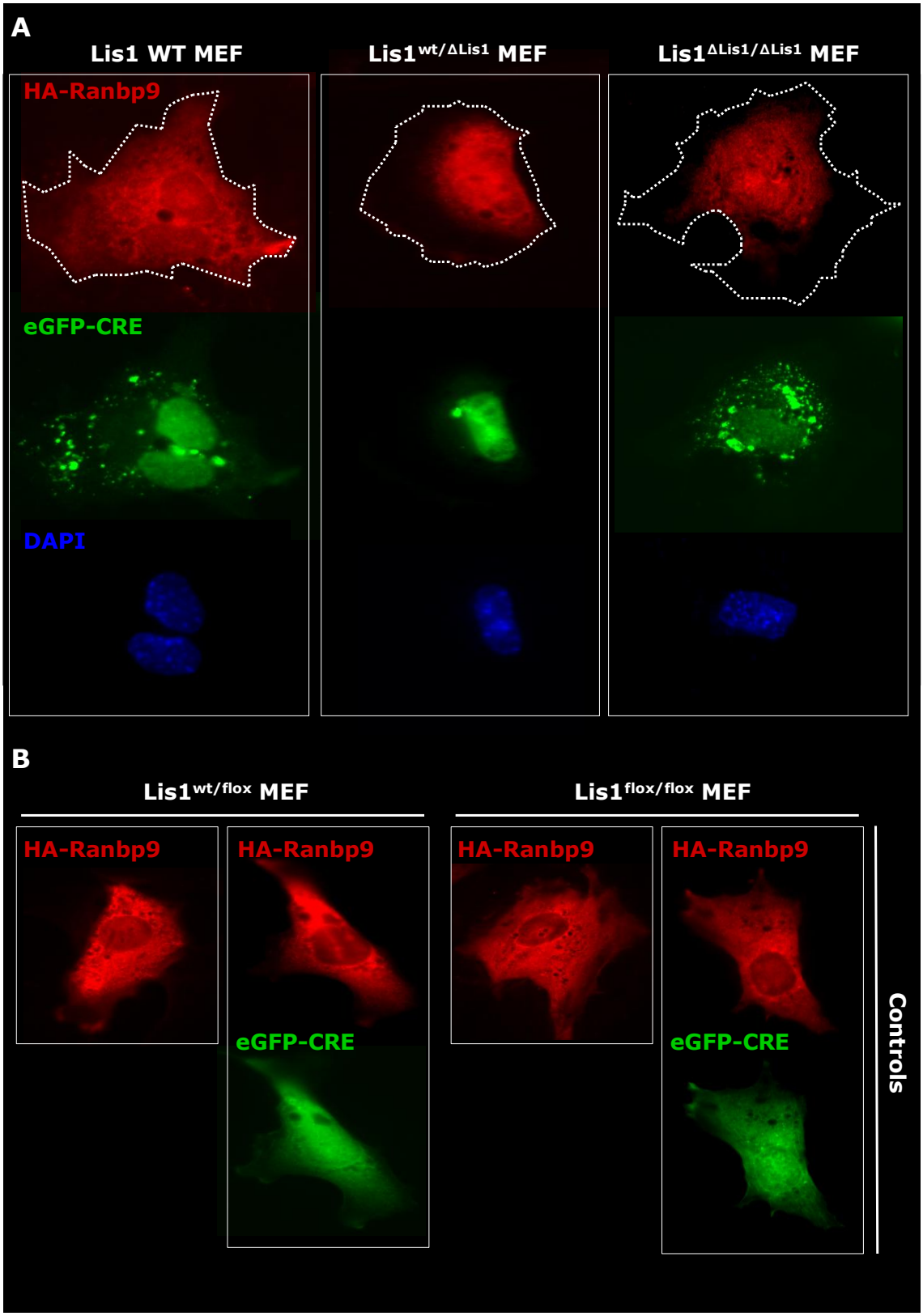
A
Lis1 WT MEF
Lis1wt/ΔLis1 MEF
Lis1ΔLis1/ΔLis1 MEF
HA-Ranbp9
eGFP-CRE
DAPI
B
Lis1wt/flox MEF
Lis1flox/flox MEF
HA-Ranbp9
HA-Ranbp9
HA-Ranbp9
HA-Ranbp9
eGFP-CRE
eGFP-CRE
Controls

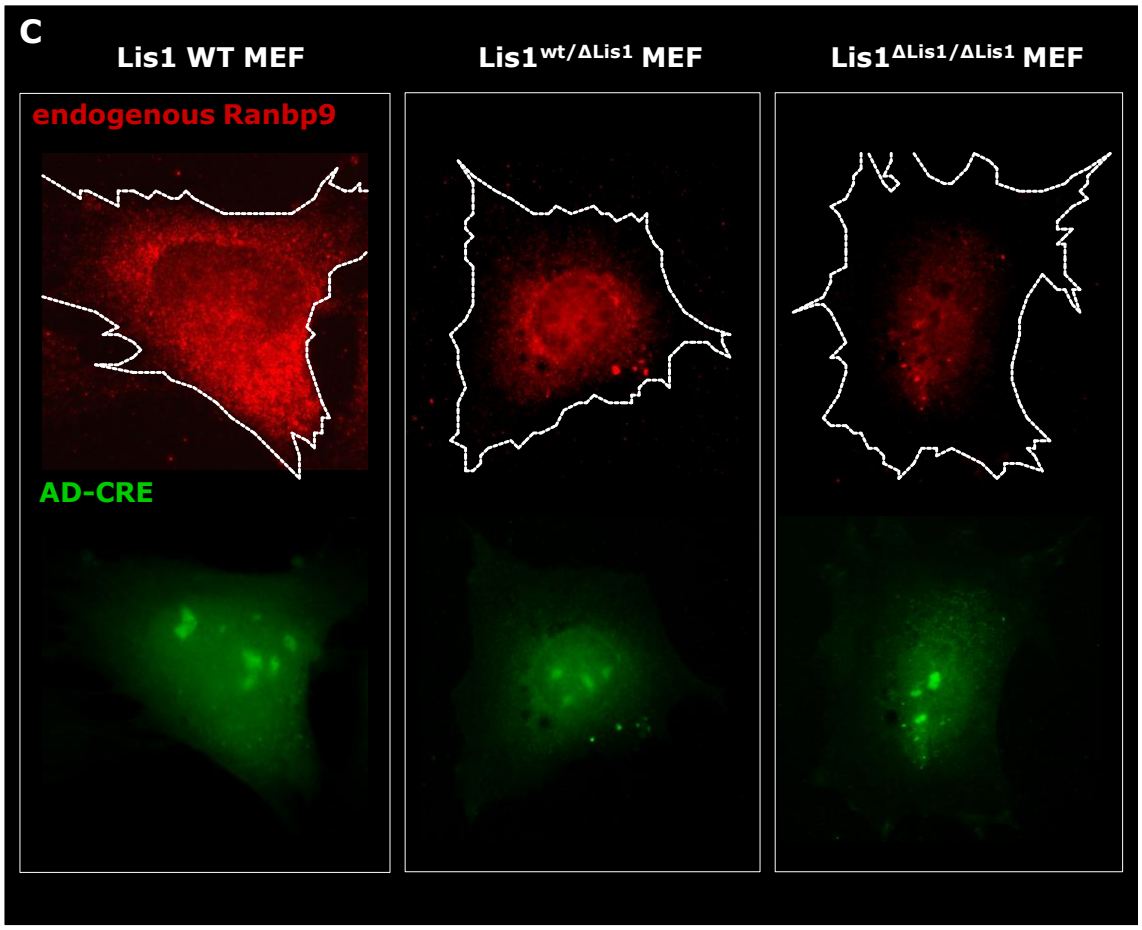

Figure 32. Low expression of Lis1 affects the level of Ranbp9 protein
A. Immunofluorescence staining displays an altered distribution of recombinant HA-Ranbp9 in MEFS with variable amounts of Lis1 48hrs after transfection with eGFP-CRE. Note that the Ranbp9 levels are significantly reduced in $Lis1^{wt/\Delta Lis1}$ and $Lis1^{\Delta Lis1/\Delta Lis1}$ MEFs, where Ranbp9 can not be detected at the cell cortex. Localization of Ranbp9 protein (red) was done with an α–HA antibody while eGFP-CRE is indicated in green. The nucleus was counterstained with DAPI (blue).
B. $Lis1^{wt/flox}$ and $Lis1^{flox/flox}$ control MEFs that do not express the CRE-recombinase show no alterations in the cellular levels and distribution of HA-Ranbp9.
C. Endogenous Ranbp9 (red) was detected in wild type and mutant MEFs 72hrs after infection with AD-CRE (green). Similar to the transfection experiments shown in Panel A, the levels of Ranbp9 protein were drastically reduced in $Lis1^{wt/\Delta Lis1}$ and $Lis1^{\Delta Lis1/\Delta Lis1}$ as compared to wild type MEFs and were completely depleted from the cell periphery. The dotted lines in A and C indicate the outer margin of the cells.

3. 3. 4. The microtubular cytoskeleton in Lis1-deficient cells

Microtubules contribute essentially to the cellular architecture and cytoskeletal functions, such as vesicular transport, cell division, and cell migration. Lis1 directly interacts with microtubules and influences microtubule dynamics (Sapir et al., 1997).

Therefore, I investigated microtubules in Lis1-deficient cells by Western blot and immunocytochemical analysis using an α-tubulin-specific antibody. While, protein extracts from wild type, Lis1$^{wt/\Delta Lis1}$ and Lis1$^{\Delta Lis1/\Delta Lis1}$ MEFs revealed no significant effects on the concentration of α-tubulin protein on Western blots (Fig. 33A), the regional distribution of α-tubulin in heterozygous and homozygous Lis1-deficient cells appeared somewhat altered compared to wild type cells (Fig. 33B). In MEFs with reduced levels of Lis1, the microtubular network determined by α-tubulin stainings seemed less complex at the periphery of the cytoplasm. This observation demonstrated that loss of Lis1 might affect the microtubule network, in agreement with previous studies (Sapir et al., 1997; Smith et al., 2000; Yingling et al., 2008).

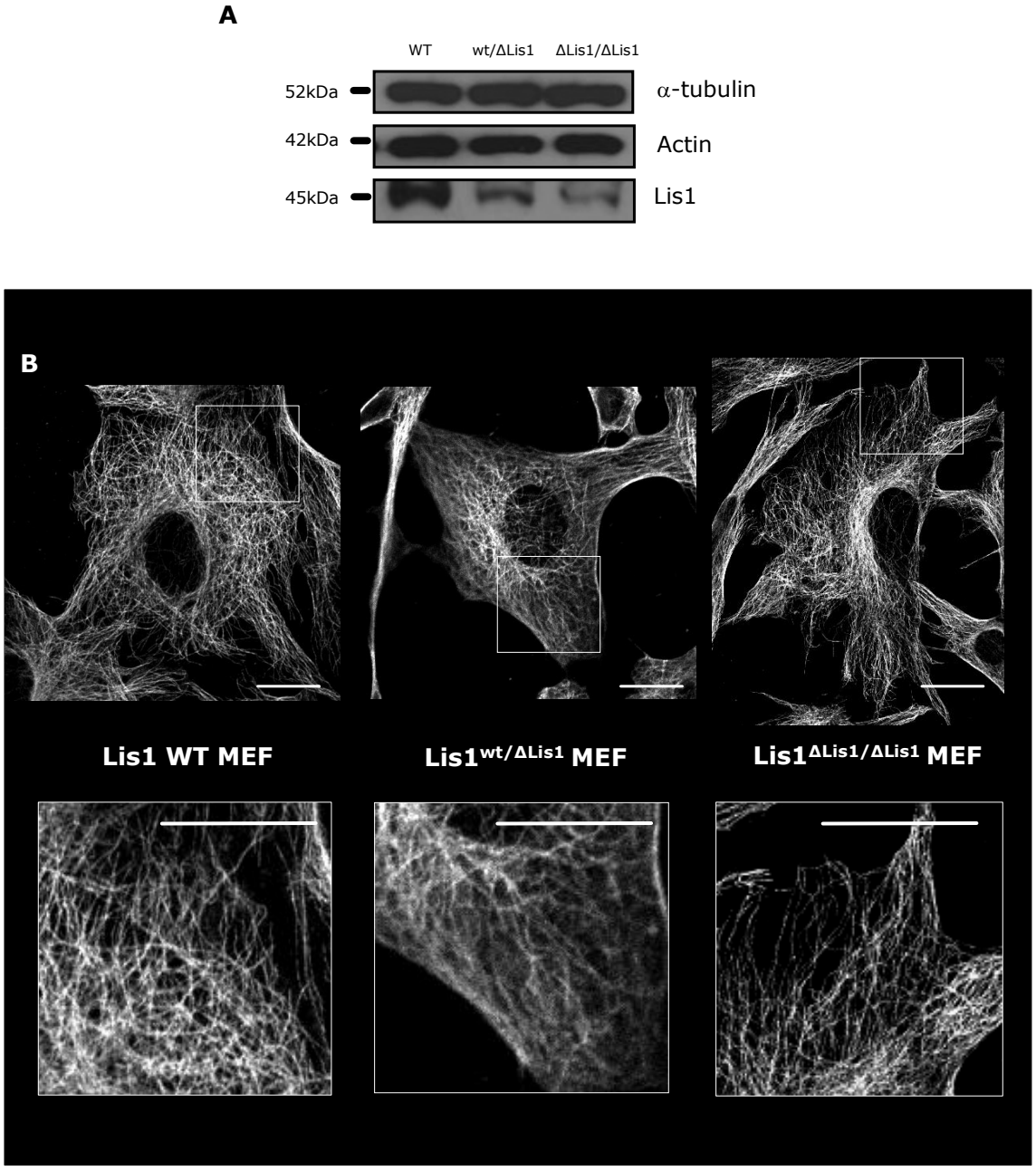

Figure 33. Determination of α-tubulin in Lis1 mutant MEF cells
72hrs after infection with AD-CRE.
A. Western blot of protein extracts (10µg total protein) from wild type and Lis1 mutant MEFs reveals no significant alteration of levels of α-tubulin expression. Gel loading was controlled with an α-actin specific antibody.
B. Immunofluorescence analysis of the distribution of α-tubulin shows that the complexity of the microtubular network was reduced at the edge of the cytoplasm in Lis1 mutants. All scale bars correspond to 20µm.

3. 3. 5. Lis1 possibly contributes to stabilize microtubules

There are a number of post-translational modifications of microtubules including phosphorylation of β-tubulin, carboxy-terminal tyrosination and acetylation of α-tubulin as well as polymodifications including glycylation and glutamylation (Barra et al., 1974; L'Hernault and Rosenbaum, 1985; Eipper, 1972; Sandoval and Cuatrecasas, 1976; Gard and Kirschner, 1985; Verhey and Gaertig, 2007; Westermann and Weber, 2003). It is known that these modification of tubulin influence the interaction with microtubule-associated proteins, such as plus-end tracking proteins suggesting that such modifications play an important role in the regulation of properties and functions of the cytoskeleton (reviewed in Hammond, Cai and J. Verhey, 2008). Acetylation of α-tubulin occurs at lysine 40 and constitutes a maker for stabilized microtubules, since it is only found in long-lived microtubules (Westermann and Weber, 2003). Recent studies suggest that acetylated tubulins play also a role in motor-based microtubule trafficking (Reed et al., 2006; Bulinski, 2007; Dompierre et al., 2007).

To examine the influence of Lis1 on the level and distribution of acetylated tubulin, Western blot and immunofluorescence stainings were performed in cultured cells with variable concentrations of Lis1. Protein extracts from $Lis1^{wt/\Delta Lis1}$, and $Lis1^{\Delta Lis1/\Delta Lis1}$ MEFs revealed significantly reduced levels of acetylated tubulins as compared to wild type controls (Fig. 34A). In agreement with this finding, a reduction of acetylated tubulins was also identified by immunofluorescence analysis (Fig. 34B). Specifically, acetylated tubulin in heterozygous and homozygous Lis1-deficient cells failed to extend to the cell cortex and appeared more sparse at the cell periphery in comparison to wild type cells.

The relative reduction of acetylated tubulin in the outer cytoplasmic regions of Lis1-depleted cells argues for a loss of stable microtubules supporting the view that in wild type cells Lis1 might possess a stabilizing influence on the microtubular network.

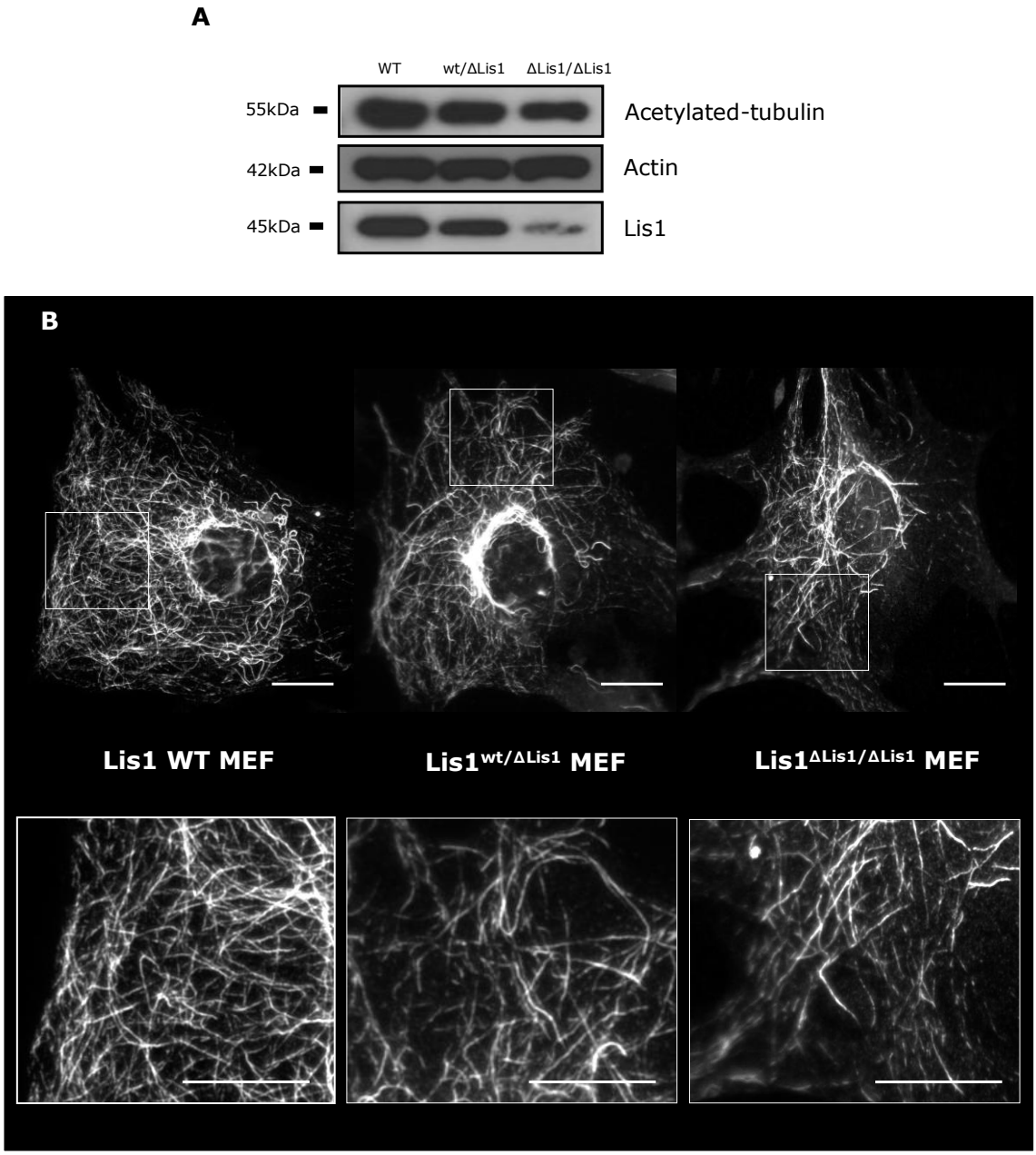

Figure 34. Reduced levels of Lis1 affect the distribution of acetylated tubulin in the cytoplasm
A. Protein extracts (10µg total protein) from wild type, $Lis1^{wt/\Delta Lis1}$, and $Lis1^{\Delta Lis1/\Delta Lis1}$ MEFs were analyzed by Western blot. Reduced levels of acetylated tubulin were detected in $Lis1^{wt/\Delta Lis1}$ and $Lis1^{\Delta Lis1/\Delta Lis1}$ MEFs. Gel loading was controlled by actin protein detection.
B. Immunofluorescence analysis of the distribution of acetylated tubulin in wild type and mutant MEFs. Note the diminished acetylated tubulin at the cell periphery when Lis1 levels are reduced. Scale bars: 20 µm. All MEFs were analyzed 72hrs after AD-CRE infections.

3. 3. 6. Analysis of MT plus-end binding proteins in Lis1-deficient cells

Microtubular dynamics are believed to be regulated by plus-end binding proteins. Lis1 has been implicated to play a role in microtubule plus-end capturing and stabilization through its interaction with plus-end binding proteins, such as CLIP-170 and $p150^{Glued}$, a subunit of dynactin. Structurally, CLIP-170 consists of a coiled-coil domain that separates the microtubule binding region located at its N-terminus from a C-terminus metal binding motif which has been shown to associate with Lis1 and dynactin (Diamantopoulos et al., 1999). CLIP-115 is structurally closely related to CLIP-170, although it lacks the C-terminal metal binding motif (De Zeeuw et al., 1997). CLIP-115 is specifically expressed in brain and in early embryonic stages during development (De Zeeuw et al., 1997). Haploinsufficiency of CLIP-115 leads to Williams Syndrome in humans, a disorder of neural development. Therefore, CLIP-115 may be involved in neurodevelopmental processes (Hoogenraad et al., 2002). Interestingly, absence of CLIP-115 leads to increased levels of CLIP-170 and dynactin at the tip of growing microtubules suggesting that CLIP-115 may regulate dynein motor functions along the microtubules (Hoogenraad et al., 2002; Lansbergen et al., 2004).

In light of these informations, I examined the distribution of the microtubule plus-end binding proteins, CLIP-170 and CLIP-115 in Lis1-deficient cells. Immunofluorescence staining on wild type, heterozygous, and homozygous Lis1-deficient MEFs with a CLIP-170 specific antibody revealed no major differences between wild type and Lis1 mutant MEFs (Fig. 35A). To measure microtubule polymerization dynamics, such as growth and shortening rate (Komarova et al., 2009; Perez et al., 1999) the average tail length of CLIP-170 comets at the microtubule plus-end was determined in wild type (380 microtubule ends in 12cells), $Lis1^{wt/\Delta Lis1}$ (n=339; 11 cells), and $Lis1^{\Delta Lis1/\Delta Lis1}$ (n=442; 11 cells) MEFs using the NIH ImageJ program (ImageJ 1.42q). No evidence for significant alterations in CLIP-170 tail length at the end of growing microtubules was observed between wild type (2.38 ± 0.16µm; mean ± standard deviation), $Lis1^{wt/\Delta Lis1}$ (2.12 ± 0.11µm) and $Lis1^{\Delta Lis1/\Delta Lis1}$ (2.26 ± 0.12µm) MEFs (Fig. 35B).

In contrast to CLIP-170, immunostaining for CLIP-115 demonstrated apparently longer comet tails of CLIP-115 end-decorations in heterozygous and homozygous Lis1-deficient cells as compared to wild type controls (Fig. 36A). For quantitative analysis, over 1000 individual comet tails of growing microtubules were measured from wild type (n=1351; 16 cells), $Lis1^{wt/\Delta Lis1}$ (n=1163; 9 cells), and $Lis1^{\Delta Lis1/\Delta Lis1}$ (n=1483; 15 cells) MEFs. Significantly longer comet tail lengths were detected in $Lis1^{wt/\Delta Lis1}$ (2.7 ± 0.13µm) and $Lis1^{\Delta Lis1/\Delta Lis1}$ (3.51 ± 0.28µm) MEFs than in wild type MEFs (1.25 ± 0.09µm) (Fig. 36B). To evaluate the total protein levels of CLIP-115 in the absence of Lis1, Western blot was performed with a specific CLIP-115 antibody. Interestingly, the overall cellular concentration of CLIP-115 was not altered in Lis1-deficient cells suggesting that most likely kinetic parameters rather than stochiometry explains the altered CLIP-115 decoration (Fig. 37). MEFs with reduced Lis1 contained also fairly normal levels of $p150^{Glued}$, a finding that is in agreement with previously described data (Fig. 37) (Smith et al., 2000).

In summary, the decoration of growing microtubule plus-ends with CLIP-115 appears modified in the absence of Lis1, although a direct interaction between both proteins has not been shown.

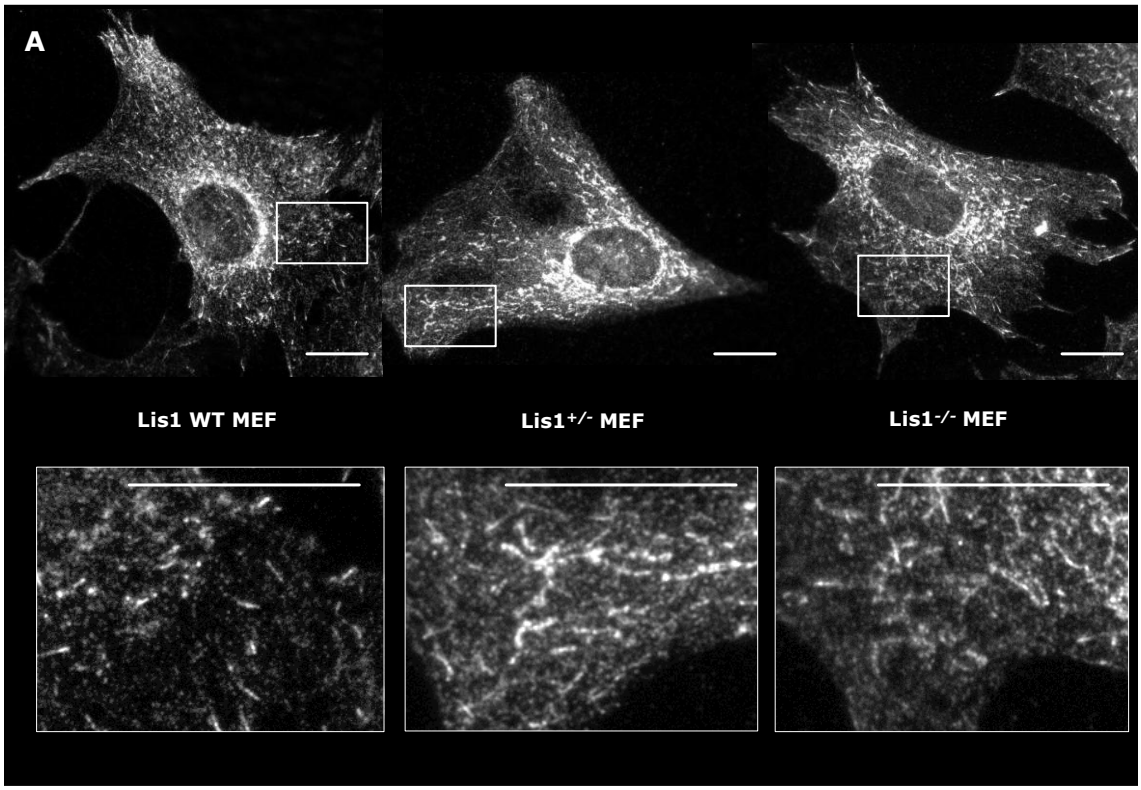

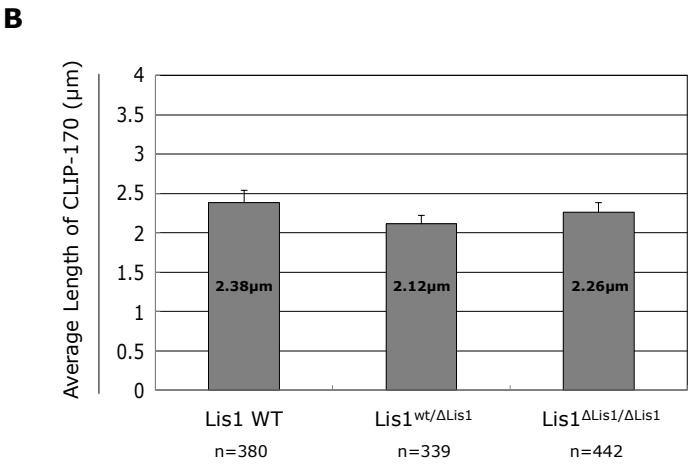

Figure 35. CLIP-170 is distributed similarly in cells with and without Lis1 protein
MEFs infected with AD-CRE were analyzed 72hrs after infections.
A. Immunofluorescence image from wild, Lis1$^{wt/\Delta Lis1}$, and Lis1$^{\Delta Lis1/\Delta Lis1}$ MEFs showed that the cytoplasmic distribution of CLIP-170 is not altered in Lis1 mutant and wild type MEFs. Scale bars: 20 µm.
B. Measuring the average comet tail length of CLIP-170 at microtubule plus-ends confirms that there is no significant difference between the experimental groups. The error bars represent the standard deviation.

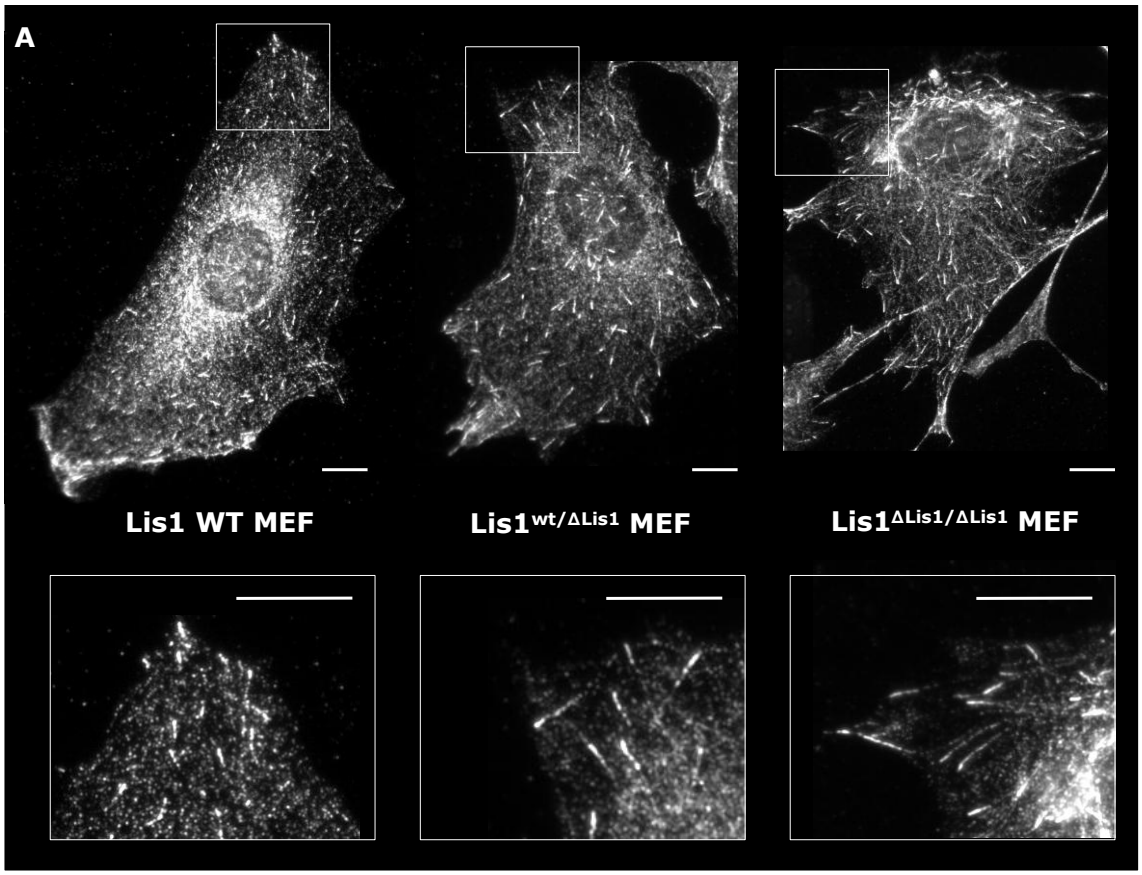

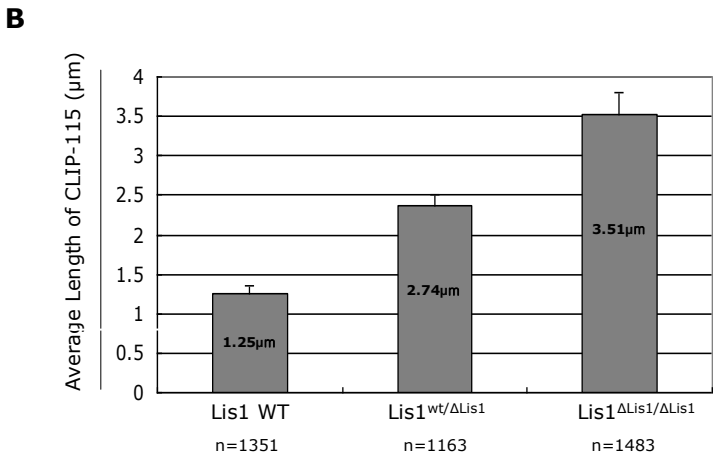

Figure 36. Low levels of Lis1 cause accumulation of CLIP-115 at the microtubule plus-end
MEFs were infected with AD-CRE and analyzed 72hrs after infections.
A. Immunofluorescence images demonstrating the altered cellular distribution of CLIP-115 in wild and Lis1 mutant MEFs. Scale bars: 10 µm.
B. Quantitative analysis of the comet tail length of CLIP-115 indicates an elongated comet tail length in Lis1 mutant MEFs. The n represents the total number of measured microtubular tips and the error bars indicate the standard deviation.

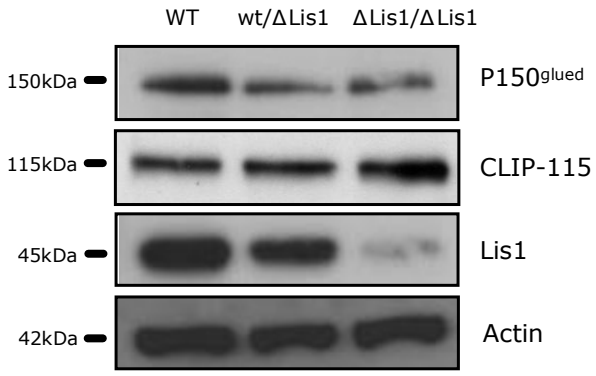

Figure 37. No significant changes in the protein levels of the plus-end binding proteins, p150^{glued} and CLIP-115, in Lis1 mutant cells
Protein (10µg total protein) form wild type, Lis1$^{wt/\Delta Lis1}$, and Lis1$^{\Delta Lis1/\Delta Lis1}$ MEFs was analyzed by Western blots with specific antibodies. Significantly reduced protein expression levels of Lis1 were detected in Lis1 mutant compared with wild type MEFs. In contrast, the protein levels of p150^{glued} and CLIP-115 were not significantly altered. Actin was served as loading control. For this experiment MEFs were infected with AD-CRE and analyzed 72hrs later.

3. 3. 7. The growth rate of microtubules appears influenced by Lis1

End binding 1 (EB1) protein is one of the growing microtubular tip binding proteins that have been suggested to regulate microtubule dynamics by stimulating growth at microtubule plus-ends (Vitre et al., 2008; reviewed in Vaughan, 2005). Dynactin, one of the Lis1 interacting proteins, directly binds to EB1 and this complex might play a role in the elongation of microtubules (Strickland et al., 2005; Askham et al., 2002). Lis1 usually colocalizes with EB1 at the plus-end tips of microtubules but EB1 is also known to exhibit a strong association with the centrosome (Caspi et al., 2003). However, the precise relationship between Lis1 and EB1 remains unclear.

To investigate whether Lis1 may play a role in the distribution of EB1, immunofluorescence staining of cultured cells with variable amounts of Lis1 was performed. As illustrated in Fig. 38, loss of Lis1 in heterozygous and homozygous MEFs had no effect on EB1, which, as expected, was specifically localized at the growing plus-ends of microtubules.

Next, fluorescently tagged EB1 was introduced into wild type and mutant MEFS to evaluate the growth rate of microtubules as reflected by the speed of the movement of the growing plus-end (Bieling et al., 2008; Binker et al., 2007). The apparent movement of the GFP label was documented by time-lapse images that were taken in 4 second intervals during a 5 minute observation period. These results were hereafter statistically evaluated (105 microtubular ends in 8 wild type and 75 ends in 5 $Lis1^{flox/flox}$ mutant MEFs) using the Metamorph image analysis software. The results indicated that the rate of plus-end growth is markedly decreased in cells lacking Lis1 with only 6.4 ± 1.09µm/min (mean ± standard deviation) in Lis1 depleted compared to 10.2 ± 1.78µm/min in wild type cells (Fig. 39B and C). This observation in Lis1-deficient cells together with the evidence for longer CLIP-115 tails at the plus-ends of microtubules strongly argues that Lis1 plays a role in controlling the speed of microtubular growth. It is unclear how this observation relates to the documented role of Lis1 in preventing catastrophic breakdown of microtubules.

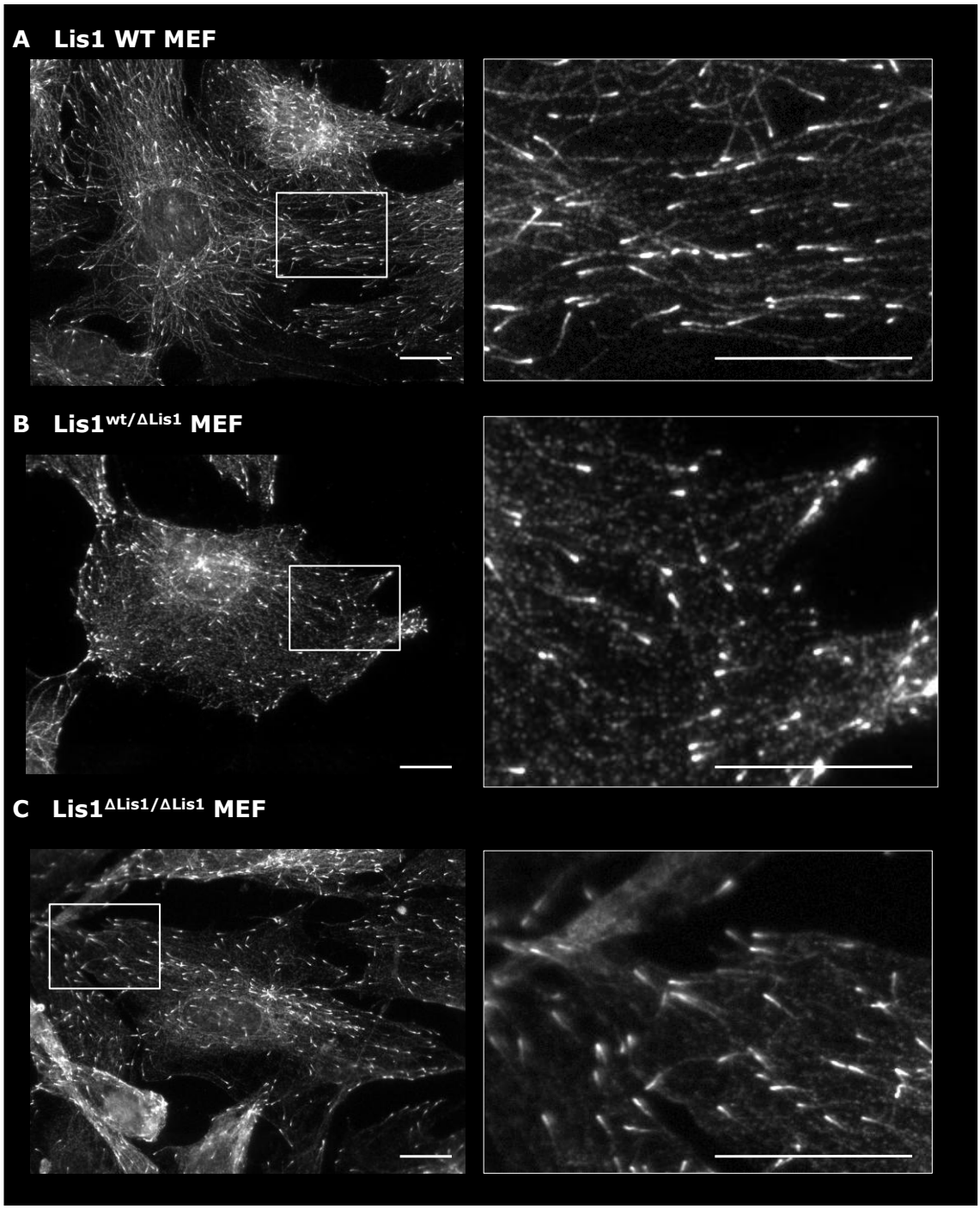

Figure 38. EB1 localization is unaffected by levels of Lis1
MEFs were analyzed 72hrs after infections with AD-CRE. The immunofluorescence detection of endogenous EB1 illustrates no significant differences in the distribution and the level of the plus-end binding protein between wild type (A) and Lis1 mutant MEFs (B, C). The left panel shows EB1 localization in an entire cell while the right panel represents the indicated detail of cell periphery. Scale bars: 20 µm.

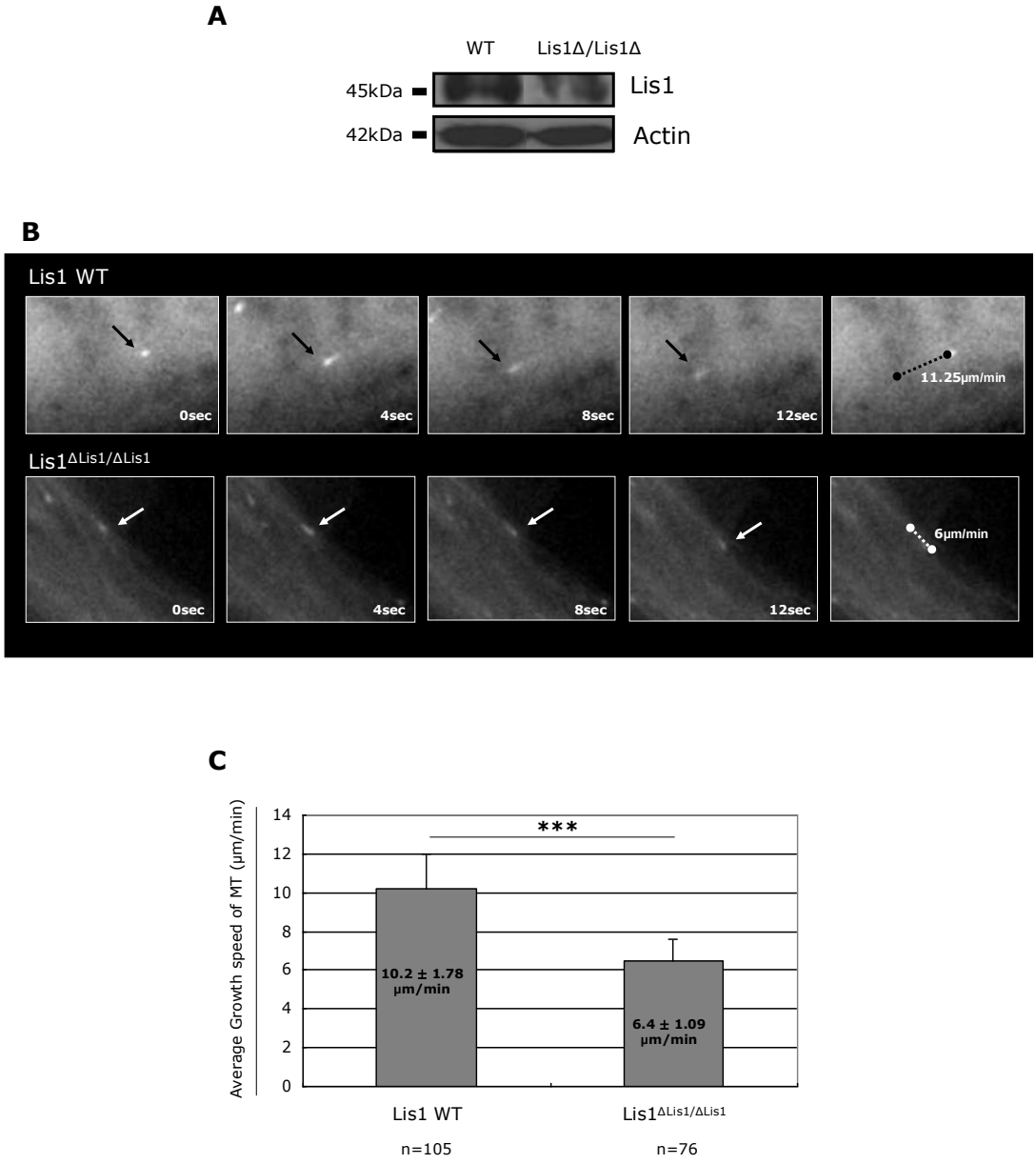

Figure 39. Lis1 affects microtubule growth speed

A. Western blot of protein extracts (10µg total protein) form wild type and Lis1 Lis1$^{\Delta Lis1/\Delta Lis1}$ MEFs 24hrs after transfection of mCherry-CRE, reveal decreased levels of Lis1 protein in Lis1$^{\Delta Lis1/\Delta Lis1}$ MEFs compared with wild type. Actin was used to monitor gel loading.

B. Representative time-lapse images of wild type and Lis1$^{\Delta Lis1/\Delta Lis1}$ MEFs transiently expressing GFP-EB1. The arrows indicate a single plus-end tip as visualized by GFP-EB1 signal that is followed in wild type and mutant MEFs during the indicated time frame. This allowed the precise determination of the microtubular growth rate.

C. Quantitative analysis of the speed of growing MT shows that the MT growth speeds in Lis1-deficient cells (6.4 ± 1.78µm/min) are slower than wild type (10.2 ± 1.09µm/min). The error bars represent the standard deviation of repeated measurement, the n of which is indicated. The statistical significance (***, P<0.001) was determined by *t*-test. For all experiments shown in panels B and C, MEFs were analyzed 24hrs after transfection with GFP-EB1 and mCherry-CRE. Double-positive cells were imaged at 4s intervals during 5mins using suitable video microscopy (Zeiss). The growth speed of microtubules was analyzed by Metamorph program.

4. Discussion

Mutations in the Lis1 gene have been reported to be responsible for type I lissencephaly. Numerous studies were performed to investigate the molecular functions of Lis1. From these investigations, it becomes clear that Lis1 plays a role as subunit of the PAF-AH complex that regulates the activity of PAF (Reiner et al., 1993). PAF is a potent phospholipid that regulates various physiological processes, particularly in the central nervous system and reproductive organs (Roudebush, 2001; Hattori et al., 1994; Umemura e tal., 2007). In addition, Lis1 interacts with the cytoskeleton and seems to regulate microtubule dynamics. These microtubule-associated roles include mitotic and meiotic cell division, nuclear migration, vesicular transport, and neuronal migration (Sapir et al., 1997; Smith et al., 2000; Sasaki et al., 2000).

Lis1 protein in testis appears to be required for proper germ cell development as Lis1 mutant males are infertile and show defects in spermatogenesis (Nayernia et al., 2003). Here, I describe the approach to investigate further details of the functional role of Lis1 during spermatogenesis. Screening of an adult mouse testis cDNA library by the yeast two-hybrid assay identified three novel candidate proteins that can bind to Lis1 protein. These include Ranbp9 (Ran binding protein 9), ACT (activator of CREM in testis), and BRAP (BRCA1 associated protein) that interact with Lis1 similar to the known binding partner NudeL.

The present study demonstrates by different methods and techniques physical interactions between Lis1 and Ranbp9, ACT, or BRAP. Moreover, it shows that the 7 WD-40 repeat motifs of Lis1 mediate the interactions with Ranbp9, ACT, and BRAP. Interestingly, the 7 WD-40 repeat motifs of Lis1 are known to be involved in a variety of protein-protein interactions and cellular functions including signal transduction, cytoskeleton regulation, and regulation of vesicular transports (reviewed in Li and Roberts, 2001).

Possible roles of Ranbp9 in its cytoplasmic association with Lis1

Ranbp9 protein constitutes a novel Lis1 binding protein that interacts with Lis1 via its SPRY domain. Interestingly, the Lis1 homology motif that is also present Ranbp9, does not mediate interaction with Lis1. I find Ranbp9 predominantly in the cytoplasm, in good agreement with previous studies (Nishitani et al., 2001). Confocal microscopy and bimolecular complementation assays in mammalian tissue culture cells indicate that Lis1 and Ranbp9 can associate in the cytoplasm and reduction of Lis1 levels result in depletion of Ranbp9, most notably in the cell periphery.

My observations suggest that Ranbp9 in association with Lis1 may be linked to the cytoskeleton. Although the relationship of Ranbp9 and microtubules is not known, recent studies on Ran binding proteins, including Ranbp9, provide arguments for such an association.

Ranbp9 was originally identified as one of several proteins that bind to the small GTPase Ran, a key molecule involved in unclear transport of macromolecules (Nakamura et al., 1998). Ran also plays a role in the assembly of the spindle complex in mitotic cells (Kalab et al., 1999; Kahana and Cleveland, 1999). Recent data suggests that Ran may also be involved in axonal transport in postmitotic neurons (reviewed in Yudin and Fainzilber, 2009).

The evolutionary conserved Ranbp1 in yeast cells (termed yrb1) is essential for the correct alignment of mitotic spindles (Ouspenski, 1998). In mammalian cells, Ranbp1 was shown *in vivo* to be part of mitosis (Guarguaglini et al., 2000). Furthermore, RanbpM, a truncated form of Ranbp9, was initially described in the centrosome of human lung fibroblasts (MRC-5), where it may control microtubular dynamics (Nakamura et al., 1998). In *Xenopus laevis*, members of the family of Ran binding proteins control mitosis (Carazo-Salas et al., 1999; Wilde and Zheng, 1999). Taken together the various reports, it seems likely that Ran and its binding partners, Ranbps, may be associated with the cytoskeleton.

This view is supported by my own investigations demonstrating that Ranbp9 binds to the microtubule-associated protein Lis1.

The newly identified Ranbp10 protein, a close relative of Ranbp9, interacts with β-tubulin via its N-terminus (Schulze et al., 2008). Interestingly, both Ranbp9 and Ranbp10 share homology with guanine nucleotide exchange factors (GEFs), in particular with Rho-GEF. Usually, small GTPase, like Ran, display weak nucleotide exchange activity that is significantly enhanced by specific GEFs. The only known Ran-GEF factor so far is the nuclear protein Rcc1 (Schulze et al., 2008). However, it was demonstrated recently that Ranbp10 is also able to mediate the exchange of GDP for GTP in the Ran protein (Schulze et al., 2008). It is therefore tempting to speculate that Ranbp9 protein on microtubules may also exert GEF activity.

The transcriptional regulator ACT forms complexes with Lis1 in the cytoplasm of spermatogenic cells in testis

Lis1 is abundantly expressed in testis and particularly enriched in meiotically dividing spermatocytes and elongating spermatids (Koizumi et al., 2003). Male Lis1 mutant mice with a homozygous gene trap integration in the Lis1 locus ($Lis1^{GT/GT}$) are infertile and display severe defects in spermatogenesis suggesting that Lis1 is essential for male germ cell development (Nayernia et al., 2003).

Here, I discovered that the germ cell specific transcription factor ACT binds to Lis1 in a yeast two-hybrid assay. ACT regulates the process of male germ cell differentiation by interacting with CREM, a key factor for the regulation of numerous postmeiotic genes during spermatid maturation (De Cesare et al., 2003). ACT expression is restricted to late spermatogenetic cells (Fimia et al., 1999). A homozygous deletion of the ACT gene results in drastic oligozoospermia, although testis development in ACT-deficient mice appears normal. This data suggests that ACT is involved in regulating genes for structural components of mature sperm (Kotaja et al., 2004).

The Lis1 gene trap integration described previously (Nayernia et al., 2003) affects nuclear condensation, formation of the tail structure, and development of the acrosome in spermatids. This phenotype is similar to ACT null mice which produce spermatids with abnormal nuclear condensation, vacuoles, defects in acrosome organization, and folded tails (Nayernia et al., 2003; Kotaja et al., 2004) suggesting that both, Lis1 and ACT, may have functions in overlapping processes during late

spermatogenesis. This hypothesis is actually supported by my observation that ACT and Lis1 are able to form complexes.

ACT is a LIM-only protein which consists of four and a half LIM domains (Fimia et al., 1999). The LIM domain is a cysteine-rich zinc-finger motif that is found in many proteins involved in the regulation of cellular processes via protein-protein interactions including gene expression, signal transduction, and cytoskeletal regulation (Review in Kadrmas and Becjerle, 2004). During spermatogenesis, ACT is initially present in the nucleus of round spermatids and translocates to the cytoplasm in elongated spermatids. The cytoplasmic localization of ACT is regulated by KIF17b, a testis-specific isoform of the brain kinesin2 motor protein KIF17 (Kotaja et al., 2005).

On tissue section of testis, I could show that endogenous ACT protein colocalizes with Lis1 in late spermatogenetic cells. BiFC assays in HeLa cells also revealed that the Lis1-ACT protein interaction occurs predominantly in the cytoplasm. Based on these results one may assume that the Lis1-ACT complex in elongated spermatids is also in the cytoplasm. Moreover, preliminary data show that overexpressed ACT in wild type MEFs distributes to the cytoplasm and to the nucleus, whereas in MEFs with reduced levels of Lis1 it predominantly goes to the nucleus (preliminary data not shown). These observations are compatible with the idea that Lis1 may function as a cytoplasmic retention protein for ACT.

Previous studies demonstrated that the third LIM domain of ACT is required for association with CREM (Fima et al., 1999) and that all LIM domains of ACT are necessary for the interaction with KIF17b (Kotaja et al., 2005). I characterized the interaction between Lis1 and ACT and demonstrated that all LIM domains are required for the interaction with Lis1. The fact that ACT binding to both, Lis1 and KIF17b requires all LIM domains is interesting, because it raises the question whether or not both proteins can interact simultaneously with ACT or alternatively bind in a competitive manner.

Formally, it can also not be ruled out that ACT functions as an adaptor protein between KIF17b and Lis1. While it is clear that ACT in association with KIF17b can be transported to the cytoplasm where it possibly also interacts with Lis1, a cytoplasmic function of ACT has not been identified yet and awaits further

investigation.

The proteins of the kinesin superfamily (KIFs) are motor proteins that participate in various cellular functions, such as chromosomal and spindle movements during cell division, and transport of organelles and molecules (reviewed in Miki et al., 2001). Kinesin-1 is a motor protein for anterograde axonal transport. Lis1 forms a complex with cytoplasmic dynein and tubulins for migration towards the microtubule plus-ends in a kinesin-1 dependent manner (Yamada et al., 2008). Interestingly, DISC1, a candidate gene for susceptibility to schizophrenia, interacts with KIF-1 that regulates the localization of Lis1 and NudeL in axons as a cargo receptor for axon elongation (Taya et al., 2007). KIF-17b associates with microtubules and mediates movement of organelles, vesicles, and proteins (reviewed in Monaco et al., 2004). Despite the structural links between Lis1, KIF-17b, and ACT the functional roles of these interactions in spermiogenesis remain to be discovered.

Putative role of the Lis1 and BRAP complex

The search for novel proteins that interact with Lis1 lead to the discovery of BRAP in the yeast two-hybrid screen. All isolated BRAP cDNA clones contained only coding sequence for the coiled-coil domain indicating that this part of BRAP is sufficient for the interaction with Lis1.

BRAP is ubiquitously expressed and particularly enriched in testis (Li et al., 1998). Expression of BRAP overlaps with Lis1 in spermatogenic cells, however, little is known about BRAP function during spermatogenesis.

BRAP was originally identified as a protein that specifically binds to the nuclear localization signal (NLS) motif of the breast cancer suppressor protein BRCA1 (Chen et al., 1996). BRAP protein is mainly found in the cytoplasm as previously shown with antibodies against BRAP and also in this study using HA or eGFP tagged BRAP (Asada et al., 2004; Li et al., 1998; Ozaki et al., 2009). Accordingly BRAP may regulate the translocation of nuclear proteins from the cytoplasm to the nucleus (Li et al., 1998).

The coiled-coil domain at the C-terminus of BRAP is sufficient to bind to the NLS motif of the cell cycle inhibitor p21 whereby it is maintained in the cytoplasm (Asada et al., 2004). I here demonstrated that the C-terminal coiled-coil domain is also sufficient for the interaction with Lis1. In contrast, the NLS motif of BRCA1 is recognized by the N-terminus of BRAP (Li et al., 1998) which is independently also able to bind to Lis1, in addition to the C-terminus. Thus, both domains of BRAP can mediate interaction with Lis1, and one can speculate that this may possibly occur in different cellular functions.

Transport between the cytoplasm and nucleus is highly regulated by translocating shuttling carriers, such as importin and exportin complexes. Cytoplasmic retention proteins control nuclear transport through the identification of NLS sequences (reviewed in Cyert, 2001). For example, subcellular localization of NF-κB is determined by IκB (reviewed in Cyert, 2001). The NF-κB family of transcription factors contains highly conserved NLS motifs which directly cooperate with IκB/MAD-3 protein. Phosphorylated IκB is released from NF-κB and this allows nuclear translocation of NF-κB.

Previous studies have demonstrated that BRAP interacts with Galectin-2, a member of galactose-binding lectins, which binds to tubulin and microtubules (Ozaki et al., 2009). This observation might be related to a peculiar perinuclear localization of BRAP that seems to reflect part of the Golgi complex (Fig. 26). Since formation and positioning of Golgi vesicles occurs along microtubules and cytoplasmic dynein and Lis1 participate in this process (Harada et al., 1998; Smith et al., 2000), BRAP may also be recruited by Lis1 or galectin-2 to microtubules that functionally interact with the Golgi apparatus. This hypothesis, however awaits further investigations.

BRAP has also been proposed to impede mitogenic signal propagation, referred to as IMP. The MAP kinase signaling pathway regulates a broad range of cellular responses, such as cell survival, cell division, proliferation, differentiation, and transformation. BRAP can play a role in the MAP kinase signal pathway acting as IMP (Matheny et al., 2004). The N-terminus of BRAP contains a putative RING-H2 domain, common in ubiquitination, with Ras-responsive E3 ubiquitin ligase activity (Matheny et al., 2004). BRAP can be modified by auto-polyubiquitination depending on Ras activity. The Ring Finger domain in the predicted structure of BRAP is followed by a Znf-UBP, and a coiled-coil domain (SMART, smart.embl-heidelberg.de)

resembling the domain architecture of the RING B-box coiled-coil (RBCC) family of proteins (Jensen et al., 2001). The RBCC proteins are involved in various cellular processes including cell cycle regulation and apoptotic cell death. Mutations of RBCC have been found in many pathological conditions (reviewed in Meroni and Diez-Roux, 2005).

Lis1 protein affects the dynamic organization of microtubules

Lis1 is an essential factor for cell viability and represents an important microtubule associated protein (Sapir et al., 1997), that interacts through most (if not all) of its WD-40 repeat domains with tubulin (Caspi et al., 2003). By immunofluorescence analysis of the cytoskeleton of MEFs I find that microtubules in the absence of Lis1 do not fully extend to the cell periphery and show decreased complexity of the microtubular network at the cell cortex, in good agreement with a recent report (Yingling et al, 2008). I also find that the level of acetylated tubulin is affected in Lis1-deficient cells suggesting that Lis1 might play a role for the stability of microtubules. Astral acetylated tubulin fibers are shortened and sparse and the level of acetylated tubulin protein is significantly decreased in cells deprived of Lis1. It is known that acetylation of α-tubulin is a post-translational modification that can control microtubular dynamics, cytoskeletal remodeling, and cell motility (Creppe et al., 2009; Tran et al., 2007; Dompierre et al., 2007; Reed et al., 2006). Failure to acetylate the tubulin network possibly results in developmental brain defects including altered radial migration and aberrant neuronal branching (Creppe et al., 2009). On the contrary, hyperacetylation of microtubule has been suggested to be associated with increased cell spreading (Tran et al., 2007). It also may provoke increased binding of motor proteins, such as kinesin-1 and cytoplasmic dynein, both proteins known to regulate bidirectional cargo transport (Dompierre et al., 2007; Reed et al., 2006).

Interestingly, microtubules are highly stabilized in spermatid manchettes (Akhmanova et al., 2005) and Nayernia et al. (2003) confirmed that spermatid manchettes are tightly associated with Lis1. It would be of interest to examine the acetylation of tubulin in the manchette of spermatids from the homozygous gene trap mutant mouse to obtain additional insights into the involvement of Lis1 and microtubules during spermatogenesis.

In general, Lis1 regulates microtubular dynamics by affecting their catastrophe rate e.g. the transition from growth to shortening of microtubules (Sapir et al., 1997). According to this view, diminishing the cellular levels of Lis1 could cause the microtubular network to become instable and result in enhanced depolymerization rate of single fibers. In addition, Lis1 may also affect the cytoskeleton by influencing the plus-ends of microtubules. Microtubules show dynamic instability with constant transitions between phases of growth and shrinkage (Horio et al., 1986). The tips of microtubules represent highly sensitive and important sites that directly control their growth (Yingling et al., 2008; reviewed in Kardon and Vale, 2009). Microtubular polymerization generates a large number of binding sites for so-called plus-end binding proteins, which include EB1, CLIP-170, and CLIP-115. During microtubular growth these molecules disappear from the growing fiber and only transiently decorate a defined area at the tip of the tubular plus-end (Dragestein et al., 2008). The equilibrium between microtubules and plus-end binding proteins might be affected by post-translational modifications, conformational changes, and protein-protein interactions (Dragestein et al., 2008).

Interestingly, in MEFs deprived of Lis1 I observed significantly augmented decoration by CLIP-115 at the tips of microtubules. A difference in plus-end accumulation of CLIP-170 was not detected.

A possible explanation for this observation might be that in the absence of Lis1 more CLIP-115 binding sites may be available at the plus-end tips of microtubules. Normally, Lis1 may facilitate the binding of specific factors to the microtubular tip-end. When concentrations of Lis1 at the cell cortex are decreasing previously occupied sites can now become available for CLIP-115 to bind. Interestingly, it is known that CLIP-115 competes with other proteins, including CLIP-170, for microtubule plus-end binding sites (Hoogenraad et al., 2002). In addition, the dynactin complex, responsible for targeting cytoplasmic dynein to the microtubule plus-end, contains a subunit, termed $p150^{glued}$, which is structurally related to the CLIP proteins (Lansbergen et al., 2004). It was shown previously that CLIP-115 competes with both $p150^{glued}$ and Lis1 for binding to the zinc fingers at the C-terminus of CLIP-170 (Lansbergen et al., 2004) and Lis1 is essential for localization of $p150^{glued}$ at the cell cortex (Smith et al., 2000). It is possible that lack of Lis1 leads to a depletion of microtubule associated $p150^{glued}$ thereby allowing more CLIP-115 at the growing microtubule plus-end. The association and dissociation of CLIP-

115 with microtubules seems to be regulated by phosphorylation and dephosphorylation cycles (Rickard and Kreis, 1991). It is interesting to speculate that reduced levels of Lis1 may affect phosphorylation of CLIP-115, thereby changing the interaction with the microtubules. In the future, CLIP-115 phosphorylation should be determined when the cellular levels of Lis1 are reduced.

The rapid growth response to various environmental signals can influence the dynamic instability of microtubules (Sapir et al., 1997). I could show by live cell imaging of $Lis1^{\Delta Lis1/\Delta Lis1}$ MEFs transfected with GFP-EB1 that the growth speed of microtubules at the plus-end was significantly reduced (as measured by GFP-EB1 velocity). This data suggests that Lis1 regulates the microtubule dynamics by affecting microtubule growth speed. The direct cause of the slow velocity of growing microtubule ends in Lis1-deficient cells remains currently unclear, but it seems to be related to the comet tail length at the plus-end of microtubules.

The microtubule plus-end decoration reflects the binding of plus-end tracking proteins to the growing end of microtubules. Hence, it is tempting to hypothesize that it might require more time to decorate the plus-end of microtubules in the absence of Lis1, measurable as a slow velocity of the growing microtubule. However these relationships need to be elucidated in detail in the future.

5. References

Abdollahi MR, Morrison E, Sirey T, Molnar Z, Hayward BE, Carr IM, Springell K, Woods CG, Ahmed M, Hattingh L, Corry P, Pilz DT, Stoodley N, Crow Y, Taylor GR, Bonthron DT, Sheridan E. (2009) Mutation of the variant alpha-tubulin TUBA8 results in polymicrogyria with optic nerve hypoplasia. Am J Hum Genet. 85(5):737-44.

Ahmad FJ, Echeverri CJ, Vallee RB, Baas PW. (1998) Cytoplasmic dynein and dynactin are required for the transport of microtubules into the axon. J Cell Biol. 140(2):391-401.

Akhmanova A, Mausset-Bonnefont AL, van Cappellen W, Keijzer N, Hoogenraad CC, Stepanova T, Drabek K, van der Wees J, Mommaas M, Onderwater J, van der Meulen H,Tanenbaum ME, Medema RH, Hoogerbrugge J, Vreeburg J, Uringa EJ, Grootegoed JA, Grosveld F, Galjart N. (2005) The microtubule plus-end-tracking protein CLIP-170 associates with the spermatid manchette and is essential for spermatogenesis. Genes Dev. 19(20):2501-15.

Angle MJ, Tom R, Jarvi K, McClure RD. (1993) Effect of platelet-activating factor (PAF) on human spermatozoa-oocyte interactions. J Reprod Fertil. 98(2):541-8.

Arai R, Nakagawa H, Kitayama A, Ueda H, Nagamune T. (2002) Detection of protein-protein interaction by bioluminescence resonance energy transfer from firefly luciferase to red fluorescent protein. J Biosci Bioeng. 94(4):362-4.

Asada M, Ohmi K, Delia D, Enosawa S, Suzuki S, Yuo A, Suzuki H, Mizutani S. (2004) Brap2 functions as a cytoplasmic retention protein for p21 during monocyte differentiation. Mol Cell Biol. 24(18):8236-43.

Askham JM, Vaughan KT, Goodson HV, Morrison EE. (2002) Evidence that an interaction between EB1 and p150(Glued) is required for the formation and maintenance of a radial microtubule array anchored at the centrosome. Mol Biol Cell. 13(10):3627-45.

Assadi AH, Zhang G, Beffert U, McNeil RS, Renfro AL, Niu S, Quattrocchi CC, Antalffy BA, Sheldon M, Armstrong DD, Wynshaw-Boris A, Herz J, D'Arcangelo G, Clark GD. (2003) Interaction of reelin signaling and Lis1 in brain development. Nat Genet. 35(3):270-6.

Bach I. (2000) The LIM domain: regulation by association. Mech Dev. 91(1-2):5-17.

Barra HS, Arce CA, Rodríguez JA, Caputto R. (1974) Some common properties of the protein that incorporates tyrosine as a single unit and the microtubule proteins. Biochem Biophys Res Commun. 60(4):1384-90.

Bennett WI, Gall AM, Southard JL, Sidman RL. (1971) Abnormal spermiogenesis in quaking, a myelin-deficient mutant mouse. Biol Reprod. 5(1):30-58.

Bieling P, Kandels-Lewis S, Telley IA, van Dijk J, Janke C, Surrey T. (2008) CLIP-170 tracks growing microtubule ends by dynamically recognizing composite EB1/tubulin-binding sites. J Cell Biol. 183(7):1223-33.

Binker MG, Zhao DY, Pang SJ, Harrison RE. (2007) Cytoplasmic linker protein-170 enhances spreading and phagocytosis in activated macrophages by stabilizing microtubules. J Immunol. 179(6):3780-91.

Brkovic A, Sirois MG. (2007) Vascular permeability induced by VEGF family members in vivo: role of endogenous PAF and NO synthesis. J Cell Biochem. 100(3):727-37.

Bulinski JC. (2007) Microtubule modification: acetylation speeds anterograde traffic flow. Curr Biol. 17(1):R18-20.

Bullock WO, Fernandez JM, Short JMS. (1987) Xl1-Blue: a high efficiency plasmid transforming recA Escherichia coli strain with beta-galactosidase selection. BioTechniques. 5(4): 376-379

Burkhard P, Stetefeld J, Strelkov SV. (2001) Coiled coils: a highly versatile protein folding motif. Trends Cell Biol. 11(2):82-8.

Cahana A, Escamez T, Nowakowski RS, Hayes NL, Giacobini M, von Holst A, Shmueli O, Sapir T, McConnell SK, Wurst W, Martinez S, Reiner O. (2001) Targeted mutagenesis of Lis1 disrupts cortical development and LIS1 homodimerization. Proc Natl Acad Sci U S A. 98(11):6429-34.

Carazo-Salas RE, Guarguaglini G, Gruss OJ, Segref A, Karsenti E, Mattaj IW. (1999) Generation of GTP-bound Ran by RCC1 is required for chromatin-induced mitotic spindle formation. Nature. 400(6740):178-81.

Caspi M, Coquelle FM, Koifman C, Levy T, Arai H, Aoki J, De Mey JR, Reiner O. (2003) LIS1 missense mutations: variable phenotypes result from unpredictable alterations in biochemical and cellular properties. J Biol Chem. 278(40):38740-8.

Chien CT, Bartel PL, Sternglanz R, Fields S. (1991) The two-hybrid system: a method to identify and clone genes for proteins that interact with a protein of interest. Proc Natl Acad Sci USA. 88: 9578–9582.

Coquelle FM, Caspi M, Cordelières FP, Dompierre JP, Dujardin DL, Koifman C, Martin P, Hoogenraad CC, Akhmanova A, Galjart N, De Mey JR, Reiner O. (2002) LIS1, CLIP-170's key to the dynein/dynactin pathway. Mol Cell Biol. 22(9):3089-102.

Creppe C, Malinouskaya L, Volvert ML, Gillard M, Close P, Malaise O, Laguesse S, Cornez I, Rahmouni S, Ormenese S, Belachew S, Malgrange B, Chapelle JP, Siebenlist U,Moonen G, Chariot A, Nguyen L. (2009) Elongator controls the migration and differentiation of cortical neurons through acetylation of alpha-tubulin. Cell. 136(3):551-64.

Curtiss J, Heilig JS. (1998) DeLIMiting development. Bioessays. 20(1):58-69.

Cyert MS. (2001) Regulation of nuclear localization during signaling. J Biol Chem. 276(24):20805-8.

Dawe AL, Caldwell KA, Harris PM, Morris NR, Caldwell GA. (2001) Evolutionarily conserved nuclear migration genes required for early embryonic development in Caenorhabditis elegans. Dev Genes Evol. 211(8-9):434-41.

Dawid IB, Breen JJ, Toyama R. (1998) LIM domains: multiple roles as adapters and functional modifiers in protein interactions. Trends Genet. 14(4):156-62.

De Cesare D, Fimia GM, Brancorsini S, Parvinen M, Sassone-Corsi P. (2003) Transcriptional control in male germ cells: general factor TFIIA participates in CREM-dependent gene activation. Mol Endocrinol. 17(12):2554-65.

Denti S, Sirri A, Cheli A, Rogge L, Innamorati G, Putignano S, Fabbri M, Pardi R, Bianchi E. (2004) RanBPM is a phosphoprotein that associates with the plasma membrane and interacts with the integrin LFA-1. J Biol Chem. 79(13):13027-34.

De Zeeuw CI, Hoogenraad CC, Goedknegt E, Hertzberg E, Neubauer A, Grosveld F, Galjart N. (1997) CLIP-115, a novel brain-specific cytoplasmic linker protein, mediates the localization of dendritic lamellar bodies. Neuron. 19(6):1187-99.

Diamantopoulos GS, Perez F, Goodson HV, Batelier G, Melki R, Kreis TE, Rickard JE. (1999) Dynamic localization of CLIP-170 to microtubule plus ends is coupled to microtubule assembly. J Cell Biol. 144(1):99-112.

Dobyns WB. (1989) The neurogenetics of lissencephaly. Neurol Clin. 7(1):89-105.

Dompierre JP, Godin JD, Charrin BC, Cordelières FP, King SJ, Humbert S, Saudou F. (2007) Histone deacetylase 6 inhibition compensates for the transport deficit in Huntington's disease by increasing tubulin acetylation. 27(13):3571-83.

Dragestein KA, van Cappellen WA, van Haren J, Tsibidis GD, Akhmanova A, Knoch TA, Grosveld F, Galjart N. (2008) Dynamic behavior of GFP-CLIP-170 reveals fast protein turnover on microtubule plus ends. J Cell Biol. 180(4):729-37.

Efimov VP, Morris NR. (2000) The LIS1-related NUDF protein of Aspergillus nidulans interacts with the coiled-coil domain of the NUDE/RO11 protein. J Cell Biol. 150(3):681-8.

Eipper BA. (1972) Rat brain microtubule protein: purification and determination of covalently bound phosphate and carbohydrate. Proc Natl Acad Sci U S A. 69(8):2283-7.

Emes RD, Ponting CP. (2001) A new sequence motif linking lissencephaly, Treacher Collins and oral-facial-digital type 1 syndromes, microtubule dynamics and cell migration. Hum Mol Genet. 10(24):2813-20.

Faulkner NE, Dujardin DL, Tai CY, Vaughan KT, O'Connell CB, Wang Y, Vallee RB. (2000) A role for the lissencephaly gene LIS1 in mitosis and cytoplasmic dynein function. Nat Cell Biol. 2(11):784-91.

Feng Y, Olson EC, Stukenberg PT, Flanagan LA, Kirschner MW, Walsh CA. (2000) LIS1 regulates CNS lamination by interacting with mNudE, a central component of the centrosome. Neuron. 28(3):665-79.

Fields S, Song O. (1989) A novel genetic system to detect protein-protein interactions. Nature. 340(6230):245-6.

Fimia GM, De Cesare D, Sassone-Corsi P. (1999) CBP-independent activation of CREM and CREB by the LIM-only protein ACT. Nature. 398(6723):165-9.

Gambello MJ, Darling DL, Yingling J, Tanaka T, Gleeson JG, Wynshaw-Boris A. (2003) Multiple dose-dependent effects of Lis1 on cerebral cortical development. J Neurosci. 23(5):1719-29.

Gard DL, Kirschner MW. (1985) A polymer-dependent increase in phosphorylation of beta-tubulin accompanies differentiation of a mouse neuroblastoma cell line. J Cell Biol. 100(3):764-74.

Geier G, Jacob E, Stöcker W, Zwilling R. (1997) Genomic organization of the zinc-endopeptidase astacin. Arch Biochem Biophys. 337(2):300-7.

Gerlitz G, Darhin E, Giorgio G, Franco B, Reiner O. (2005) Novel functional features of the Lis-H domain: role in protein dimerization, half-life and cellular localization. Cell Cycle. 4(11):1632-40.

Gilbert, S. F. (2003). Developmental Biology, 7th edn. Sunderland, MA: Sinaue Associates.

Gluzman Y. (1981) SV40-transformed simian cells support the replication of early SV40 mutants. Cell. 23(1):175-82.

Gossen M, Bujard H. (1992) Tight control of gene expression in mammalian cells by tetracycline-responsive promoters. Proc Natl Acad Sci U S A. 89(12):5547-51.

Graham FL, Smiley J, Russell WC, Nairn R. (1977) Characteristics of a human cell line transformed by DNA from human adenovirus type 5. J Gen Virol. 36(1):59-74.

Guarguaglini G, Renzi L, D'Ottavio F, Di Fiore B, Casenghi M, Cundari E, Lavia P. (2000) Regulated Ran-binding protein 1 activity is required for organization and function of the mitotic spindle in mammalian cells in vivo. Cell Growth Differ. 11(8):455-65.

Guerrini R, Parrini E. (2009) Neuronal migration disorders. Neurobiol Dis.

Haase A, Nordmann C, Sedehizade F, Borrmann C, Reiser G. (2008) RanBPM, a novel interaction partner of the brain-specific protein p42(IP4)/centaurin alpha-1. J Neurochem. 105:2237-2248.

Hammond JW, Cai D, Verhey KJ. (2008) Tubulin modifications and their cellular functions. Curr Opin Cell Biol. 20(1):71-6.

Harada A, Takei Y, Kanai Y, Tanaka Y, Nonaka S, Hirokawa N. (1998) Golgi vesiculation and lysosome dispersion in cells lacking cytoplasmic dynein. J Cell Biol. 141(1):51-9.

Hattori M, Adachi H, Tsujimoto M, Arai H and Inoue K. (1994) Miller-Dieker lissencephaly gene encodes a subunit of brain platelet-activating factor. Nature 370: 216-218.

He TC, Zhou S, da Costa LT, Yu J, Kinzler KW, Vogelstein B. (1998) A simplified system for generating recombinant adenoviruses. Proc Natl Acad Sci U S A. 95(5):2509-14.

Hilton DJ, Richardson RT, Alexander WS, Viney EM, Willson TA, Sprigg NS, Starr R, Nicholson SE, Metcalf D, Nicola NA. (1998) Twenty proteins containing a C-terminal SOCS box form five structural classes. Proc Natl Acad Sci U S A. 95(1):114-9.

Holzbaur EL, Vallee RB. (1994) DYNEINS: molecular structure and cellular function. Annu Rev Cell Biol. 10:339-72.

Hoogenraad CC, Akhmanova A, Grosveld F, De Zeeuw CI, Galjart N. (2000) Functional analysis of CLIP-115 and its binding to microtubules. J Cell Sci. 113(Pt 12):2285-97.

Hoogenraad CC, Koekkoek B, Akhmanova A, Krugers H, Dortland B, Miedema M, van Alphen A, Kistler WM, Jaegle M, Koutsourakis M, Van Camp N, Verhoye M, van der Linden A, Kaverina I, Grosveld F, De Zeeuw CI, Galjart N. (2002) Targeted mutation of Cyln2 in the Williams syndrome critical region links CLIP-115 haploinsufficiency to neurodevelopmental abnormalities in mice. Nat Genet. 32(1):116-27.

Horio T, Hotani H. (1986) Visualization of the dynamic instability of individual microtubules by dark-field microscopy. 321(6070):605-7.

Hirokawa N. (1998) Kinesin and dynein superfamily proteins and the mechanism of organelle transport. Science. 279(5350):519-26.

Hirotsune S, Fleck MW, Gambello MJ, Bix GJ, Chen A, Clark GD, Ledbetter DH, McBain CJ, Wynshaw-Boris A. (1998) Graded reduction of Pafah1b1 (Lis1) activity results in neuronal migration defects and early embryonic lethality. Nat Genet. 19(4):333-9.

Jaglin XH, Poirier K, Saillour Y, Buhler E, Tian G, Bahi-Buisson N, Fallet-Bianco C, Phan-Dinh-Tuy F, Kong XP, Bomont P, Castelnau-Ptakhine L, Odent S, Loget P, Kossorotoff M, Snoeck I, Plessis G, Parent P, Beldjord C, Cardoso C, Represa A, Flint J, Keays DA, Cowan NJ, Chelly J. (2009) Mutations in the beta-tubulin gene TUBB2B result in asymmetrical polymicrogyria. Nat Genet.

James P, Halladay J, Craig EA. (1996) Genomic libraries and a host strain designed for highly efficient two-hybrid selection in yeast. Genetics. 144: 1425–1436.

Jensen K, Shiels C, Freemont PS. (2001) PML protein isoforms and the RBCC/TRIM motif. Oncogene. 20(49):7223-33.

Kadrmas JL, Beckerle MC. (2004) The LIM domain: from the cytoskeleton to the nucleus. Nat Rev Mol Cell Biol. 5(11):920-31.

Kahana JA, Cleveland DW. (1999) Beyond nuclear transport. Ran-GTP as a determinant of spindle assembly. J Cell Biol. 146(6):1205-10.

Kalab P, Pu RT, Dasso M. (1999) The ran GTPase regulates mitotic spindle assembly. Curr Biol. 9(9):481-4.

Keays DA, Tian G, Poirier K, Huang GJ, Siebold C, Cleak J, Oliver PL, Fray M, Harvey RJ, Molnár Z, Piñon MC, Dear N, Valdar W, Brown SD, Davies KE, Rawlins JN, Cowan NJ, Nolan P, Chelly J, Flint J. (2007) Mutations in alpha-tubulin cause abnormal neuronal migration in mice and lissencephaly in humans. Cell. 128(1):45-57.

Kerjan G, Gleeson JG. (2007) Genetic mechanisms underlying abnormal neuronal migration in classical lissencephaly. Trends Genet. 23(12):623-30.

Kim MH, Cooper DR, Oleksy A, Devedjiev Y, Derewenda U, Reiner O, Otlewski J, Derewenda ZS. (2004) The structure of the N-terminal domain of the product of the lissencephaly gene Lis1 and its functional implications. Structure. 12(6):987-98.

Koizumi H, Yamaguchi N, Hattori M, Ishikawa TO, Aoki J, Taketo MM, Inoue K, Arai H. (2003) Targeted disruption of intracellular type I platelet activating factor-acetylhydrolase catalytic subunits causes severe impairment in spermatogenesis. J Biol Chem. 278(14):12489-94.

Komarova Y, De Groot CO, Grigoriev I, Gouveia SM, Munteanu EL, Schober JM, Honnappa S, Buey RM, Hoogenraad CC, Dogterom M, Borisy GG, Steinmetz MO, Akhmanova A. (2009) Mammalian end binding proteins control persistent microtubule growth. J Cell Biol. 184(5):691-706.

Kotaja N, De Cesare D, Macho B, Monaco L, Brancorsini S, Goossens E, Tournaye H, Gansmuller A, Sassone-Corsi P. (2004) Abnormal sperm in mice with targeted deletion of the act (activator of cAMP-responsive element modulator in testis) gene. Proc Natl Acad Sci U S A. 101(29):10620-5.

Kotaja N, Macho B, Sassone-Corsi P. (2005) Microtubule-independent and protein kinase A-mediated function of kinesin KIF17b controls the intracellular transport of activator of CREM in testis (ACT). J Biol Chem. 280(36):31739-45.

Lansbergen G, Komarova Y, Modesti M, Wyman C, Hoogenraad CC, Goodson HV, Lemaitre RP, Drechsel DN, van Munster E, Gadella TW Jr, Grosveld F, Galjart N, Borisy GG, Akhmanova A. (2004) Conformational changes in CLIP-170 regulate its binding to microtubules and dynactin localization. J Cell Biol. 166(7):1003-14.

Lebkowski JS, Clancy S, Calos MP. (1985) Simian virus 40 replication in adenovirus-transformed human cells antagonizes gene expression. Nature. 317(6033):169-71.

L'Hernault SW, Rosenbaum JL. (1985) Chlamydomonas alpha-tubulin is posttranslationally modified by acetylation on the epsilon-amino group of a lysine. Biochemistry. 24(2):473-8.

Li D, Roberts R. (2001) WD-repeat proteins: structure characteristics, biological function, and their involvement in human diseases. Cell Mol Life Sci. 58(14):2085-97.

Li S, Ku CY, Farmer AA, Cong YS, Chen CF, Lee WH. (1998) Identification of a novel cytoplasmic protein that specifically binds to nuclear localization signal motifs. J Biol Chem. 273(11):6183-9.

Liu Z., Steward R., Luo L. (2000) Drosophila Lis1 is required for neuroblast proliferation, dendritic elaboration and axonal transport. Nat. Cell Biol. 2:767–775.

Lo Nigro C, Chong CS, Smith AC, Dobyns WB, Carrozzo R, Ledbetter DH. (1997) Point mutations and an intragenic deletion in LIS1, the lissencephaly causative gene in isolated lissencephaly sequence and Miller-Dieker syndrome. Hum Mol Genet. 6(2):157-64.

Lyon MF, Hawkes SG. (1970) X-linked gene for testicular feminization in the mouse. Nature. 227(5264):1217-9.

Macho B, Brancorsini S, Fimia GM, Setou M, Hirokawa N, Sassone-Corsi P. (2002) CREM-dependent transcription in male germ cells controlled by a kinesin. Science. 298(5602):2388-90

Mason JM, Arndt KM. (2004) Coiled coil domains: stability, specificity, and biological implications. Chembiochem. 5(2):170-6.

Mateja A, Cierpicki T, Paduch M, Derewenda ZS, Otlewski J.(2006) The dimerization mechanism of LIS1 and its implication for proteins containing the LisH motif. J Mol Biol. 357(2):621-31.

Matheny SA, Chen C, Kortum RL, Razidlo GL, Lewis RE, White MA. (2004) Ras regulates assembly of mitogenic signalling complexes through the effector protein IMP. Nature. 427(6971):256-60.

Meroni G, Diez-Roux G. (2005) TRIM/RBCC, a novel class of 'single protein RING finger' E3 ubiquitin ligases. Bioessays. 27(11):1147-57.

Mesngon MT, Tarricone C, Hebbar S, Guillotte AM, Schmitt EW, Lanier L, Musacchio A, King SJ, Smith DS. (2006) Regulation of cytoplasmic dynein ATPase by Lis1. J Neurosci. 26(7):2132-9.

Mimori-Kiyosue Y, Shiina N, Tsukita S. (2000) The dynamic behavior of the APC-binding protein EB1 on the distal ends of microtubules. Curr Biol. 2000 10(14):865-8.

Miki H, Setou M, Kaneshiro K, Hirokawa N. (2001) All kinesin superfamily protein, KIF, genes in mouse and human. Proc Natl Acad Sci U S A. 98(13):7004-11.

Monaco L, Kotaja N, Fienga G, Hogeveen K, Kolthur US, Kimmins S, Brancorsini S, Macho B, Sassone-Corsi P. (2004) Specialized rules of gene transcription in male germ cells: the CREM paradigm. Int J Androl. 27(6):322-7.

Morell M, Espargaro A, Aviles FX, Ventura S. (2008) Study and selection of in vivo protein interactions by coupling bimolecular fluorescence complementation and flow cytometry. Nat Protoc. 3(1):22-33.

Moutier R, Toyama K, Cotton WR, Gaines JF. (1976) Three recessive genes for congenital osteopetrosis in Norway rat. J Hered. 67(3):189-90.

Murrin LC, Talbot JN. (2007) RanBPM, a scaffolding protein in the immune and nervous systems. J Neuroimmune Pharmacol. 2(3):290-5.

Nakamura M, Masuda H, Horii J, Kuma K, Yokoyama N, Ohba T, Nishitani H, Miyata T, Tanaka M, Nishimoto T. (1998) When overexpressed, a novel centrosomal protein, RanBPM, causes ectopic microtubule nucleation similar to gamma-tubulin. J Cell Biol. 143(4):1041-52.

Nayernia K, Vauti F, Meinhardt A, Cadenas C, Schweyer S, Meyer BI, Schwandt I, Chowdhury K, Engel W, Arnold HH. (2003) Inactivation of a testis-specific Lis1 transcript in mice prevents spermatid differentiation and causes male infertility. J Biol Chem. 278(48):48377-85.

Niethammer M, Smith DS, Ayala R, Peng J, Ko J, Lee MS, Morabito M, Tsai LH. (2000) NUDEL is a novel Cdk5 substrate that associates with LIS1 and cytoplasmic dynein. Neuron. 28(3):697-711.

Nishitani H, Hirose E, Uchimura Y, Nakamura M, Umeda M, Nishii K, Mori N, Nishimoto T. (2001) Full-sized RanBPM cDNA encodes a protein possessing a long stretch of proline and glutamine within the N-terminal region, comprising a large protein complex. Gene. 272(1-2):25-33.

Ozaki K, Sato H, Inoue K, Tsunoda T, Sakata Y, Mizuno H, Lin TH, Miyamoto Y, Aoki A, Onouchi Y, Sheu SH, Ikegawa S, Odashiro K, Nobuyoshi M, Juo SH, Hori M, Nakamura Y, Tanaka T. (2009) SNPs in BRAP associated with risk of myocardial infarction in Asian populations. Nat Genet. 41(3):329-33.

Ouspenski II. (1998) A RanBP1 mutation which does not visibly affect nuclear import may reveal additional functions of the ran GTPase system. Exp Cell Res. 244(1):171-83.

Palmer JS, Cromie WJ, Plzak LF, Leff AR. (1997) A platelet activating factor antagonist attenuates the effects of testicular ischemia. J Urol. 158(3 Pt 2):1186-90.

Perez, F., Diamantopoulos, G.S., Stalder, R., and Kreis, T.E. (1999) CLIP-170 highlights growing microtubule ends in vivo. Cell. 96, 517-527.

Péterfy M, Gyuris T, Grosshans D, Cuaresma CC, Takács L. (1998) Cloning and characterization of cDNAs and the gene encoding the mouse platelet-activating factor acetylhydrolase Ib alpha subunit/lissencephaly-1 protein. Genomics. 47(2):200-6.

Piehl M, Cassimeris L. (2003) Organization and dynamics of growing microtubule plus ends during early mitosis. Mol Biol Cell. 14(3):916-25.

Pierre P, Scheel J, Rickard JE, Kreis TE. (1992) CLIP-170 links endocytic vesicles to microtubules. Cell. 70(6):887-900.

Presley JF, Cole NB, Schroer TA, Hirschberg K, Zaal KJ, Lippincott-Schwartz J. (1997) ER-to-Golgi transport visualized in living cells. Nature. 389(6646):81-5.

Reed NA, Cai D, Blasius TL, Jih GT, Meyhofer E, Gaertig J, Verhey KJ. (2006) Microtubule acetylation promotes kinesin-1 binding and transport. Curr Biol. 16(21):2166-72.

Reiner O, Carrozzo R, Shen Y, Wehnert M, Faustinella F, Dobyns WB, Caskey CT, Ledbetter DH. (1993) Isolation of a Miller-Dieker lissencephaly gene containing G protein beta-subunit-like repeats. Nature. 364(6439):717-21.

Rickard JE, Kreis TE. (1991) Binding of pp170 to microtubules is regulated by phosphorylation. J Biol Chem. 266(26):17597-605.

Rooij DG, Boer P. (2003) Specific arrests of spermatogenesis in genetically modified and mutant mice. Cytogenet Genome Res. 103(3-4):267-76.

Roudebush WE. (2001) Role of platelet-activating factor in reproduction: sperm function. Asian J Androl. 3(2):81-5.

Sambrook J, Fritsch EF, Maniatis T. (1989) Molecular Cloning: A Laboratory Manual (Cold Spring Harbor Laboratory, Cold Spring Harbor, NY).

Sandoval IV, Cuatrecasas P. (1976) Opposing effects of cyclic AMP and cyclic GMP on protein phosphorylation in tubulin preparations. Nature, Lond. 262:511-514.

Sankaran S, Starita LM, Groen AC, Ko MJ, Parvin JD. (2005) Centrosomal microtubule nucleation activity is inhibited by BRCA1-dependent ubiquitination. Mol Cell Biol. 25(19):8656-68.

Sapir T, Elbaum M, Reiner O. (1997) Reduction of microtubule catastrophe events by LIS1, platelet-activating factor acetylhydrolase subunit. EMBO J. 16(23):6977-84.

Sasaki S, Shionoya A, Ishida M, Gambello MJ, Yingling J, Wynshaw-Boris A, Hirotsune S. (2000) A LIS1/NUDEL/cytoplasmic dynein heavy chain complex in the developing and adult nervous system. Neuron. 28(3):681-96.

Sassone-Corsi P. (1998) Regulating the balance between differentiation and apoptosis: role of CREM in the male germ cells. J Mol Med. 76(12):811-7.

Sattler M, Salgia R. (2007) c-Met and hepatocyte growth factor: potential as novel targets in cancer therapy. Curr Oncol Rep. 9(2):102-8.

Schulze H, Dose M, Korpal M, Meyer I, Italiano JE, Jr and Shivdasani RA. (2008) RanBP10 is a cytoplasmic guanine nucleotide exchange factor that modulates noncentrosomal microtubules. J Biol Chem. 283: 14109-14119.

Siller KH, Serr M, Steward R, Hays TS, Doe CQ. (2005) Live imaging of Drosophila brain neuroblasts reveals a role for Lis1/dynactin in spindle assembly and mitotic checkpoint control. Mol Biol Cell. 16(11):5127-40.

Smith DS, Niethammer M, Ayala R, Zhou Y, Gambello MJ, Wynshaw-Boris A, Tsai LH. (2000) Regulation of cytoplasmic dynein behaviour and microtubule organization by mammalian Lis1. Nat Cell Biol. 2(11):767-75.

Stewart RM, Richman DP, Caviness VS Jr. (1975) Lissencephaly and Pachygyria: an architectonic and topographical analysis. Acta Neuropathol. 31(1):1-12.

Strickland LI, Wen Y, Gundersen GG, Burgess DR. (2005) Interaction between EB1 and p150glued is required for anaphase astral microtubule elongation and stimulation of cytokinesis. Curr Biol. 15(24):2249-55.

Studier FW, Rosenberg AH, Dunn JJ, Dubendorff JW. (1990) Use of T7 RNA polymerase to direct expression of cloned genes. Methods Enzymol. 185:60-89.

Tai CY, Dujardin DL, Faulkner NE, Vallee RB. (2002) Role of dynein, dynactin, and CLIP-170 interactions in LIS1 kinetochore function. J Cell Biol. 156(6):959-68.

Tanenbaum ME, Macůrek L, Galjart N, Medema RH. (2008) Dynein, Lis1 and CLIP-170 counteract Eg5-dependent centrosome separation during bipolar spindle assembly. EMBO J. 27(24):3235-45.

Taya S, Shinoda T, Tsuboi D, Asaki J, Nagai K, Hikita T, Kuroda S, Kuroda K, Shimizu M, Hirotsune S, Iwamatsu A, Kaibuchi K. (2007) DISC1 regulates the transport of the NUDEL/LIS1/14-3-3epsilon complex through kinesin-1. J Neurosci. 27(1):15-26.

Tjoelker LW, Wilder C, Eberhardt C, Stafforini DM, Dietsch G, Schimpf B, Hooper S, Le Trong H, Cousens LS, Zimmerman GA, et al. (1995) Anti-inflammatory properties of a platelet-activating factor acetylhydrolase. Nature. 374(6522):549-53.

Toyo-oka K, Shionoya A, Gambello MJ, Cardoso C, Leventer R, Ward HL, Ayala R, Tsai LH, Dobyns W, Ledbetter D, Hirotsune S, Wynshaw-Boris A. (2003) 14-3-3epsilon is important for neuronal migration by binding to NUDEL: a molecular explanation for Miller-Dieker syndrome. Nat Genet. 34(3):274-85.

Tran AD, Marmo TP, Salam AA, Che S, Finkelstein E, Kabarriti R, Xenias HS, Mazitschek R, Hubbert C, Kawaguchi Y, Sheetz MP, Yao TP, Bulinski JC. (2007) HDAC6 deacetylation of tubulin modulates dynamics of cellular adhesions. J Cell Sci. 120(Pt 8):1469-79.

Tsai JW, Chen Y, Kriegstein AR, Vallee RB. (2005) LIS1 RNA interference blocks neural stem cell division, morphogenesis, and motility at multiple stages. J Cell Biol. 170(6):935-45.

Umemura K, Kato I, Hirashima Y, Ishii Y, Inoue T, Aoki J, Kono N, Oya T, Hayashi N, Hamada H, Endo S, Oda M, Arai H, Kinouchi H, Hiraga K. (2007) Neuroprotective role of transgenic PAF-acetylhydrolase II in mouse models of focal cerebral ischemia. Stroke. 38(3):1063-8.

Valiyaveettil M, Bentley AA, Gursahaney P, Hussien R, Chakravarti R, Kureishy N, Prag S, Adams JC. (2008) Novel role of the muskelin-RanBP9 complex as a nucleocytoplasmic mediator of cell morphology regulation. J Cell Biol. 182(4):727-39.

Vaughan KT. (2005) TIP maker and TIP marker; EB1 as a master controller of microtubule plus ends. J Cell Biol. 171(2):197-200.

Verhey KJ, Gaertig J. (2007) The tubulin code. Cell Cycle. 6(17):2152-60.

Vitre B, Coquelle FM, Heichette C, Garnier C, Chrétien D, Arnal I. (2008) EB1 regulates microtubule dynamics and tubulin sheet closure in vitro. Nat Cell Biol. 10(4):415-21.

Vojtek AB, Hollenberg SM, Cooper JA. (1993) Mammalian Ras interacts directly with the serine/threonine kinase Raf. Cell. 74(1):205-14.

Wang D, Li Z, Messing EM, Wu G. (2002) Activation of Ras/Erk pathway by a novel MET-interacting protein RanBPM. J Biol Chem. 277(39):36216-22.

Westermann S, Weber K. (2003) Post-translational modifications regulate microtubule function. Nat Rev Mol Cell Biol. 4(12):938-47.

Wilde A, Zheng Y. (1999) Stimulation of microtubule aster formation and spindle assembly by the small GTPase Ran. Science. 284(5418):1359-62.

Wynshaw-Boris A. (2007) Lissencephaly and LIS1: insights into the molecular mechanisms of neuronal migration and development. Clin Genet. 72(4):296-304.

Xiang X, Osmani AH, Osmani SA, Xin M, Morris NR (1995) NudF, a nuclear migration gene in Aspergillus nidulans, is similar to the human LIS-1 gene required for neuronal migration. Mol Biol Cell. 6(3):297–310

Yamada M, Toba S, Yoshida Y, Haratani K, Mori D, Yano Y, Mimori-Kiyosue Y, Nakamura T, Itoh K, Fushiki S, Setou M, Wynshaw-Boris A, Torisawa T, Toyoshima YY, Hirotsune S. (2008) LIS1 and NDEL1 coordinate the plus-end-directed transport of cytoplasmic dynein. EMBO J. 27(19):2471-83.

Yan W, Assadi AH, Wynshaw-Boris A, Eichele G, Matzuk MM, Clark GD. (2003) Previously uncharacterized roles of platelet-activating factor acetylhydrolase 1b complex in mouse spermatogenesis. Proc Natl Acad Sci U S A. 100(12):7189-94.

Yingling J, Youn YH, Darling D, Toyo-Oka K, Pramparo T, Hirotsune S, Wynshaw-Boris A. (2008) Neuroepithelial stem cell proliferation requires LIS1 for precise spindle orientation and symmetric division. Cell. 132(3):474-86.

Yudin D, Fainzilber M. (2009) Ran on tracks--cytoplasmic roles for a nuclear regulator. J Cell Sci. 122(Pt 5):587-93.

Zimmermann S, Steding G, Emmen JM, Brinkmann AO, Nayernia K, Holstein AF, Engel W, Adham IM. (1999) Targeted disruption of the Insl3 gene causes bilateral cryptorchidism. Mol Endocrinol. 13(5):681-91.

Zou Y, Lim S, Lee K, Deng X, Friedman E. (2003) Serine/threonine kinase Mirk/Dyrk1B is an inhibitor of epithelial cell migration and is negatively regulated by the Met adaptor Ran-binding protein M. J Biol Chem. 278(49):49573-81.

Acknowledgements

First of all, I thank the International Graduate College: "Molecular Complexes of Biomedical Relevance" for the Georg-Christoph-Lichtenberg Fellowship financed by the state of Lower Saxony.

I would like to express my great gratitude to Prof. Dr. Hans-Henning Arnold for giving me the opportunity to work in the Department of Cell and Molecular Biology. For Prof. Dr. Hans-Henning Arnold excellent scientific guidance, persistent support, and impressive enthusiasm and also Dr. Andreas Holz encouragement and supporting discussions as well as their constructive ideas over last four years I am very thankful. I would like to thank Prof. Dr. Brigitte M. Jockusch and Prof. Dr. Martin Korte for their kind acceptance to be part of the thesis committee and the final stage of my dissertation.

Dr. Barbara Winter, Dr. Astrid Buchberger, Dr. Franz Vauti, Dr. Vita Dauksaite, and Sabine Buchmeier I would like to thank for their tenacious support, research-based direction, and especially Barbara for her kind help in official and private matters. Congcong Zhang I would like to thank for his help in the FACS experiments and express my appreciation to Dr. Marco Van Ham and Marcin Ura for their great helps related to the microtubules. Mrs. Charlotte Klaue and Dr. Manuela Schüngel have effectively managed many matters for me concerning the German bureaucracy.

Many thanks go to lab colleagues (Bastian, Ines, Jana, Alex, Iris, Franziska, and Friederike) and our former bachelor students (Franziska, Nicole, Dagmar, and Robert) for their aid and the warm atmosphere.

Last but not least I would like to thank my family and my best friends (Bujin, Mijung and Sunyoung) for their persistent support and encouragement. I am also greatly thankful to my love Patrick and his family.

Without all the support by my side I could not have reached my goal within time.